THE ROLE OF RHO KINASE 2 IN THE DEVELOPMENT OF ISCHEMIA/REPERFUSION INJURY IN NORMAL AND DIABETIC HEARTS

by

Marysol Garcia Patino

B.Sc. Tecnológico de Monterrey, 2008

M.Sc., Tecnológico de Monterrey, 2010

A THESIS SUBMITTED IN PARTIAL FULFILLMENT OF

THE REQUIREMENTS FOR THE DEGREE OF

DOCTOR OF PHILOSOPHY

in

THE FACULTY OF GRADUATE AND POSTDOCTORAL STUDIES

(Pharmaceutical Sciences)

THE UNIVERSITY OF BRITISH COLUMBIA

(Vancouver)

December 2017

Abstract

During myocardial infarction, the heart enters into an ischemic state that, if untreated, leads to cell death. To avoid this, reperfusion must be instituted. However, this causes a type of cardiac damage known as myocardial ischemia-reperfusion (I/R) injury. Concomitant diseases such as diabetes not only increase the risk of myocardial infarction, but also intensify susceptibility to I/R injury. Over-activation of Rho kinase (ROCK) has been reported to contribute to I/R injury; however, it is unknown whether ROCK1, ROCK2 or both isoforms, is/are responsible for this effect. Furthermore, it has not been determined if the cardioprotective activity of ROCK inhibition is maintained under diabetic conditions. Here, we evaluated the contribution of ROCK2 to myocardial I/R injury, as well as its role during diabetes.

The induction of I/R injury impaired cardiac function in wild-type (WT) but not heterozygous ROCK2-knockdown (ROCK2+/-) mice. Infarct size was also lower in ROCK2+/- mice than in their WT counterparts, while an I/R-induced increase in ROCK activity was detected only in WT hearts. The cardioprotection observed in ROCK2+/- mice was associated with increased Akt and GSK-3β phosphorylation and a reduction of I/R-induced cytokine production. Compared to their ROCK2-expressing counterparts, cardiac-specific ROCK2 knockout (cROCK2-/-) mice subjected to I/R also had a smaller infarct size, suggesting that the deleterious effects of I/R are at least partially regulated by cardiomyocyte ROCK2. However, the induction of diabetes by streptozotocin treatment abrogated the protective effect of cardiomyocyte-specific ROCK2 deletion. ROCK activity was comparable in control and diabetic post-I/R cROCK2-/- hearts, but the increase in Akt and GSK-3β phosphorylation was no longer detected under diabetic conditions. Furthermore, cytokine production in non-diabetic cROCK2-/-

mice was higher than in their ROCK2 expressing counterparts, and this was normalized in diabetic conditions.

Overall, these results show that ROCK2 plays a significant role in the development of myocardial I/R injury, and that its inhibition is associated with activation of the pro-survival RISK-pathway. Moreover, the cardioprotection obtained by the cardiac-specific deletion of this isoform suggests that I/R-induced ROCK2 activation takes place in the cardiomyocyte. However, this cardioprotective effect is lost during diabetes, possibly due to impaired Akt and GSK-3β phosphorylation.

Lay Summary

When a person suffers a heart attack, blood stops flowing through a portion of the heart. This portion no longer receives the oxygen and nutrients carried in blood, so the heart enters a state known as *ischemia*. In order to avoid tissue death on that portion of the heart, blood flow has to be restored, in a procedure known as *reperfusion.* However, this sudden change of conditions causes a type of damage known as *myocardial ischemia-reperfusion (I/R) injury.* Because diabetic patients are at a greater risk of developing cardiovascular diseases, they are also more prone to I/R injury. The present thesis focuses on a specific protein, Rho kinase 2 (ROCK2), and its role in the development of this disease in both diabetic and non-diabetic conditions. Our data show that hearts that do not express ROCK2 are protected against I/R injury; however, this cardioprotection is lost in the presence of diabetes.

Preface

All of the experiments reported in chapter 2 were carried out by me under the very valuable guidance of my supervisor, Dr. Kathleen M. MacLeod. Dr. Shelly McErlane and Kris Andrews, from the Centre for Comparative Medicine at the University of British Columbia provided advice and support for the development of the *in vivo* protocol of myocardial I/R injury here employed.

A version of chapter 3 has been submitted for publication with the following title: Contribution of ROCK2 to myocardial ischemia-reperfusion injury. The authors are: Marysol Garcia-Patino, Vongai Nyamandi, Julia Nogueira Varela, Guorong Lin, Hesham Soliman, Zhengping Jia, James K. Liao and Kathleen M. MacLeod. The study was designed and conceived jointly by me and Dr. Kathleen M. MacLeod. I conducted all the experimental studies and data analysis. Vongai Nyamandi and Julia Nogueira Varela provided support for the development of animal studies. Dr. Guorong Lin and Dr. Hesham Soliman offered guidance on the development of the ROCK and PTEN assays, as well as the immunohistochemical staining. Dr. Zhengping Jia and Dr. James K. Liao kindly provided the transgenic mouse models.

A version of chapter 4 will be submitted for publication. The working title is: Diabetes impairs the cardioprotective effect of cardiomyocyte-specific ROCK2 deletion in myocardial I/R injury. The study was designed and conceived by me and Dr. Kathleen M. MacLeod. I conducted all the experiments and data analyisis. Vongai Nyamandi and Dr. Hesham Soliman offered guidance on the animal breeding and the immunohistochemical staining that was performed. Dr. James K. Liao kindly provided the transgenic mouse model.

The present thesis conforms to the Canadian Council on Animal Care Guidelines on the

Care and Use of Experimental Animals and to the Guide for Care and Use of Laboratory Animals published by the United States National Institutes of Health (NIH publication no. 85–23, revised 1996). The animal work reported in this thesis was approved by the University of British Columbia Animal Care Ethics Committee, protocol number A14-0215.

Table of Contents

List of Tables

List of Figures

List of Abbreviations

A1C	Glycated hemoglobin
AAR	Area at risk
AGEs	Advanced glycation end-products
AIF	Apoptosis-inducing factor
α-MHC	Alpha-myosin heavy chain
ANT	Adenine nucleotide translocase
AON	Area of necrosis
AT1	Angiotensin II type 1
ATP	Adenosine triphosphate
BAD	Bcl-2-associated death promoter
BB	Bio-breeder rats
CAD	Caspase-activated deoxyribonuclease
cROCK2-/-	ROCK2$^{flox/flox}$-αMHC-*MerCreMer* mice
cROCK2+/+	ROCK2$^{flox/flox}$ non-αMHC-*MerCreMer* mice
DAMP	Damage-associated molecular patterns
DNA	Deoxyribonucleic acid
DTT	1,4-dithiothreitol
E/A	Early to late ventricular filling ratio
eNOS	Endothelial nitric oxide synthase
ER	Endoplasmic reticulum
Erk1/2	Extracellular signal regulated kinase 1/2
$FADH_2$	Flavin adenine dinucleotide

GAP	GTPase-activating protein
GEF	Guanine nucleotide exchange factor
GLUT2	Glucose transporter 2
GSK-3β	Glycogen synthase kinase-3β
GTP	Guanosine-5'-triphosphate
H&E	Hematoxylin and eosin
H_2O_2	Hydrogen peroxide
I/R	Ischemia/reperfusion
ICAD	Inhibitor of caspase-activated DNAse
IHC	Immunohistochemical
IKK	Inhibitor of NFκB kinase
IL-1β	Interleukin 1β
IL-6	Interleukin 6
INTERHEART	A large international study across 52 countries that examined the effects of potentially modifiable risk factors associated with myocardial infarction
JAK2	Janus kinase 2
JNK	NH_2-terminal Jun kinases
LAD	Left anterior descending
LDH	Lactate dehydrogenase
LDLR	Low-density lipoprotein receptor
LEW.1AR1	Lewis rats with a defined MHC haplotype
LIMK	LIM-Kinase
LV	Left ventricular

MCP-1	Monocyte chemotactic protein-1
MerCreMer	Cre recombinase
MLCP	Myosin light chain phosphatase
MPI	Myocardial performance index
MPTP	Mitochondrial permeability transition pore
mTOR	Mammalian target of rapamycin
MYPT	Myosin phosphatase targeting protein
NADH	Nicotinamide adenine dinucleotide (reduced form)
NADPH	Nicotinamide adenine dinucleotide phosphate (reduced form)
NCX	Na^+/Ca^{2+} exchanger
NFκB	Nuclear factor kappa B
NHE	Na^+/H^+ exchanger
NOD	Non-obese diabetic mice
O_2^-	Superoxide
PARP	Poly ADP-ribose polymerase
PDK1	Phosphoinositide-dependent protein kinase 1
PH	Pleckstrin-homology
PI3K	Phosphoinositide 3-kinase
PIP2	Phosphatidylinositol (3,4)-biphosphate
PIP3	Phosphatidylinositol (3,4,5)-trisphosphate
PKC	Protein kinase C
POST	ST-Segment Elevation Myocardial Infarction trial
PTEN	Phosphatase and tensin homolog deleted on chromosome 10

RAGE	Receptor for AGEs
RISK	Reperfusion injury signaling kinase pathway
RNA	Ribonucleic acid
ROCK	Rho kinase
ROCK1	Rho kinase 1
ROCK2	Rho kinase 2
ROCK2+/-	ROCK2 heterozygous whole-body knockdown
ROS	Reactive oxygen species
RT-PCR	Real time-polymerase chain reaction
SAFE	Survivor activating factor enhancement pathway
SAPK	Stress-activated protein kinases
SC	Subcutaneous
SE	Standard error
SOD	Superoxide dismutase
SOD1	Superoxide dismutase 1
SOD2	Superoxide dismutase 2
STAT3	Signal transducer and activator of transcription 3
STZ	Streptozotocin
TAC	Transverse aortic constriction
TGF-β1	Transforming growth factor-β1
TLR	Toll-like receptor
TNFα	Tumor necrosis factor α
TTC	Triphenyltetrazolium chloride

WT	Wild-type

Acknowledgements

I would first like to thank my PhD supervisor, Dr. Kathleen M. MacLeod, for guiding me through this journey, and for her patience, commitment and unconditional support throughout these years. I will always be grateful to her for giving me the opportunity of being part of her research group, as well as for all the lessons she taught me, not only in research but in many other aspects of life.

I also would like to thank the members of my PhD committee, Dr. Brian Rodrigues, Dr. Roger Brownsey, and Dr. Glen Tibbits, as well as my PhD committee chair, Dr. Mary Ensom, for their valuable advice, support and dedication. Thank you for helping me to enhance the quality of my work and allowing me to be a better critic of myself.

I would also like to thank the Faculty of Pharmaceutical Sciences for their continuous support; with special thanks to Dr. Thomas Chang and Ms. Shirley Wong, for making their best effort to assure that all students achieve the goals of their graduate studies. I would also like to thank CONACyT for supporting me with a full scholarship the first four years of my studies.

Also, I would like to thank all the past and present members of our lab, Vongai, Julia, Carolyn, Hesham, Lin and Girish, for their support, advice and assistance. Special thanks to Vongai for putting up with me for more than five years - you certainly made the difficult moments less harsh. I am also grateful for the support of the members of the Rodrigues lab: Amy, Bahira, Nate, Ying and Fulong - thanks.

I would like to thank my parents, Salvador and Korina, for always being there for me, for their love, and for helping me to follow my dreams. I certainly would not be at the place I am at without you, and I will always be grateful for that. Thanks to my *abuelita* Maria Elena and my aunt Minerva for always caring for me and for giving me the confidence to move forward.

Finally, I would like to thank my dear husband Hector, for his unconditional love, his understanding and for being there the moments that I needed him the most. I would not have been able to accomplish this without you, you are the force that makes me go forward. I love you.

To my dear parents, Salvador and Korina, my *abuelita* Maria Elena, and my aunt Minerva, for being my pillars of support and my source of motivation,

and to my beloved husband Hector, for being the light of my life.

Chapter 1: Background

1.1 Cardiovascular disease and myocardial I/R injury

Cardiovascular disease is the number one cause of death worldwide. In 2015, 17.7 million people in the world died from cardiovascular disease, representing more than 30% of the total deaths and of these, 7.4 million were due to heart disease (1). Cardiovascular disease is also the leading cause of death in Canada. In 2004, 32.1% of all deaths in Canada were due to cardiovascular disease, and 54% of these were caused by heart disease (2). High blood pressure, elevated levels of blood cholesterol and triglycerides, diabetes, obesity, smoking, unhealthy diet, lack of exercise and stress are some of the risk factors that have been associated with the development of heart disease (3).

One of the most prevalent forms of heart disease is atherosclerosis, a condition caused by the buildup of plaque in the arteries. Over time, this plaque may rupture, causing the formation of a thrombus. This thrombus can then block the artery, stopping blood from flowing to a section of the heart, and causing a myocardial infarction (also known as heart attack). People who suffer a myocardial infarction have a higher risk of having another one; it has been estimated that after three years, about 20% of them will have a second event (4).

When a myocardial infarction takes place, the normal blood flow and therefore the supply of oxygen and nutrients to the myocardium is interrupted. As a consequence, the heart enters into an ischemic state that, if untreated, will cause the death of cardiomyocytes in the damaged area (5). In order to avoid this, myocardial reperfusion by thrombolytic therapy, percutaneous coronary intervention, or coronary artery bypass is performed. However, the prompt normalization of ischemic conditions during reperfusion causes an irreversible myocardial

damage known as ischemia/reperfusion (I/R) injury (5). Myocardial I/R injury can also happen in other settings where the heart is subjected to ischemic conditions and then reperfused, such as a cardiac transplant, where the heart is subjected to global I/R injury (6).

Myocardial I/R injury manifests in four different forms: myocardial stunning, microvascular obstruction, I/R-induced arrhythmias and lethal myocardial I/R injury, with each one of them being more severe than the previous one. Myocardial stunning is a form of reversible contractile dysfunction linked to short periods of ischemia, and recovery also depends on the length of ischemia before reperfusion (7). Microvascular obstruction is caused by capillary compression and cardiomyocyte swelling, and it is characterized by neutrophil infiltration and fibrin deposition. In patients who have suffered myocardial I/R injury, coronary blood flow may appear to be normal, but more sensitive tests, such as myocardial contrast echocardiography, will confirm the presence of microvascular obstruction. This manifestation of myocardial I/R injury has been linked to reductions of ejection fraction, left ventricular remodeling and large infarct sizes (7). I/R-induced arrhythmias are dependent on the duration of ischemia, but can be treated (7). Lethal myocardial I/R injury refers to the death of cardiomyocytes that were viable at the end of ischemia (7).

Many forms of treatment have been proposed for the reduction or prevention of myocardial I/R injury (8). Of these, two therapeutic strategies, known as ischemic preconditioning and ischemic postconditioning, have been especially well studied. Ischemic preconditioning is defined as the cardioprotection achieved by subjecting the heart to brief periods of ischemia and reperfusion before an extended period of ischemia; while ischemic postconditioning is the cardiac tolerance against I/R injury provided by brief periods of ischemia and reperfusion after a long period of ischemia has occurred (9). Both ischemic preconditioning

and postconditioning have been demonstrated to reduce the deleterious effects of myocardial I/R injury by avoiding the sudden physiological changes that occur in this condition (6). However, since ischemic preconditioning can only be employed in planned procedures such as a cardiac transplant or a previously scheduled percutaneous coronary intervention, ischemic postconditioning is the only one of the two therapies that is possible in patients that have suffered a myocardial infarction (6). Clinical trials have been conducted in order to evaluate the efficiency of these two forms of therapy; however, the results have so far been ambiguous or negative (10). For instance, the ST-Segment Elevation Myocardial Infarction randomized trial (POST) has recently shown that in patients undergoing percutaneous coronary intervention after suffering a myocardial infarction, ischemic postconditioning did not improve the outcomes of I/R injury (11). Therefore, the search for treatments that reduce or eliminate the detrimental effects of myocardial I/R injury continues.

1.2 Molecular mechanisms of myocardial I/R injury

The development of myocardial I/R injury is a complex process that involves many different mechanisms (Fig 1.1) and the most relevant are discussed below.

1.2.1 Rapid change of pH and intracellular Ca^{2+} overload

During ischemia, oxygen levels are significantly lower, and anaerobic glycolysis is performed in order to maintain ATP levels. The production of ATP by this process is much less efficient (5%), and this inhibits ATP-dependent processes such as Na^+/K^+ ATPase activity, ATP-dependent Ca^{2+} reuptake and active Ca^{2+} excretion. Furthermore, both intra- and extracellular pH are decreased due to the large amount of H^+ produced by the conversion of glucose to lactate via

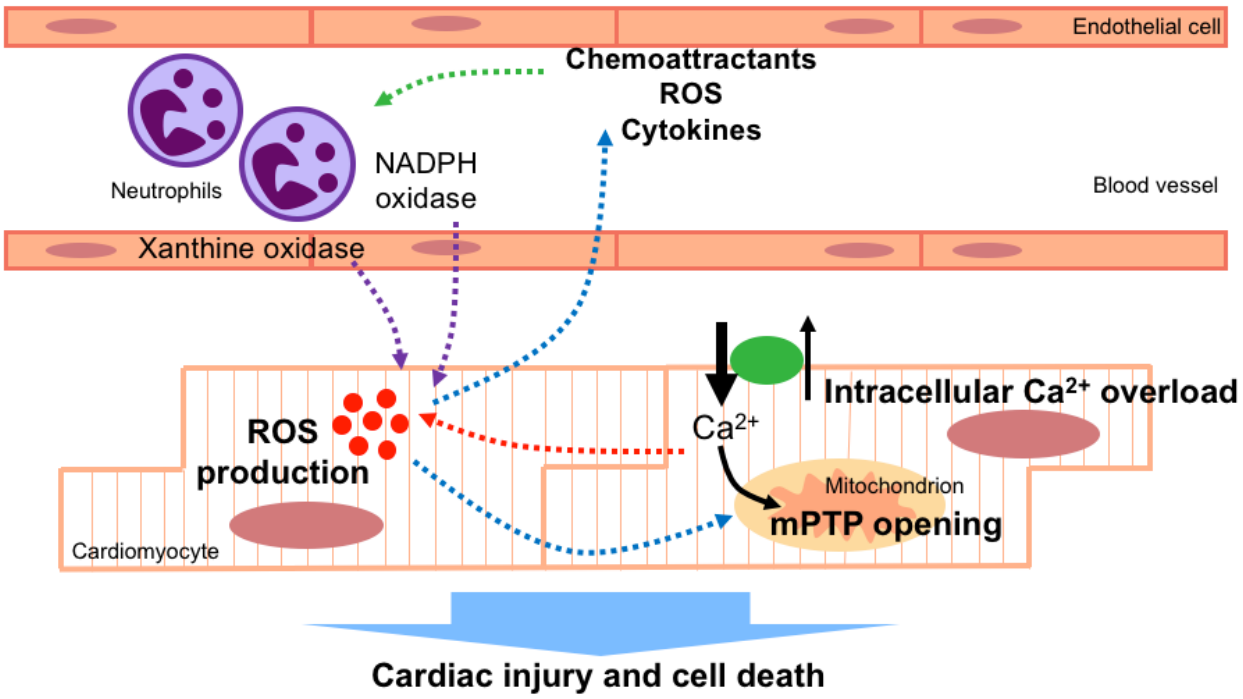

Figure 1.1 Mechanisms involved in the development of myocardial I/R injury

During ischemia, oxygen and pH levels are significantly decreased; however, the rapid change of conditions that occurs during reperfusion can translate into many deleterious effects. The abrupt change in pH, as well as the depolarization of the cell membrane, promotes an overload of intracellular Ca^{2+}. The excess of intracellular Ca^{2+} can then promote Ca^{2+} uptake into the mitochondria via the mitochondrial calcium uniporter. The elevated levels of mitochondrial Ca^{2+} promote the opening of the MPTP, which induces ROS production (red dashed arrow). Likewise, ROS can also further promote MPTP opening and stimulate an inflammatory response (blue dashed arrows). Pro-inflammatory cytokines and chemoattractants promote neutrophil infiltration (green dashed arrow), and the NADPH oxidase in these cells, as well as xanthine oxidase in endothelial cells (purple dashed arrows) stimulate the production of ROS (12).

anaerobic glycolysis (13).

During reperfusion, only the extracellular pH is rapidly brought to a normal level, creating a gradient across the membrane. The high level of intracellular H^+ stimulates Na^+/H^+ exchange by the Na^+/H^+ exchanger (NHE), resulting in an increase of intracellular Na^+. This increase in intracellular Na^+ and the depolarization of the cell membrane drive the Na^+/Ca^{2+} exchanger (NCX) in the reverse direction, causing an overload of intracellular Ca^{2+} (14). The excess intracellular Ca^{2+} can then promote Ca^{2+} uptake into the mitochondria via the mitochondrial calcium uniporter (12).

1.2.2 Production of reactive oxygen species

At the onset of reperfusion, cardiac tissue switches from anaerobic glycolysis to aerobic metabolism, increasing ATP production. However, the sudden recovery of oxygen levels causes a drastic increase in the production of reactive oxygen species (ROS) (15). Most oxygen (95%) is reduced to water (H_2O) by tetravalent reduction in complex IV of the mitochondrial electron transport chain, while the rest (5%) is reduced by univalent pathways that generate free radical intermediates. In normal conditions, the univalent pathway generates superoxide (O_2^-) when oxygen accepts an electron, and the presence of H^+ promotes the formation of hydrogen peroxide (H_2O_2). Superoxide dismutase (SOD) can also convert O_2^- to its ordinary molecular form or to H_2O_2, and H_2O_2 can then be reduced to H_2O by catalase or glutathione peroxidase (16). However, in myocardial I/R injury, the presence of these antioxidant enzymes of ROS homeostasis is affected, and a large amount of ROS accumulates (15). Furthermore, high levels of ROS can also affect the components of the electron transport chain, promoting an even higher production of O_2^- and potentiating ROS production (12).

1.2.3 The opening of the mitochondrial permeability transition pore

The mitochondrial permeability transition pore (MPTP) is a large non-specific channel located at the inner membrane of the mitochondria (17). During reperfusion, the elevated levels of mitochondrial Ca^{2+} and ROS promote the opening of this pore, allowing the passage of any molecule smaller than 1.5 kDa. The opening of the MPTP greatly diminishes the mitochondrial membrane potential and proton gradient, thereby uncoupling oxidative phosphorylation and reducing mitochondrial ATP production (18). Cyclophilin D can also promote the opening of the MPTP by associating with adenine nucleotide translocase (ANT) and binding to the inner mitochondrial membrane, in a process also regulated by Ca^{2+} and ROS (19). If the damage induced by myocardial I/R injury is large enough, and most of the mitochondria undergo MPTP opening, ATP production is severely limited and mitochondrial homeostasis is lost. The mitochondrial matrix then swells, causing the outer mitochondrial membrane to break (12).

1.2.4 Cell death induced by I/R injury

The high levels of intracellular Ca^{2+}, the accumulation of ROS, and the opening of the MPTP along with other factors induced by myocardial I/R injury, eventually lead to cell death by apoptosis, necrosis or autophagy (20). Apoptosis is a mechanism of regulated cell death characterized by DNA fragmentation and cell shrinkage. The dying cell expresses cell surface markers that promote phagocytosis, avoiding the leakage of cytosolic contents (21). In myocardial I/R injury, apoptosis can be initiated by two different pathways: the extrinsic receptor-specific pathway or the intrinsic mitochondrial-dependent pathway. In the extrinsic receptor-specific pathway, a ligand binds to a death receptor and initiates the cleavage of pro-

caspases 2, 8 and 10, which then activate pro-caspases 3, 6 and 7. These pro-caspases are also known as effector caspases, and they cleave proteins that initiate the apoptotic process in myocardial I/R injury, such as inhibitor of caspase-activated DNAse (ICAD) and poly ADP-ribose polymerase (PARP) (22). The cleaved form of ICAD promotes the translocation of caspase-activated deoxyribonuclease (CAD) from the cytosol to the nucleus. There, CAD promotes DNA rupture, and therefore apoptosis (22). PARP, on the other hand, is an anti-apoptotic protein that functions as a sensor of DNA damage. Cleavage by caspase 3 separates the DNA-binding domain of PARP from its catalytic domain, rendering this protein inactive (23).

In the intrinsic mitochondrial-dependent pathway, pro-apoptotic and anti-apoptotic signals regulate the release of proteins from the inner mitochondrial membrane. Bcl-2, an anti-apoptotic protein located at the outer mitochondrial membrane, regulates the release of cytochrome c and maintains the integrity of the mitochondrial membrane. However, during myocardial I/R injury, Ca^{2+} overload and the opening of the MPTP promotes the translocation of pro-apoptotic Bax from the cytosol to the outer mitochondrial membrane (22). Here, Bax promotes the release of apoptosis-inducing factor (AIF) and cytochrome c from the inter-membrane space by pore formation or Bcl-2 association, since the association of Bax with Bcl-2 inactivates the latter through heterodimerization. In animal models of myocardial I/R injury, it has been suggested that the inhibition of Bax (24) and the activation of Bcl-2 (25) reduce the extent of cell death. Moreover, because of the relationship between these two proteins, the ratio of Bax/Bcl-2 is commonly used as an indicator of apoptosis susceptibility (26). The release of AIF and cytochrome c from the mitochondria can then trigger a series of detrimental effects. AIF induces caspase-independent nuclear degradation, while cytochrome c disrupts cell homeostasis and activates caspase 9. Similarly to caspases 2, 8 and 10 from the extrinsic receptor-specific

pathway, caspase 9 also activates pro-caspases 3, 6 and 7 (22). In myocardial I/R injury, the initiation of the apoptotic cascade is almost immediate. Cytochrome c release can be detected only within minutes of starting reperfusion. However, apoptosis only becomes apparent after several hours (27).

In contrast to apoptosis, necrosis is normally regarded as an unregulated mechanism of cell death characterized by cell swelling and rupture. However, it has been suggested that this autolytic process can be promoted by an increased protease activity and ion dysregulation (20). In the development of myocardial I/R injury, MPTP opening plays a key role in necrosis. At an early stage, MPTP opening induces apoptosis; however when the MPTP remains open, necrosis is induced due to the loss of membrane potential and ATP depletion (12). Calpain activation has been also implicated in the development of I/R-induced necrosis. These proteins are cysteine proteases activated by elevated concentrations of intracellular Ca^{2+}, and they are responsible for membrane degradation during myocardial I/R injury (28). Necrosis has also been detected in cells that undergo apoptosis, in a process known as "secondary necrosis". Phagocytosis is not performed in these cells, and this causes a progressive loss of structural integrity that eventually leads to cell rupture (29).

Autophagy is a mechanism used to remove damaged organelles or to supply nutrients during starvation; however, when excessively activated, it induces cell death. When autophagy is initiated, an isolation membrane engulfs cytoplasmic substrates, and an autophagosome is formed. Lysosomes are then fused to autophagosomes to promote their degradation (30). Beclin-1 has been implicated in autophagy initiation induced by myocardial I/R injury. In normal conditions, this protein remains inactive when bound to Bcl-2, but in starvation conditions, Beclin-1 is released. Beclin-1 functions as a molecular scaffold that allows the interaction of

several regulators of autophagosome formation, therefore, its release promotes autophagy. During myocardial I/R injury, autophagy can be classified either as protective or as damaging; however, recent reports agree that its effects will differ depending when and how it is initiated (12, 31).

1.2.5 Inflammation

Myocardial I/R injury induces an inflammatory response that is vital for cardiac tissue repair. Within minutes, chemokines and pro-inflammatory cytokines are secreted by endogenous cardiac cells and cells of the immune system. Chemokines then attract monocytes, while pro-inflammatory cytokines activate neutrophil recruitment (32), and both monocytes and neutrophils clear debris in areas of necrosis and augment cytokine release. Nonetheless, the inflammatory response elicited by myocardial I/R injury is often excessive, having a detrimental effect on the heart (33). Inflammation, along with the activation of both the innate and adaptive immune systems, plays an important role in the pathogenesis of myocardial I/R injury.

Since no pathogens are involved in the development of myocardial I/R injury, the type of inflammation elicited is known as “sterile inflammation”. In this process, toll-like receptors (TLRs) are activated by endogenous ligands known as damage-associated molecular patterns (DAMPs). In normal conditions, DAMPs are located inside the cell; however, when the membrane is damaged, DAMPs are released and free to bind TLRs (34). TLRs are predominantly expressed in leukocytes, and it has been shown that TLR2, 3, 4, and 6 are also expressed in cardiomyocytes (35). TLR activation leads to the nuclear translocation of nuclear factor kappa B (NFκB), a transcription factor that promotes the expression of pro-inflammatory cytokines such as tumor necrosis factor alpha (TNFα), interleukin 6 (IL-6) and interleukin 1-beta

(IL-1β), and chemokines such as monocyte chemotactic protein 1 (MCP-1) (33). It has been shown that TLR activation contributes to the development of myocardial I/R injury. For instance, Hua et al. (36) reported that TLR4 knockout mice had significantly lower infarct sizes compared to their wild-type (WT) counterparts, and that this cardioprotection was associated with the activation of anti-apoptotic pathways. Similarly, Arslan et al. (37) reported that in an *in vivo* mouse model of myocardial I/R injury, anti-TLR2 therapy is cardioprotective against the development of this condition.

The increased production of pro-inflammatory cytokines has been detected in many different models of myocardial I/R injury. Several reports show that mRNA and protein levels of TNFα, IL-1β and IL-6 are significantly increased by I/R-induction (38-40). Neutrophils also play an important role in the development of myocardial I/R injury. They are attracted to the site of injury within minutes of reperfusion, and their presence peaks after 24 hours (41). In order for them to infiltrate the cardiac tissue, pro-inflammatory cytokines TNFα, IL-1β and IL-6 activate endothelial cells and promote the production of adhesion molecules that will allow neutrophil migration through the endothelium (32). Once they are recruited to the cardiac tissue, neutrophils can then amplify the production of pro-inflammatory cytokines and chemokines, and release ROS and proteases that will contribute to the damage caused by myocardial I/R injury (41). The deleterious role of neutrophils is supported by reports that suggest that neutrophil depletion achieved by anti-neutrophil serum administration (42) or neutrophil-filtered blood perfusion (43), reduces the severity of myocardial I/R injury.

However, as previously mentioned, the role of inflammation in the development of myocardial I/R injury is not purely detrimental. There is also evidence that pro-inflammatory cytokines, such as TNFα have an ambivalent role during myocardial I/R injury (44). Lecour et al.

(45) showed that in hearts subjected to I/R injury *ex vivo*, a low dose of TNFα has the same cardioprotective effects as those obtained by ischemic preconditioning, but at higher doses, TNFα-treated hearts have larger infarct sizes compared to their untreated counterparts. Similarly, blocking the IL-6 receptor for four weeks after inducing myocardial I/R injury worsens systolic cardiac function, suggesting that this cytokine plays a protective role in the long-term development of I/R injury (46).

1.3 Pro-survival pathways against the development of myocardial I/R injury

It has been demonstrated that the activation of specific cardioprotective pathways during reperfusion can attenuate the detrimental effects of myocardial I/R injury. At the onset of reperfusion, cardioprotection can be achieved by activating the reperfusion injury signaling kinase (RISK) pathway (47). This pathway is activated by G-coupled protein receptor ligands and growth factors, and it is formed by two signaling cascades, the phosphoinositide 3-kinase (PI3K)/Akt and the extracellular signal regulated kinase (Erk1/2, also known as p44/p42). Each one of these cascades can be selectively activated; for instance, it has been reported that insulin only activates PI3K/Akt, and that transforming growth factor-β1 (TGF-β1) only recruits Erk1/2 (47).

The activation of both PI3K/Akt and Erk1/2 leads to the phosphorylation and inactivation of pro-apoptotic proteins such as Bcl-2-associated death promoter (BAD), Bax, BIM and p53, and the inhibition of cytochrome c release by Bax-independent mechanisms. Meanwhile, the specific activation of the PI3K/Akt signaling cascade induces the phosphorylation of glycogen synthase kinase-3 (GSK-3β) and endothelial nitric oxide synthase (eNOS), inactivating the former and activating the latter. When GSK-3β is phosphorylated, it binds to ANT, and reduces

the affinity of this protein for cyclophilin D, inhibiting MPTP opening. GSK-3β inhibition also preserves mitochondrial ATP, prevents the overload of mitochondrial Ca^{2+} and decreases ROS formation (48). The activation of eNOS leads to the formation of nitric oxide, which prevents leukocyte adhesion, maintains the integrity of the endothelium (49), and inhibits the opening of the MPTP (50). PI3K/Akt signaling can also phosphorylate and activate the inhibitor of NFκB kinase (IKK)-α, inducing NFκB activation and its translocation to the nucleus (51). Although NFκB is recognized as a trigger of the inflammatory response induced by myocardial I/R injury, its transient activation can promote the transcription of anti-apoptotic proteins such as Bcl-2 (52).

As noted in the previous section, it has been reported that small amounts of TNFα promote cardioprotection against I/R injury. However, this protective effect is maintained even when Akt or Erk1/2 are inhibited, suggesting that this is an alternative cardioprotective pathway (53). This pathway was later defined as the survivor activating factor enhancement (SAFE) pathway, and it is formed by Janus kinase 2 (JAK2) and signal transducer and activator of transcription 3 (STAT3) (54). The JAK/STAT signaling that forms part of the SAFE pathway had been previously related to the development of cardiac hypertrophy, apoptosis and inflammation; however, in the setting of myocardial I/R injury, it appears to have positive outcomes (54). The SAFE pathway regulates cardioprotection by inducing the expression of anti-apoptotic Bcl-2 and down-regulating pro-apoptotic Bax (55), reducing the extent of I/R-induced apoptosis. Even though the SAFE and RISK pathways have shown to be independent from each other, it has been suggested that cross-talk might occur. Serine phosphorylation of STAT3 can be promoted by the p85 regulatory subunit of PI3K, allowing it to form homodimers and achieve a more stable form (56). Additionally, Nguyen et al. (57) showed that after JAK2 binds to PI3K, it is phosphorylated and activated by Akt.

A vast amount of research has been conducted in order to find pharmacological agents and techniques that promote the activation of these prosurvival pathways. Some of these agents have seemed promising, although the positive preclinical results have not always translated into positive clinical outcomes. For example, glucose-insulin-potassium administration, which is known to activate PI3K/Akt, consistently decreased infarct size in animal models of myocardial I/R injury (58, 59). Nonetheless, randomized clinical trials showed no significant differences between treated and untreated patients (60, 61). However, other pharmacological therapies such as exenatide, a glucagon-like peptide analog that also activates the RISK pathway, have shown cardioprotective properties against the development of I/R injury in both animal models (62) and clinical trials (63). Furthermore, although the precise mechanism is not completely clear, both ischemic preconditioning (53, 64) and postconditioning (65, 66) are known to exert their cardioprotective effects by activating the RISK and SAFE pathways. Nonetheless, it should be pointed out that none of these pharmacological or mechanical therapies have been transferred to clinical practice, and that the presence of comorbidities may interfere with the cardioprotective mechanisms of these phenomena (9).

1.4 The role of diabetes during myocardial I/R injury

1.4.1 Diabetes mellitus

Diabetes mellitus is a metabolic disorder characterized by hyperglycemia due to deficient insulin secretion, deficient insulin action or both. Chronic hyperglycemia in diabetic patients leads to the development of microvascular complications that notably affect the eyes, kidneys and nerves, and the overall risk of cardiovascular disease is much higher in those with diabetes than in non-diabetics. In 2015, the International Diabetes Federation estimated that 415 million

adults in the world suffer from diabetes (67). Even though the prevalence of diabetes is much higher in developing countries, Canada has seen a drastic increase in its incidence. In 2009, 6.8% of the population was diabetic, representing a 230% increase since 1998 (68). Diabetes can be classified into several types, the most common being type 1 diabetes, type 2 diabetes, and gestational diabetes mellitus (68). Other types of specific diabetes, such as those derived from genetic conditions or drug use, have been identified, but their prevalence is much lower (68).

Type 1 diabetes is an autoimmune disease characterized by the destruction of pancreatic beta cells. Since these cells are the ones that produce insulin, hyperglycemia is induced. Patients with this type of diabetes produce islet autoantibodies that promote the accumulation of islet-specific T cells that recognize and destroy beta cells (69). Growing evidence shows that this process is triggered by environmental factors in patients with a genetic predisposition. Therefore, it is believed that the modern pro-inflammatory environment is one of the main causes of the increase in the incidence of type 1 diabetes in the last 50 years (70). Compared to the rest of the world, countries of European descent have a higher prevalence of type 1 diabetes, and this condition is normally diagnosed during childhood. Of all children that develop this type of diabetes by the age of 18, 80% have detectable autoantibodies before they are 3 years old (70). Lifelong insulin therapy is required to treat type 1 diabetes, and frequent blood glucose self-monitoring is necessary. Type 1 diabetes is also distinguished by its proclivity for ketoacidosis, due to the lack of insulin (68).

Type 2 diabetes is characterized by different degrees of insulin resistance and insulin deficiency, and is by far the most common form, representing 90-95% of all cases (71). Many risk factors have been associated with the development of type 2 diabetes: a sedentary lifestyle, lack of physical activity, obesity, smoking, advanced age, genetic predisposition, and a low fiber

diet with a high glycemic index (71). The progression of type 2 diabetes is characterized by an initial state of insulin resistance, which can be caused by lipotoxicity, inflammation, glucotoxicity and mitochondrial dysfunction (72). Insulin resistance is compensated by an overproduction of insulin by the pancreatic beta cells, in order to maintain normal glucose levels. However, as insulin resistance increases, beta cells gradually decline in function, resulting in impaired glucose tolerance. Eventually, beta cells become exhausted, and this leads to patent diabetes and elevated glucose levels (73).

Gestational diabetes mellitus is a condition suffered by pregnant women characterized by the presence of glucose intolerance (68). As pregnancy progresses, insulin requirements become higher in both healthy women and those with gestational diabetes mellitus. However, women with gestational diabetes mellitus have a reduced insulin response to nutrients, and therefore develop hyperglycemia (74). It has been suggested that inadequate beta cell function is one of the underlying causes of gestational diabetes mellitus. The beta cells of healthy pregnant women undergo a series of changes so that the higher demand for insulin is met. For instance, glucose-stimulated insulin secretion is increased. However, in women with gestational diabetes, beta cells are incapable of adapting (75). When controlled, this type of diabetes ceases at the end of pregnancy; nonetheless, women who have previously suffered gestational diabetes mellitus have a higher risk of developing it in later pregnancies. If untreated, it may lead to an increase in maternal and perinatal morbidity (68).

In order to diagnose someone as diabetic, at least one of the following criteria should be met: 1) a fasting plasma glucose higher than 7.0 mM, 2) a 2 hour-plasma glucose higher than 11.1 mM in a 75 g oral glucose tolerance test, or 3) a random plasma glucose higher than 11.1 mM. In adult patients, a glycated hemoglobin (A1C) test can also be performed, and diabetes is

diagnosed when A1C is higher than 6.5% (68). However, this test should not be performed when factors that affect its accuracy are present. For instance, patients with chronic anemia will have falsely low A1C values due to the decreased survival of red blood cells; while patients with suspected type 1 diabetes who commonly present iron deficiency anemia will have falsely elevated A1C values (76).

1.4.2 Diabetes and cardiac disease

Patients with both type 1 and type 2 diabetes are at a significantly high risk of developing cardiovascular disease. In the Framingham study, it was found that the presence of diabetes increases the incidence of cardiovascular disease 2-fold in men and 3-fold in women (77). Furthermore, 68% of diabetic patients over the age of 65 die from heart disease (78), making it the greatest threat to patients suffering from this condition.

Diabetes affects cardiovascular function by increasing the presence of coronary plaques, which later lead to coronary artery disease. This process is mediated by mechanisms stimulated by chronic hyperglycemia, such as the accumulation of ROS, microvascular dysfunction, insulin resistance, enhanced inflammation and the reversed transport of cholesterol (79). Coronary artery disease then translates to ischemic heart disease, making diabetic patients more prone to suffer a myocardial infarction. Their risk of suffering a myocardial infarction for the first time is comparable to the risk of non-diabetic patients with a previous myocardial infarction (80); and according to data obtained in the INTERHEART study, if diabetes were eliminated, the rate of myocardial infarction would decrease by 19.1% for women and 10.1% for men (81).

The presence of diabetes can also impair cardiac function independently of changes in vascular function, coronary artery disease or hypertension. This cardiac disease is known as

diabetic cardiomyopathy, and it is characterized by three clinical stages: 1) patients develop an asymptomatic left ventricular diastolic dysfunction, that can be detected by tissue Doppler imaging or conventional Doppler echocardiography, 2) diastolic dysfunction is evident and early signs of systolic dysfunction can be detected with echocardiography, 3) the heart has developed hypertrophy and both diastolic and systolic dysfunction are present, leading to heart failure (79, 82). Diabetic cardiomyopathy is induced by hyperglycemia, hyperinsulinemia and insulin resistance, as well as the metabolic shift from glucose to fatty acid oxidation (83).

1.4.3 Diabetes and myocardial I/R injury

The increased incidence of myocardial infarction in diabetic patients makes them more prone to experience myocardial I/R injury. Moreover, the outcomes of this procedure are much worse under diabetic conditions. When reperfusion is performed by either percutaneous coronary intervention or thrombolytic therapy, diabetic patients have larger infarcts, lower ejection fraction, and greater mortality (84, 85). The mechanisms that lead to an increased susceptibility of the diabetic heart to I/R injury remain to be fully elucidated. However, two main factors are known to play an important role: the increased levels of oxidative stress, and the exacerbated inflammatory response (86, 87).

Oxidative stress is one of the principal causes of all diabetes complications. In the diabetic heart subjected to I/R injury, increased oxidative stress is due to a higher basal production of ROS and/or the depletion of the antioxidant defense system (88). A large part of hyperglycemia-induced ROS overproduction takes place in the mitochondria (89). In normal conditions, nicotinamide adenine dinucleotide (NADH), a reducing agent, and pyruvate, are generated by glycolysis in the cytoplasm. The oxidation of pyruvate then produces other four

molecules of NADH and a molecule of flavin adenine dinucleotide ($FADH_2$). NADH and $FADH_2$ donate electrons to complexes I and II of the electron transport chain, respectively. The transfer of these electrons generates a mitochondrial membrane potential that drives ATP synthase, allowing the production of ATP (87). However, under hyperglycemic conditions, the formation of NADH and $FADH_2$ is significantly increased, and the mitochondrial membrane potential generated is much higher. This increases the half-life of electron transport intermediates, such as ubisemiquinone, which produce high amounts of O_2^- (87, 90).

The production of ROS under diabetic conditions can also be modulated by non-mitochondrial mechanisms. For instance, the activity of nicotinamide adenine dinucleotide phosphate (NADPH) oxidase, an enzyme located in the membrane of intracellular organelles, is much higher in the diabetic myocardium (91, 92). NADPH oxidase promotes the formation of O_2^- by transferring NADPH electrons to molecular oxygen; therefore, its increased activity becomes deleterious for cell function (93). Similarly, xanthine oxidase, an enzyme that promotes ROS production by catalyzing the oxidation of hypoxanthine to xanthine and its subsequent conversion to uric acid, is overactivated during hyperglycemia (94). Furthermore, the activity of nitric oxide synthase, which stimulates the production of O_2^-, is also uncoupled during diabetes (94).

The diabetes-induced depletion of the antioxidant system causes a further increase in oxidative stress. For example, under hyperglycemic conditions, superoxide dismutase 2 (SOD2) activity is significantly decreased, and in compensation, superoxide dismutase 1 (SOD1) increases its activity. Both SOD1 and SOD2 form H_2O_2 from O_2^-, which is then converted to water by glutathione peroxidase or catalase. However, the depletion of these last two antioxidant enzymes and the increased activity of SOD1, translates into H_2O_2 accumulation, which increases

oxidative stress (87). This depletion of the antioxidant system has also been detected in diabetic patients (95).

The diabetes-induced accumulation of ROS can then activate several deleterious mechanisms. For example, high levels of ROS lead to the activation of the polyol pathway, which reduces carbonyl compounds to their polyol form using NADPH. However, since NADPH is required for the regeneration of reduced glutathione, a major scavenger of ROS, its overconsumption exacerbates oxidative stress (89). The ROS-induced inhibition of glycolysis also promotes the formation of diacylglycerol, a metabolite capable of activating protein kinase C (PKC). Overactivation of PKC due to hyperglycemia has been linked to decreased eNOS activity (96). Therefore, the levels of endothelium-derived nitric oxide, a molecule known to preserve vascular homeostasis, are lower in the presence of diabetes (97). It has been suggested that in hyperglycemic conditions, PKC phosphorylates PI3K at Thr86, decreasing its insulin induced-activation (98). Therefore, eNOS, as a downstream target of PI3K/Akt, is inactivated by the hyperglycemia-induced overactivation of PKC (98). Furthermore, PKC-β2, an isoform of PKC, has been implicated in the development of myocardial I/R injury under diabetic conditions, via caveolin-3/Akt signaling (99). Liu et al. (99) showed that PKC-β2 inhibits caveolin-3, a structural membrane protein required to maintain the integrity of cardiomyocyte caveolae. Since the knockdown of caveolin-3 inactivated Akt, a kinase involved in cardioprotective mechanisms against I/R injury, the authors suggested that both proteins were affected by hyperglycemia-induced PKC-β2 overactivation (99).

Another mechanism affected by the overload of ROS due to hyperglycemia is the higher production of advanced glycation end-products (AGEs). AGEs are formed by the non-enzymatic reaction of proteins with glucose and other glycating agents. This modification alters the function

of these proteins, affecting their ability to interact with other components and promoting their binding to the receptor for AGEs (RAGE), which then promotes ROS production and NFκB activation (89). During diabetes, the elevated levels of O_2^- inhibit enzymes of the glycolysis pathway, and a higher concentration of glucose and glycating agents is available to form AGEs (100). Moreover, it has been suggested that the activation of RAGE is linked to the development of myocardial I/R injury in the diabetic heart; since diabetic RAGE-knockout mice hearts subjected to *ex vivo* I/R injury show improved cardiac function compared to their WT counterparts (101).

Under hyperglycemic conditions, basal inflammation is also higher. It has been reported that hyperglycemia increases the level of circulating pro-inflammatory cytokines such TNFα and IL-6 (102), and that high levels of TNFα affect both insulin signaling and secretion (103). Furthermore, diabetes also promotes leukocyte production and the infiltration of neutrophils (104). Therefore, under diabetic conditions, the inflammatory response is constantly activated, leaving diabetic patients in a state of chronic inflammation. The mechanisms that lead to chronic inflammation under diabetic conditions have not been fully elucidated. However, it has been suggested that the overproduction of ROS induced by hyperglycemia activates IKK/NFκB, the NH_2-terminal Jun kinases/stress-activated protein kinases (JNK/SAPK) and the p38 MAPK pro-inflammatory pathways (105). These pathways affect insulin signaling by altering the phosphorylation of the insulin receptor and/or the insulin receptor substrate (IRS) (105). When I/R injury is induced in the diabetic heart, an exacerbated inflammatory response is triggered. For instance, it has been suggested that in diabetic hearts subjected to I/R injury, leukocyte accumulation, as well as the adhesion of leukocytes to endothelial cells are much higher than in normal conditions (106, 107).

1.4.4 Impairment of pro-survival pathways against I/R injury in the diabetic heart

There is increasing evidence suggesting that cardioprotective mechanisms, such as preconditioning and postconditioning, are not effective against the development of myocardial I/R injury under diabetic conditions (108-110). For instance, it has been reported that in normal rats, one cycle of preconditioning is sufficient to lower infarct size, but in diabetic Goto-Kakizaki rats, a minimum of three cycles is necessary (111). Both preconditioning and postconditioning achieve cardioprotection by activating the RISK and SAFE pathways; however, during diabetes, the activation of these pro-survival pathways is impaired (112).

The abrogation of the RISK pathway and its PI3K/Akt signaling cascade plays an important role in the susceptibility of the diabetic heart to I/R injury. There are many reports supporting the concept that Akt inactivation is linked to the increase in cardiac damage observed in models of both type 1 (99, 113, 114) and type 2 diabetes (111, 115). Several mechanisms have been suggested, but two appear to be most important: the deficiency of insulin action or secretion, and the activation of phosphatase and tensin homolog deleted on chromosome 10 (PTEN) (87).

It has been reported that the administration of insulin before (116) or shortly after reperfusion (117), protects the heart against the development of I/R injury via activating PI3K/Akt signaling. However, in type 1 and type 2 diabetes, the activation of this signaling mechanism is compromised by insulin resistance, leading to a decrease in Akt activity and therefore an increase of cardiac damage. PTEN, on the other hand, counteracts the activity of the PI3K/Akt signaling cascade. In its active form, PI3K phosphorylates phosphatidylinositol (3,4)-biphosphate (PIP2) and generates phosphatidylinositol (3,4,5)-trisphosphate (PIP3). PIP3 serves

as a plasma membrane docking site for proteins that have a pleckstrin-homology (PH) domain, such as phosphoinositide-dependent protein kinase-1 (PDK1) and Akt. In the presence of PIP3, Akt is recruited to the plasma membrane where it is phosphorylated and activated by PDK1 (118). However, PTEN is able to dephosphorylate PIP3, converting it to PIP2 (119). Compared to their normal counterparts, the hearts of diabetic Goto-Kakizaki rats exhibit a higher level of PTEN expression (120), and it has been suggested that this increase is responsible for the loss of the cardioprotective activity of postconditioning during diabetes (121).

Less research has been done on the effects of diabetes on the SAFE pathway and its main component, the JAK2/STAT3 signaling cascade. However, there is some evidence suggesting that the activation of this prosurvival pathway is abrogated under hyperglycemic conditions. Hotta et al. (122) reported that in diabetic rats subjected to myocardial I/R injury, treatment with valsartan, an angiotensin II type 1 (AT1) receptor blocker, restored calcineurin and erythropoietin-induced JAK2 activity. Therefore, the authors suggested that diabetes-induced AT1 receptor-mediated upregulation of calcineurin impairs JAK2 signaling (122). It has also been reported that the decrease of STAT3 activity in diabetic rat hearts subjected to *ex vivo* I/R injury is regulated by the activation of mammalian target of rapamycin (mTOR) (123). Furthermore, STAT3 has been implicated in the hyperglycemia-induced loss of cardioprotection of ischemic postconditioning (124).

1.5 Rho kinase and its role in cardiovascular disease and myocardial I/R injury

1.5.1 Rho kinase

Rho kinases (ROCKs) are serine/threonine kinases involved in a wide range of physiological functions, such as smooth muscle contraction, cell migration, adhesion and

motility. The ROCK kinase domain is located towards the amino terminus, while a coiled-coil region contains other functional motifs such as the Rho-binding domain, the PH domain and the cysteine-rich domain (Fig 1.2) (125). The two isoforms of ROCK that have been detected, Rho kinase 1 (ROCK1) and Rho kinase 2 (ROCK2), are highly homologous, sharing an overall amino acid identity of 65%, and an identity of 92% at the kinase domain (126). ROCK1 is widely expressed in all human tissues except brain and muscle, while ROCK2 is mainly found in brain, muscle, heart, lungs and placenta (127).

ROCK is the major downstream effector of RhoA, a small guanosine-5'-triphosphate (GTP)-binding protein activated by the stimulation of G-protein coupled receptors and tyrosine kinase (126). In their inactive state, ROCK keeps a closed autoinhibitory loop by binding the amino terminus to the Rho-binding and the PH domains. But when RhoA is activated by GTP-binding, it attaches to the Rho-binding domain, opening the autoinhibitory loop and exposing the kinase domain (Fig 1.2) (125). Both ROCK isoforms are also activated by arachidonic acid, which binds to the PH domain (126), and ROCK1 and ROCK2 can be selectively activated by caspase-3 and granzyme-B, respectively, by cleaving the carboxyl terminus and uncovering the kinase domain (128) (Fig 1.2).

Mechanisms of ROCK inhibition have also been reported. RhoE inhibits ROCK1 by preventing RhoA from binding the Rho-binding domain (125), while ROCK1 and ROCK2 are inhibited by small G-proteins Gem and Rad, respectively, by an unknown mechanism (129). Additionally, ROCK activity can be regulated by phosphorylation (130, 131), and it was recently reported that autophosphorylation at Ser1366 reflects the activation status of this protein (132).

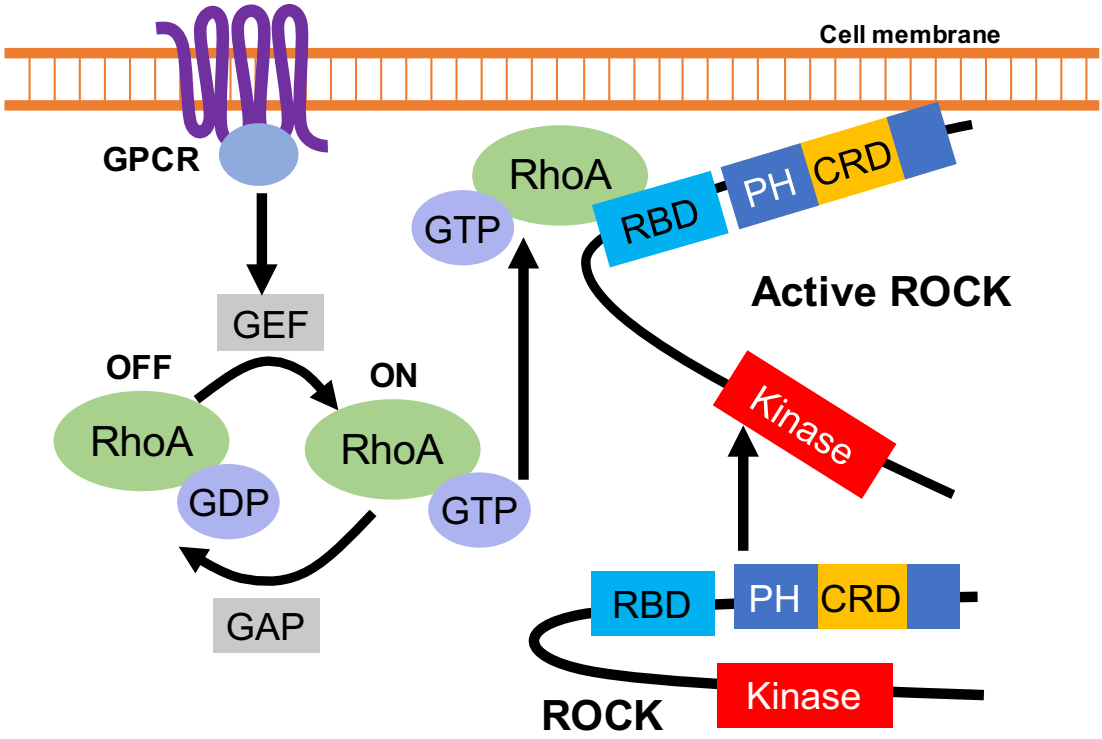

Figure 1.2 Structure and activation of ROCK

ROCK is formed by an amino terminus, where a kinase domain is located, and a coiled-coil region, that contains the Rho-binding domain (RBD) and the PH domain, where the cysteine-rich domain can be found. In its inactive form, ROCK forms a closed autoinhibitory loop by binding the amino terminus to the PH domain. The main activator of ROCK, RhoA, is a small G-protein that is activated when bound to GTP, and deactivated when bound to guanosine 5′-diphosphate (GDP). In order to switch from one state to another, GTPase-activating proteins (GAPs) and guanine nucleotide exchange factors (GEFs) regulate the activity of RhoA. GEFs, activated by G-protein coupled receptor activation, activate RhoA by promoting the exchange of GDP for GTP, while GAPs promote the hydrolysis of GTP. When RhoA is activated by GTP-binding, it attaches to the RBD, opening the autoinhibitory loop and exposing the kinase domain (125).

ROCK phosphorylates more than 30 downstream substrates at the consensus amino acid sequences R/KXS/T and R/KXXS/T (R: arginine, K: lysine, X: any amino acid, S: serine, T: threonine). Myosin phosphatase targeting protein (MYPT) is one of the most relevant ones (125, 133). This protein is a subunit of myosin light chain phosphatase (MLCP), an enzyme that dephosphorylates the light chain of myosin II and promotes smooth muscle relaxation. When MYPT is phosphorylated by ROCK, MLCP is inhibited, stimulating smooth muscle contraction (133). However, ROCK1 and ROCK2 activate MYPT by different mechanisms. Only ROCK2 is able to bind directly and phosphorylate MYPT, while ROCK1 requires intermediaries (134). Other downstream substrates of ROCK are LIM-Kinase (LIMK), adducin and ezrin-radixin-moesin (ERM) (125). ROCK-activated LIMK phosphorylates and inactivates cofilin, a protein that promotes actin depolymerization and actin filament turnover (135). Adducin, activated by ROCK phosphorylation, binds to actin filaments and promotes the association of actin to spectrin, a mechanism that plays an important role in membrane ruffling and cell motility (136). ERM, phosphorylated and activated by ROCK, promotes the crosslinking of transmembrane proteins to F-actin (137).

1.5.2 Rho kinase in cardiovascular disease and diabetes

Even though ROCK is involved in many basic cellular processes, its overactivation has been linked to the pathogenesis of several cardiovascular diseases. In some cases, each isoform has a different role in the development of these conditions. For instance, it has been reported that ROCK inhibition reduces the extent of cardiac hypertrophy induced by G-protein-coupled receptor agonists, such as angiotensin II, and endothelin-1 (138-140). However, further research suggested, that ROCK2, but not ROCK1, was involved in the development of angiotensin II-

induced hypertrophy (141). Compared to their ROCK2-expressing counterparts, the induction of hypertrophy by angiotensin II infusion or transverse aortic constriction (TAC) resulted in a smaller heart-to-body weight ratio and a lower left ventricular mass in cardiac-specific ROCK2-knockout mice (142). TAC-induced fibrosis and cardiac remodeling are also significantly reduced by ROCK inhibition (143), and the results from studies using knockout mice have revealed that ROCK1 is the isoform involved in this mechanism (141, 144, 145).

The inhibition of ROCK can also reduce the inflammatory process that takes place in atherosclerosis. In a model of mice deficient in low-density lipoprotein receptor (LDLR-/-), Y-27632, a non-isoform selective ROCK inhibitor, reduced inflammation and the infiltration of T-lymphocytes promoted by this condition (146). Similar results were observed when the bone marrow of ROCK1 and ROCK2 knockout mice was transplanted to LDLR-/- mice, suggesting that both isoforms are involved in this process. However, each one of them acted by a different mechanism and had different functions (147, 148). ROCK has also been implicated in the development of hypertension. The treatment of this condition by non-isoform specific inhibitors such as Y-27632 and fasudil has successfully lowered blood pressure (149-151), although the role of each ROCK isoform is less clear.

Since a large proportion of patients with cardiac complications also have type 1 or type 2 diabetes, it is important to understand how these conditions might affect the role of ROCK in the development of cardiovascular diseases. For instance, it has been reported that in a rat model of type 2 diabetes, ROCK inhibition reduces the extent of myocardial fibrosis by inhibiting JNK and TGF-β1 (152). Also, it has been suggested that an increase in ROCK expression at an early stage of type 1 diabetes contributes to the development of coronary dysfunction (153), and that in a type 2 diabetic model, ROCK contributes to the increase of blood pressure (154).

ROCK has also been implicated in the development of diabetic cardiomyopathy and the cardiac abnormalities characteristic of this disease. In type 1 diabetic mice, ROCK inhibition improved both *ex vivo* and *in vivo* cardiac function, in association with attenuation of actin polymerization (155). A subsequent study showed that, under diabetic conditions, ROCK inhibition attenuated PKCβ2 and iNOS activity, and that the inhibition of PKC-β2 and iNOS normalized the hyperglycemia-induced overactivation of both RhoA and ROCK, suggesting that RhoA/ROCK, PKCβ2 and iNOS interact in a positive feedback loop that promotes the development of diabetic cardiomyopathy (156). Furthermore, it was later determined that ROCK2 is the isoform involved in this process, given its ability to directly phosphorylate and activate PKCβ2, interfering with the PDK1-mediated phosphorylation of Akt (157).

1.5.3 Rho kinase and myocardial I/R injury

ROCK has also been implicated in the development of myocardial I/R injury. Bao et al. (158) were the first to suggest that ROCK had a role in the development of myocardial I/R injury. They reported that in an *in vivo* mouse model of myocardial I/R injury, the expression of RhoA and ROCK activity in the ischemic heart were increased. Furthermore, Y-27632, a non-isoform selective ROCK inhibitor, had a cardioprotective effect on hearts subjected to myocardial I/R injury. They proposed that the cardioprotective effect of Y-27632 was mediated by anti-apoptotic mechanisms, since Bcl-2 was downregulated during I/R injury and upregulated when ROCK was inhibited. Necrosis was also inhibited, and inflammatory mechanisms such as neutrophil infiltration and cytokine and chemokine production were affected by ROCK inhibition. Similarly, Wolfrum et al. (159) reported that fasudil, another non-isoform selective ROCK inhibitor, exhibited cardioprotective activity in an *in vivo* rat model of myocardial I/R.

The administration of hydroxyfasudil increased the activity and phosphorylation of Akt. Since this process was blocked by the inhibition of PI3K, the authors were able to confirm that ROCK inhibition promoted the activation of PI3K/Akt signaling.

Hamid et al. (160) confirmed that the effects of ROCK during myocardial I/R injury in an *ex vivo* rat model were mediated by the inhibition of elements of the RISK pathway. Furthermore, they demonstrated that ROCK was activated during early reperfusion and not during ischemia, suggesting that this protein has a highly significant role in the development of myocardial I/R injury. On the other hand, Li et al. (161) reported that the cardioprotective mechanism triggered by ROCK inhibition was different depending on the stage of reperfusion. They confirmed in an *in vivo* rat model that the PI3K/Akt signaling cascade of the RISK pathway was activated with fasudil at an early stage, but not at a late phase of reperfusion. They suggested that at this later stage, ROCK inhibition activated JAK2/STAT3 signaling from the SAFE pathway instead. Also, they demonstrated that the I/R-induced increase of caspase-3 activity is also attenuated by fasudil treatment.

Although Bao et al. (158) had previously shown that I/R-induced neutrophil infiltration is affected by ROCK inhibition, Kitano et al. (162) evaluated the mechanism involved in this process. Using an *in vivo* mouse model of I/R injury, they observed that fasudil administration reduced I/R-induced leukocyte accumulation, and that this was correlated with a reduction of pro-inflammatory cytokines in serum. Moreover, the mRNA production of IL-6, MCP-1 and TNFα was significantly lower in the cardiac tissue and leukocytes of mice treated with fasudil (162).

Even though these reports provide a better understanding of the role of ROCK in the development of myocardial I/R injury, none of them investigated the specific role of either one

of the two ROCK isoforms. Until a couple of years ago, isoform-specific ROCK inhibitors were not commercially available, making this a complicated task. In order to assess the contribution of each ROCK isoform, transgenic knockout models need to be used. Because of the relevant progress that has been done assessing the role of ROCK1 and ROCK2 in other cardiovascular diseases, it is of importance to investigate their individual contributions in myocardial I/R injury. Furthermore, the effect of ROCK inhibition in the development of I/R injury in the presence of comorbidities, such as diabetes, has not been evaluated. Due to the prevalence of myocardial I/R injury in diabetic patients, it is crucial to determine whether diabetes affects the cardioprotective activity of ROCK inhibition.

Whether ROCK1, ROCK2 or both isoforms are responsible for the development of myocardial I/R injury in normal and diabetic conditions is not known. However, since recent results from our research group indicate that the expression of ROCK2 but not ROCK1 is elevated in type 1 diabetic hearts (157), we are currently focused on the activity of this ROCK isoform. Therefore, this thesis work will focus on understanding the role of ROCK2 in the development of myocardial I/R injury in the absence and presence of type 1 diabetes.

1.6 Experimental models of myocardial I/R injury and type 1 diabetes

In order to understand the role of a protein or a pharmacological agent in the development of myocardial I/R injury, the proper experimental model should be selected. The three main types of models of I/R injury reported in the literature are *in vitro*, *ex vivo* and *in vivo* models. In the *in vitro* model of myocardial I/R injury (also known as simulated I/R injury or hypoxia-reoxygenation) cultured cells are first exposed to conditions that simulate ischemia: low levels or absence of oxygen, slightly acidic media, and low glucose. After a period of time, they

return to normoxic conditions and normal cell culture media is provided. This model provides a limited understanding of the complex dynamics between different types of cells that take place in I/R injury. Nonetheless, the *in vitro* model is useful in scenarios where genetic effects or complex mechanistic relationships need to be studied (163).

In the *ex vivo* model of myocardial I/R injury, isolated hearts are first subjected to global or regional ischemia and then returned to normal perfusion. This can be done either by Langendorff perfusion, where the aorta is cannulated and perfused in a retrograde manner, or using the isolated working heart, where perfusion starts from the left atrium and exits the aorta, mimicking the normal perfusion of the heart. In both types of *ex vivo* myocardial I/R injury, a physiologic solution such as the Krebs-Hensleit buffer, replaces blood, and constant pressure or flow may be instituted. An *ex vivo* isolated heart system allows the measurement of cardiac contractile function without the interference of other organ systems, systemic circulation or neuronal regulation (164). However, this is a non-physiological model, which can be a limitation if the systemic effects of myocardial I/R injury need to be assessed. In this case, an *in vivo* model should be used. The transient ligation of the left anterior descending (LAD) coronary artery is the most common model of *in vivo* myocardial I/R injury, and it is normally performed by a left thoracotomy (164). This model has the capacity to evaluate cardiac function, infarct size, protein expression and activity, and the systemic effects of inflammation, allowing a more comprehensive understanding of the development of myocardial I/R injury. Therefore, this was the model used in the present work.

1.7 Experimental models of type 1 diabetes

Type 1 diabetes is an autoimmune condition that targets the destruction of pancreatic beta cells in the islets of Langerhans. Therefore, an animal model of type 1 diabetes should focus on selectively inducing the death of these cells. This can be achieved by the following approaches: induction by autoimmune diabetes, genetic induction, viral induction and chemical induction (165).

Mice that are able to develop autoimmune type 1 diabetes such as the non-obese diabetic (NOD) mice, the bio-breeder (BB) rats and the Lewis rats with a defined MHC haplotype (LEW.1AR1) can be used as an experimental model for this condition (165). All of them develop insulitis due to the infiltration of inflammatory cells to the islets of Langerhans, causing beta cell destruction. Alternatively, non-autoimmune models of genetically induced type 1 diabetes such as the AKITA mouse have also been developed. These mice have a mutation at the *Insulin 2* gene, which causes a defective processing of pro-insulin. Misfolded pro-insulin then aggregates at the endoplasmic reticulum (ER), causing ER stress and beta cell death (166). Due to their characteristics, the autoimmune and the genetically induced type 1 diabetic mice are commonly used in studies that focus on beta cell inflammation and the genetics of this condition. However, neither one of these models of type 1 diabetes are convenient to use if a transgenic model, such as the ROCK2 knockout mice, is already being employed. Type 1 diabetes can also be induced by viral infection, where viruses such as the coxsackie B virus, the encephalomyocarditis virus and the Kilham rat virus are used to promote beta cell destruction (165). Nonetheless, this last method is the most complicated to manage, and therefore the least applied.

The induction of beta cell death by chemical toxicity is one of the most common and affordable methods used to establish a model of type 1 diabetes. Alloxan and streptozotocin

(STZ) are the two drugs normally employed for this purpose. The chemical structure of both drugs is highly similar to glucose, and this characteristic allows them to enter the pancreatic beta cells through the glucose transporter 2 (GLUT2). The pancreas, kidney and liver are the main organs expressing this transporter; however, the last two are better protected against the deleterious effects of alloxan and STZ (166). Therefore, by using a controlled dose, the induction of cell death is beta cell-selective.

Alloxan and STZ lead to cell death by different mechanisms. When alloxan enters the beta cells, it is reduced to dialuric acid by ROS. Dialuric acid can then re-oxidize alloxan, in a process that generates O_2^- and other free radicals. The high level of free radicals damages the DNA, induces its fragmentation and leads to cell death. With doses that range from 50 to 150 mg/kg for rodents, alloxan generates a quick hyperglycemic response. Chronic hyperglycemia can also be generated using this drug; however, there are reports that show that glucose levels can be normalized over time, possibly due to beta cell-regeneration (166). STZ follows several mechanisms that lead to beta cell-destruction. This drug can accumulate inside the cell and form diazomethane, an alkylating product that induces DNA alkylation and promotes cell death. STZ also acts as a nitric oxide donor, promoting DNA damage, and in a very similar mechanism to that of alloxan, it can also stimulate free radical production. This production of free radicals not only causes cell damage directly, but it can also disrupt ATP production and lead to a decrease of insulin synthesis and secretion. Unlike alloxan, STZ has a better toxicity profile, and its beta cell-regeneration incidence is much lower (166). Two different doses of STZ can be used to induce type 1 diabetes: a single high dose and a multiple low dose. A single high dose of STZ induces a high level of DNA damage that translates into to a drastic reduction of ATP levels as well as the loss of membrane integrity, therefore leading to beta cell necrosis (167). For mice, a single high

dose of STZ may range from 100 to 300 mg/kg, and it can lead to hyperglycemia within a few hours. However, mice have high risk of hypoglycemia, as well as renal and hepatic toxicity, shortly after STZ administration. On the other hand, the induction of diabetes by multiple low doses of STZ more closely resembles the development of type 1 diabetes in humans. By administering 20-50 mg/kg STZ to mice over 3 to 5 days, two peaks of beta cell apoptosis can be detected: one at the end of STZ treatment, and another one 11 days later, when lymphocyte-cell infiltration to the islets of Langerhans takes place (167). Multiple low doses of STZ can induce both hyperglycemia and insulitis, and the risk of immediate hypoglycemia is much lower (166).

1.8 Research hypothesis and specific aims

Based on the observations that have been made on the role of ROCK inhibition in myocardial I/R injury, the relevance of evaluating the contribution of the ROCK2 isoform and the importance of understanding how diabetes can affect the response to I/R injury, we proposed to investigate the following hypothesis: *The overactivation of ROCK2 contributes to I/R injury in the normal and diabetic heart.*

In order to test this hypothesis, three specific aims were pursued in the present thesis:

1. Establish an *in vivo* model of myocardial I/R injury in non-diabetic and diabetic conditions:

In order to properly evaluate the role of ROCK2 in the development of myocardial I/R injury, we first evaluated the most appropriate conditions for the research model selected. Two preliminary studies were performed for this purpose. In the first, cardiac function was evaluated in diabetic and non-diabetic mice with a ROCK2 partial deletion. In the second, we developed a protocol of *in vivo* myocardial I/R injury for both control and diabetic mice.

2. Investigate the whole-body and cardiomyocyte-specific contribution of ROCK2 in myocardial I/R injury:

In order to evaluate the role of ROCK2 in the development of myocardial I/R injury, we measured the infarct size of whole-body heterozygous and cardiomyocyte-specific ROCK2 knockout mice subjected to *vivo* myocardial I/R injury. Cardiac function, ROCK activity, the activation of the RISK pathway, and the extent of inflammation were also evaluated.

3. Evaluate the role of cardiomyocyte ROCK2 in the development of myocardial I/R injury in diabetic conditions.

In order to assess the role of ROCK2 in the development of myocardial I/R injury during diabetes, we compared the responses of diabetic and non-diabetic cardiomyocyte-specific ROCK2 knockout mice to the induction of myocardial I/R injury. Infarct size, cardiac function, ROCK activity, the activation of the RISK pathway, and the extent of inflammation were also evaluated in this study.

Chapter 2: Characterization of the myocardial I/R injury *in vivo* model

2.1 Overview

In vivo cardiac studies allow us to not only understand the effects of a specific disease on cardiovascular function and signaling, but also to evaluate its interdependent physiology. In the present thesis, we evaluated the role of ROCK2 in the development of myocardial I/R injury *in vivo* in both non-diabetic and diabetic mice. In order to achieve this, it was first necessary to determine the most appropriate conditions for these experiments.

As mentioned in Chapter 1, selective inhibitors of ROCK2 are not commercially available, so in order to investigate the isoform-specific contribution of ROCK2, it was necessary to use a genetically modified mouse model. Two types of genetically modified mice were available to us: the ROCK2 heterozygous whole-body knockdown (ROCK2+/-) and the tamoxifen-inducible cardiac-specific ROCK2 knockout. The first model enabled us to understand the systemic role of ROCK2 during myocardial I/R injury, as well as the sum of the effects that it had on the many different types of cardiac cells, while the second one allowed us to isolate the role of ROCK2 in the cardiomyocyte.

In order to establish our experimental conditions, we conducted two preliminary studies. In the first one, we evaluated the effect of STZ-induced diabetes on the cardiac function of ROCK2+/- mice. STZ was selected to induce type 1 diabetes given its effectiveness for this purpose. In the second study, we developed an *in vivo* myocardial I/R injury protocol for both control and diabetic mice, and assessed the role of STZ-induced diabetes on the development of I/R injury by measuring cardiac function over the course of 5 weeks.

2.2 Study 1: Evaluation of cardiac function in non-diabetic and diabetic WT and ROCK2+/- mice

2.2.1 Introduction

Mice are one of the most relevant animal models in research; however, each strain has different characteristics that need to be taken into consideration. For instance, CD-1 mice are an outbred strain, meaning that they are more robust and have a greater genetic diversity (168); while C57BL/6J are inbred mice, making them highly genetically similar (169). There are even strains of mice, such as the FVB/N, that have demonstrated cardioprotection against the development of myocardial I/R injury, making them unsuitable for this type of experiment (170).

Furthermore, genetically modified mice might respond in different ways depending on the gene that has been knocked out. Although no major physiological or behavioral changes were found in ROCK2+/- mice (171), when we began this work it was unknown whether partial ROCK2 deletion had a significant effect on cardiac function under either non-diabetic or diabetic conditions. Therefore, the main aim of this study was to evaluate cardiac function in non-diabetic and diabetic WT and ROCK2+/- mice.

2.2.2 Materials and methods

Animals

Homozygous ROCK2 mice (ROCK2-/-) have an embryonic lethality as high as 90%, (171, 172). Therefore, ROCK2+/- mice, provided by Dr. Zhengping Jia, a collaborator at the Faculty of Neurosciences and Mental Health at the University of Toronto, were used in the present thesis. Mice were bred on a CD-1 background; no remarkable differences between them and their WT counterparts have been identified (171).

At 8 weeks of age, male ROCK2+/- and WT mice were treated with STZ (40 mg/ml/day for 3 days) or its citrate buffer vehicle (0.1 M, pH 4.5). This STZ dose was chosen based on preliminary work in our lab showing that it produced a marked increase in blood glucose in CD-1 mice within 2 weeks after administration of the final dose. Eight weeks after STZ treatment, non-fasting blood glucose levels were measured using One Touch Ultra test strips and a One Touch Ultra 2 glucometer (LifeScan, Burnaby, BC, Canada). At all times, mice were housed under identical conditions, and had free access to food and water. Two groups of mice were employed in this study, one for the echocardiographic measurements, and another one for the isolated heart perfusion and western blotting.

This investigation conforms to the Canadian Council on Animal Care Guidelines on the Care and Use of Experimental Animals and the Guide for Care and Use of Laboratory Animals published by the United States National Institutes of Health (NIH publication no. 85–23, revised 1996). All protocols were approved by the University of British Columbia Animal Care Committee.

Echocardiographic measurements

Eight and eleven weeks after STZ or vehicle treatment, systolic cardiac function was assessed in the first group of diabetic and non-diabetic mice using the Vevo 2100 echocardiography system (Fujifilm VisualSonics, Toronto, ON, Canada). In brief, mice were anesthetized using 4-4.5% of isoflurane, and kept at a constant temperature of 37±0.5°C using a heated echocardiography platform. The level of isoflurane was then lowered to 1-2%, and all measurements were done at a heart rate of 500±30 bpm. Mice were positioned at a parasternal

short-axis view, and 2-D M-mode scans were obtained in order to calculate ejection fraction, fractional shortening, cardiac output, and left ventricular (LV) mass.

Heart perfusion and western blotting

The original purpose of the second group of mice was to assess the effect of I/R injury *ex vivo* in non-diabetic and diabetic mice. To this end, 16 weeks after STZ or vehicle treatment, mice were deeply anesthetized with 4% isoflurane, and euthanized by cervical dislocation. Hearts were quickly excised and perfused in the Langendorff mode with Krebs-Henseleit buffer (118 mM NaCl, 4.7 mM KCl, 1.2 mM $MgSO_4$, 1.2 mM KH_2PO_4, 25 mM $NaHCO_3$, 2.5 mM $CaCl_2$, 0.05 mM EDTA, 0.5 mM sodium pyruvate, and 11 mM glucose, pH 7.4, bubbled with 95% O_2 and 5% CO_2). Hearts were stabilized for 10 minutes, and in order to simulate ischemia, the perfusion line was closed for 20 minutes. Reperfusion was then allowed by re-opening the perfusion line, and 40 minutes later, hearts were removed and snap frozen in liquid nitrogen.

Cardiac function following induction of myocardial I/R injury *ex vivo* was highly variable, making it very difficult to evaluate the effects of either partial deletion of ROCK2 or of diabetes. As a result, we decided to not pursue this model further. However, the hearts were used to evaluate the effect of STZ-induced diabetes on ROCK1 and ROCK2 expression levels in ROCK2+/- hearts and their WT counterparts. In brief, frozen tissues were homogenized in RIPA buffer (Tris HCl 50 mM pH 7.4, NP-40 1%, SDS 0.1%, sodium deoxycholate 0.5%, NaCl 150 mM, EDTA 2 mM and protease and phosphatase inhibitor), Laemmli buffer was added (2x), and samples were heated at 95° for 5 minutes. Proteins were separated using 8% SDS-PAGE gels and immunoblotted using ROCK2 primary antibody (Santa Cruz Biotechnology, Santa Cruz, CA). GAPDH (Santa Cruz Biotechnology, Santa Cruz, CA) protein expression was used as a

loading control. Membranes were then stripped and re-probed for ROCK1 (BD Biosciences, Franklin Lakes, NJ). ImageJ v1.46r (NIH, Bethesda, MD) was used to perform densitometry.

Statistical analysis

All results are expressed as means ± standard error (SE), and n represents the number of animals in each group. GraphPad Prism version 5.00 for Mac (GraphPad Software, San Diego, CA) was used to analyze for statistical significance ($p<0.05$) using one-way ANOVA followed by Neuman-Keuls test.

2.2.3 Results

Eight weeks after vehicle treatment, there were no significant differences in the body weight of non-diabetic ROCK2+/- mice and that of their WT counterparts (Fig 2.1A). Similarly, the non-fasting blood glucose level of non-diabetic mice of both genotypes was comparable (Fig 2.1B). Eight week-diabetic ROCK2+/- and WT mice had a significantly lower body weight compared to their control counterparts; however, no differences were detected between the two genotypes (Fig 2.1A). As expected, non-fasting blood glucose levels were much higher in diabetic mice, but there were no differences between the diabetic ROCK2+/- and WT mice (Fig 2.1B). These results indicate that the partial deletion of ROCK2 does not have an effect on the decrease of body weight and the increase of non-fasting blood glucose induced by STZ treatment.

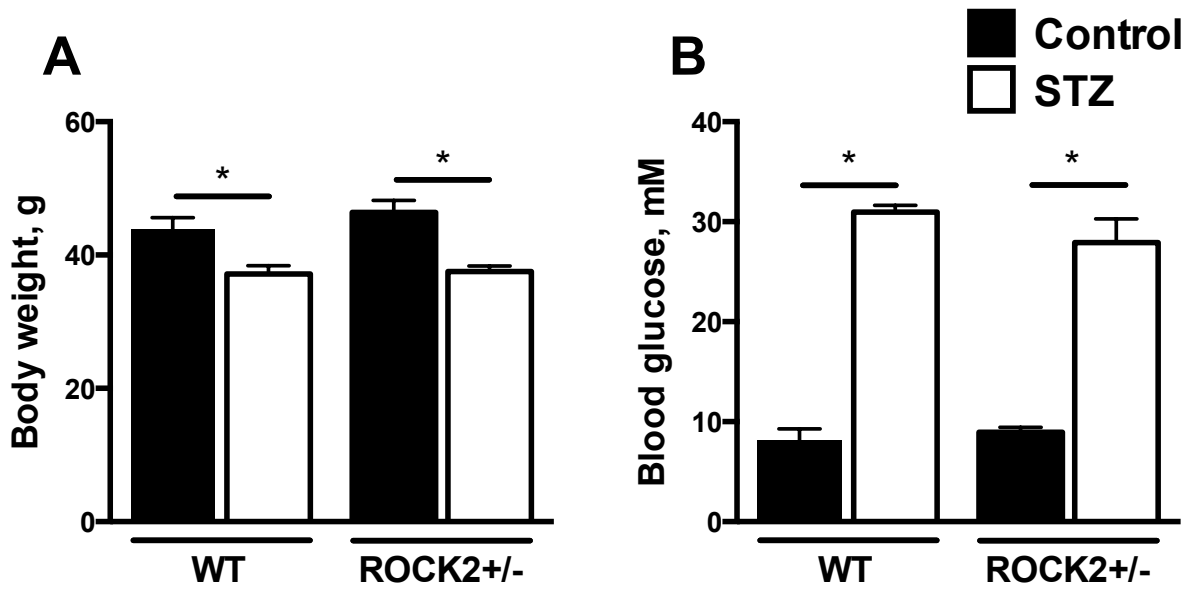

Figure 2.1 Physiologic parameters of ROCK2+/- and WT mice 8 weeks after STZ treatment.

Body weight (A) and non-fasting blood glucose levels (B) of ROCK2+/- and WT mice 8 weeks after STZ treatment (n=4-5, * $p<0.05$).

At both 8 (Fig 2.2) and 11 (Fig 2.3) weeks after vehicle treatment, no significant differences in ejection fraction, fractional shortening, cardiac output, or LV mass were found between non-diabetic ROCK2+/- mice and their WT counterparts, indicating that partial deletion of ROCK2 does not impair systolic cardiac function. Furthermore, both 8 (Fig 2.2) and 11 (Fig 2.3) weeks after induction of diabetes, the ejection fraction, fractional shortening, cardiac output, and LV mass of diabetic WT mice were similar to those observed in their non-diabetic counterparts, suggesting that even after a long period of hyperglycemia, the systolic cardiac function of WT CD-1 mice is not significantly affected. Similarly, no significant differences in systolic cardiac function were detected between diabetic ROCK2+/- mice and their WT counterparts.

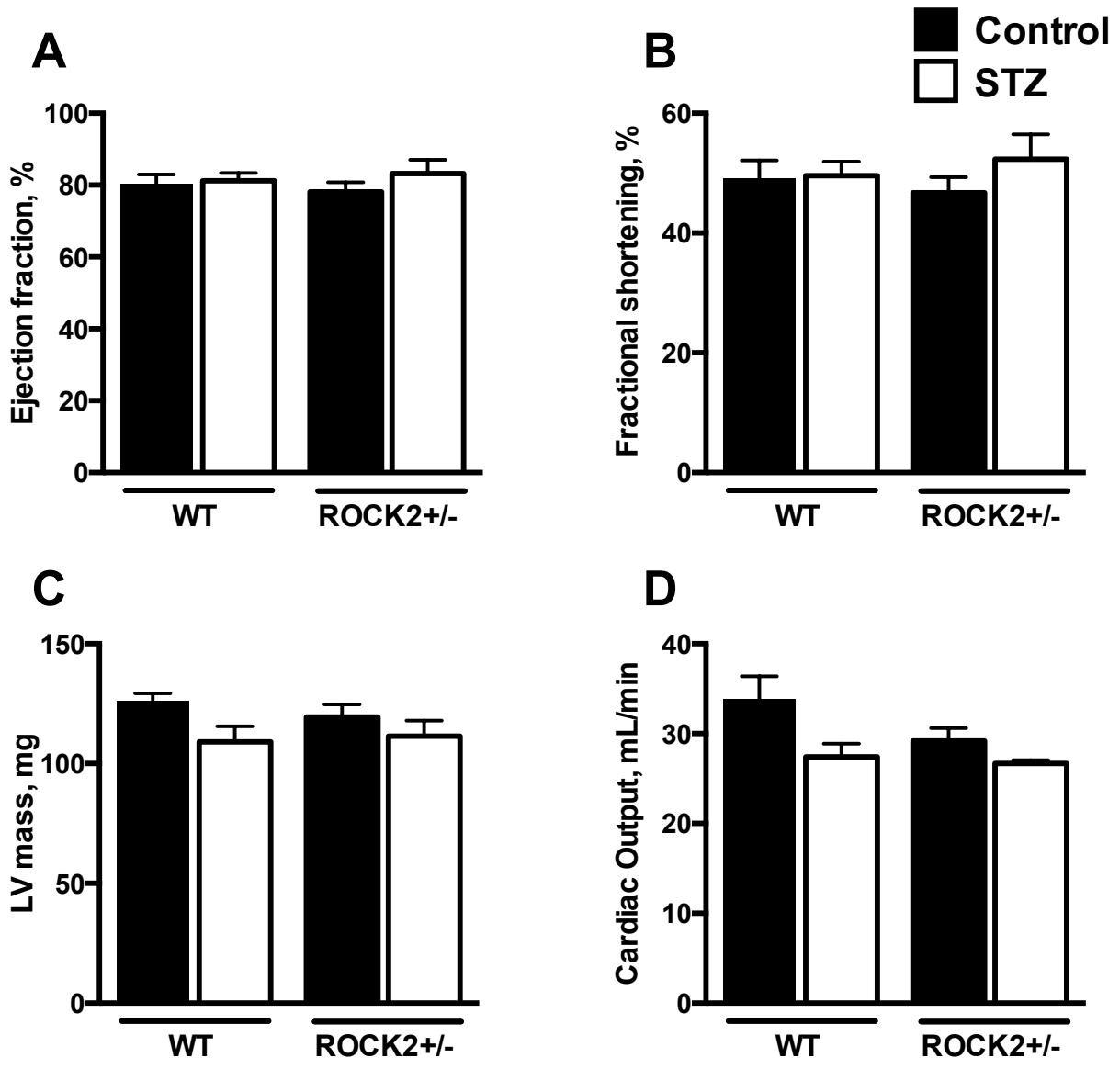

Figure 2.2 Cardiac parameters of ROCK2+/- and WT mice 8 weeks after STZ treatment.

Ejection fraction (A), fractional shortening (B), LV mass corrected (C) and cardiac output (D) were determined using 2-D M-mode (n=4-5, $p>0.05$).

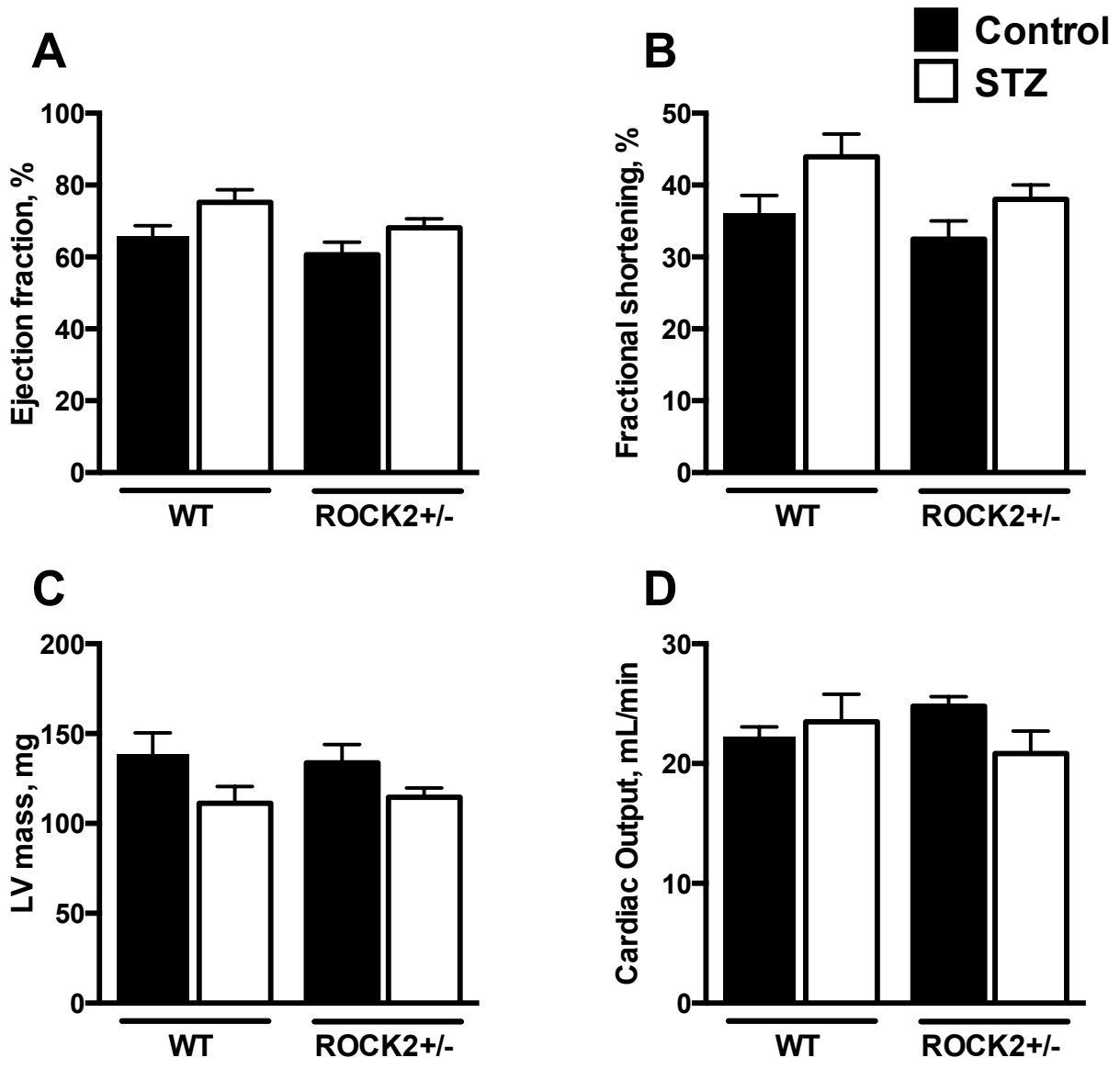

Figure 2.3 Cardiac parameters of ROCK2+/- and WT mice 11 weeks after STZ treatment.

Ejection fraction (A), fractional shortening (B), LV mass corrected (C) and cardiac output (D) were determined using 2-D M-mode (n=4-5, $p>0.05$).

As expected, ROCK2 expression was significantly lower in isolated non-diabetic ROCK2+/- hearts than in their WT counterparts (Fig 2.4A). In hearts from diabetic WT mice, there was a significant increase in ROCK2 expression, but no corresponding differences were detected between diabetic ROCK2+/- hearts and their non-diabetic counterparts (Fig 2.4A). These results suggest that the diabetes-induced increase in ROCK2 expression in the heart is avoided by the partial deletion of ROCK2. ROCK1 expression was similar among groups (Fig 2.4B), suggesting that in this model, the induction of diabetes does not have an effect on ROCK1 expression, and that the knockdown of ROCK2 does not cause a compensatory upregulation of this other isoform.

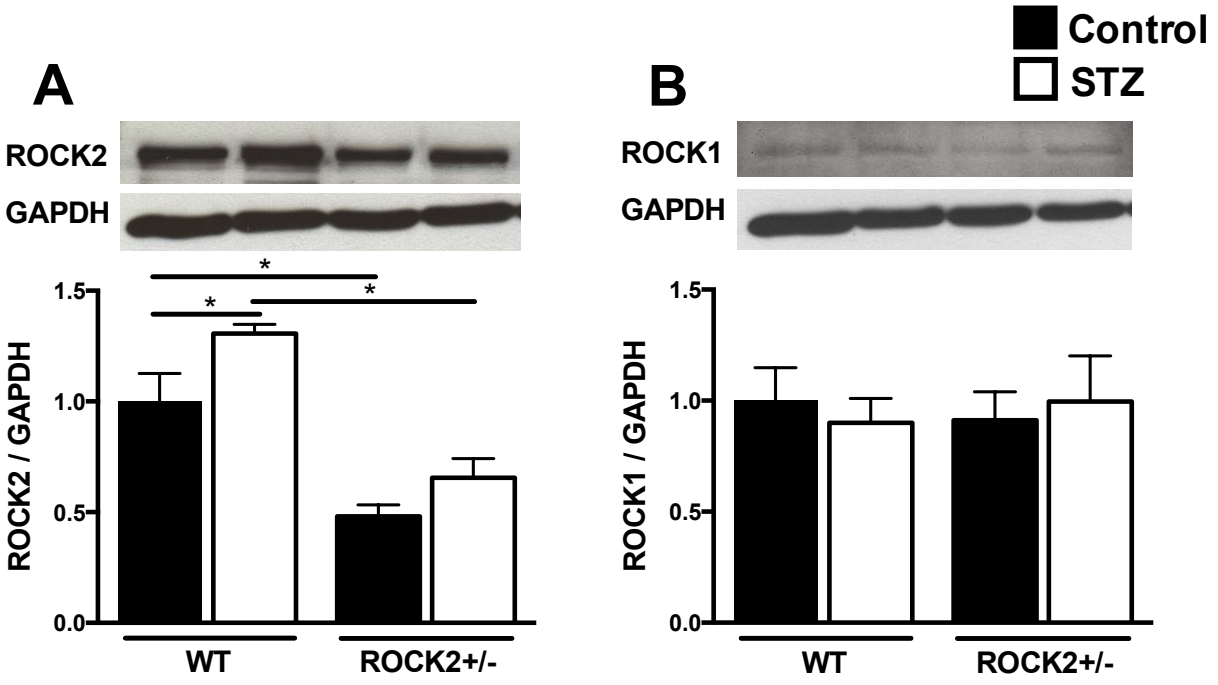

Figure 2.4 ROCK isoforms expression in diabetic and non-diabetic ROCK2+/- and WT mice subjected to *ex vivo* I/R injury.

ROCK2 (A) and ROCK1 (B) protein expression was evaluated in WT and ROCK2+/- mice hearts 16 weeks after STZ treatment (n=4-5 for all groups, * $p<0.05$).

2.2.4 Discussion

It is well known that the presence of diabetes is associated with the development of cardiac dysfunction. However, when the cardiac abnormalities of diabetes occur in the absence of changes in coronary artery disease or hypertension, it results in a condition known as diabetic cardiomyopathy (79). Although this condition is known to develop in STZ-treated diabetic rodents (173), in the present study, there was no evidence of systolic cardiac dysfunction in diabetic WT mice 11 weeks after STZ treatment. As previously mentioned, these mice have a CD-1 background, and in an unpublished study performed by our research group, we were unable to detect a decrease in systolic cardiac function in CD-1 mice even 13 weeks after induction of diabetes. Moreover, diastolic dysfunction, which usually accompanies and often precedes systolic cardiac dysfunction in the development of diabetic cardiomyopathy, was not detected at 13 weeks either. These observations, together with the fact that both ROCK2+/- and WT mice were overtly diabetic by 8 weeks after STZ treatment, suggest that CD-1 mice are resistant to the development of myocardial dysfunction associated with diabetic cardiomyopathy.

It has been previously suggested that animal strain can have an independent influence on the development of diabetic cardiomyopathy (174). In rats, these changes depended on the susceptibility of each strain to STZ treatment (174). However, the reason for strain differences in mice is not as clear. Male C57BL/6 mice were found to display a significant decrease in systolic cardiac function 12 weeks after STZ treatment (175, 176). Moreover, using magnetic resonance imaging, a decrease in ejection fraction, fractional shortening and cardiac output could be detected in this strain of mice as early as 4 weeks after STZ treatment (177). On the other hand, male CD-1 mice were not found to develop systolic cardiac dysfunction until 16 weeks after induction of diabetes, although significant diastolic dysfunction was detected at 12 weeks (178).

Our data showing an absence of systolic dysfunction in WT CD-1 mice 13 weeks after diabetes induction are consistent with the results of the latter study, and suggest that the development of diabetic cardiomyopathy in this strain of mice is delayed.

Since cardiac dysfunction did not develop in the animal model used in the present study within the time period investigated, the role of ROCK2 in diabetic cardiomyopathy could not be evaluated. Previously, our research group had demonstrated the presence of diabetic cardiomyopathy in 12 week diabetic rats, and had found that acute inhibition of ROCK normalized cardiac function in diabetic rats while having no effect on cardiac function in control animals (155). Furthermore, it was later shown that ROCK2 expression was higher in diabetic rat hearts, while ROCK1 expression remained the same, suggesting that the former is the isoform involved in the development of diabetic cardiomyopathy (157). In the present study, we detected a significant increase in ROCK2 expression in diabetic WT mice 16 weeks after STZ treatment, which was prevented in diabetic ROCK2+/- mice; and in the unpublished study performed by our research group that was mentioned above, ROCK2 expression was significantly higher in diabetic CD-1 mice 13 weeks after STZ treatment. Since cardiac dysfunction was not detected in either case, the data suggests that the diabetes-induced elevation of ROCK2 expression occurs well before the onset of diabetic cardiomyopathy.

In spite of these observations, it was important to determine if the induction of myocardial I/R injury resulted in differences in cardiac function in diabetic and non-diabetic CD-1 mice. Therefore, we also conducted a preliminary study in which CD-1 mice were treated with STZ and then subjected to myocardial I/R injury, following which systolic and diastolic cardiac function were evaluated.

2.3 Study 2: Establishing a model of *in vivo* myocardial I/R injury in non-diabetic and diabetic mice

2.3.1 Introduction

The use of *in vivo* myocardial I/R injury models has allowed researchers to study many different factors around the development of this condition. Reproducible results can be obtained by controlling the duration and the location of ischemic injury, as well as the length of reperfusion. The most common technique used to induce myocardial I/R injury *in vivo* is the temporary ligation of the LAD coronary artery (179). In larger animals, such as pigs or dogs, the ligation is done using a strip of moistened umbilical tape, while in small animals, such as rats or mice, a thread or a fine suture is used (179). Since a thoracotomy needs to be performed to visualize the hearts, animals have to be intubated and ventilated during this procedure. Intubation can be performed by tracheostomy or by endotracheal intubation, with the latter method being the safest (180).

For the project in this thesis, we established a detailed surgical protocol that allowed us to perform myocardial I/R injury *in vivo* in both normal and type 1 diabetic CD-1 mice. The protocol was developed under the guidance and supervision of Dr. Shelly McErlane and Kris Andrews, from the Centre for Comparative Medicine at the University of British Columbia. Once this protocol was established, we induced myocardial I/R injury in mice subjected to different lengths of STZ treatment. Afterwards, changes in both systolic and diastolic cardiac function were evaluated.

2.3.2 Materials and methods

Animals

At 8 weeks of age, male CD-1 mice were treated with two different doses of STZ: 40 mg/ml for 3 days (treatment 1), or 60, 50 and 40 mg/ml for 3 days (treatment 2). Preliminary work from our lab has shown that with both doses, mice become diabetic within 2 weeks. Control mice were given citrate buffer vehicle (0.1 M, pH 4.5) for the same length of treatment. Non-fasting glucose levels were measured using One Touch Ultra test strips and a One Touch Ultra 2 glucometer (LifeScan, Burnaby, BC, Canada). Ultimately, no significant differences were detected between the two doses of STZ in either blood glucose (treatment 1, 18.3±3.5 mM; treatment 2, 24.0±4.6 mM; $p>0.05$) or cardiac function following I/R injury, so results from the two treatment groups were pooled for the analyses.

All mice were housed under the same conditions, and had free access to food and water. This investigation conforms to the Canadian Council on Animal Care Guidelines on the Care and Use of Experimental Animals and the Guide for Care and Use of Laboratory Animals published by the United States National Institutes of Health (NIH publication no. 85–23, revised 1996). All protocols were approved by the University of British Columbia Animal Care Committee.

Surgical preparation

Diabetic and non-diabetic mice were divided in two groups: one was subjected to myocardial I/R injury 1 week after STZ treatment, and another one had I/R injury induced 3 weeks after STZ treatment. The day of surgery, mice were weighed and anesthetized using a subcutaneous (SC) injection of a ketamine/xylazine mixture. Control mice received 80 and 5 mg/kg of ketamine and xylazine, respectively; while STZ-treated mice received 40 and 1.25

mg/kg. If mice were still moving after 5 minutes, additional ketamine/xylazine was given. After mice were sedated, 1 ml of warm saline (SC) was provided and corneal lubricant was applied.

Intubation and Ventilation

Mice were placed on a slanted table with their abdomen facing up before starting the intubation procedure. The tip of an otoscope was inserted into the mouth and the tongue was gently pressed down in order to expose the throat and vocal cords. Xylocaine (2%) jelly was applied and a 22G catheter was inserted into the trachea. Proper intubation was verified. The appropriate ventilation rate and volume were determined using the values provided by the ventilator manufacturer (Harvard Apparatus, Holliston, MA). Mice were placed on their side over a heating pad, and ventilated using a mixture of oxygen and isoflurane (1-2.5%). A SC injection of buprenorphine (0.05 mg/kg for control mice and 0.025 mg/kg for STZ-treated mice) was provided. A rectal probe thermometer (Braintree Scientific, Braintree, MA) was used to monitor body temperature, which ranged between 36.8-37.1°C.

LAD coronary artery ligation

Before starting surgery, anesthesia was verified by testing the pedal withdrawal reflex. A SC injection of bupivacaine 0.25% on the incision site (30-60 µl) was provided, and the skin was disinfected with surgical scrub. A skin incision parallel to the midline and on the right side of the sternum was made. The pectoral muscles were separated and the rib cage exposed. A thoracotomy between the 3rd and 4th rib was made, and the heart was exposed using a small retractor. The pericardium was removed and the LAD coronary artery was ligated using Vicryl 8-0 (Ethicon, Somerville, NJ). If the ligation was successful, an immediate "blanching" was

observed in the myocardium downstream from the ligation. In sham-operated mice, Vicryl 8-0 was passed underneath the LAD artery, but a ligation was not performed. The chest cavity was then covered with a small piece of moistened sterile gauze during ischemia. After 40 minutes, the knot was carefully removed without damaging the cardiac muscle in order to allow reperfusion. The rib cage, the muscle and the skin were then sutured using Vicryl 6-0 (Ethicon, Somerville, NJ).

Recovery

To wean mice from the ventilator, a SC injection of atipamizole (1 mg/kg for control mice and 0.5 mg/kg for STZ-treated mice) was provided and the percentage of isoflurane was lowered by half. Isoflurane was turned off when mice started to battle the ventilator, and the tracheal cannula was removed when signs of consciousness were detected. Mice were then placed in recovery cages (heated, easily accessible food and gel water), and after 20-40 minutes of constant monitoring, another SC injection of buprenorphine (0.05 mg/kg for control mice and 0.0125 mg/kg for STZ-treated mice) was provided. Mice were then monitored for the next 3-5 hours, and at the end of the day, an extra dose of buprenorphine (0.05 mg/kg for control mice and 0.025 mg/kg for STZ-treated mice) was given. The first week after surgery, additional fluids and buprenorphine were given as needed. Mice were monitored on a daily basis for 1 week, and then every week.

Echocardiographic measurements

Cardiac function was evaluated by echocardiography 1, 3 and 5 weeks after surgery using the Vevo 2100 echocardiography system (Fujifilm VisualSonics, ON, Canada). In brief, mice

were anesthetized using 4-4.5% of isoflurane, and placed on an echocardiography platform with their nose inside an anesthesia nose cone. Temperature was maintained at 37±0.5°C. The level of isoflurane was then lowered to 1-2% before proceeding with the echocardiographic measurements. Anesthetized mice, with a heart rate of 400±30 bpm, were positioned at an apical four-chamber view in order to image the mitral valve. The early to late ventricular filling (E/A) ratio and the left ventricular myocardial performance index (LV MPI) were calculated from scans obtained by pulse wave Doppler. The E/A ratio is a measurement of diastolic cardiac function, while the MPI incorporates both systolic and diastolic cardiac function. Mice were then positioned at a parasternal short-axis view, and 2-D M-mode scans were obtained at a heart rate of 500±30 bpm. Fractional shortening and ejection fraction were calculated from these scans as indicators of systolic cardiac function. After the last echocardiographic assessment, body weight and non-fasting glucose levels were measured. Mice were then euthanized and hearts were removed and weighed.

Statistical analysis

Data were expressed as means ± SE, and the number of animals in each group is represented by n. Results were analyzed using GraphPad Prism version 5.00 for Mac (GraphPad Software, San Diego, CA). Physiological data were analyzed by one-way ANOVA followed by Neuman-Keuls test for multiple comparisons. Echocardiographic data were analyzed using two-way ANOVA followed by Neuman-Keuls test. Results were considered statistically significant at $p<0.05$.

2.3.3 Results

No significant differences in mortality rate were found between non-diabetic (11.1%) and diabetic mice (12.5%), suggesting that the surgical protocol developed here is a safe method for the induction of myocardial I/R injury *in vivo* in both diabetic and non-diabetic mice. Before the induction of myocardial I/R injury, the non-fasting blood glucose levels of mice that had been treated with STZ one week previously were not significantly higher than those of untreated mice (Table 2.1). Also, at this point, no significant differences in body weight were detected between STZ-treated and untreated mice (Table 2.1). The first week after surgery, there were no differences in systolic or diastolic cardiac function among groups (Fig 2.5). However, 3 weeks after inducing I/R injury, both control and STZ-treated mice hearts had a significantly higher E/A ratio and LV MPI compared to sham-operated mice (Fig 2.5C and D). A high E/A ratio is a sign of elevated left atrial pressure, which could be secondary to an increase in left ventricular filling pressure during diastole (181, 182), while a higher LV MPI indicates a global deterioration in cardiac function (183). Therefore, the increase in both of these parameters could reflect the induction of myocardial I/R injury. Nonetheless, by 5 weeks after surgery, the E/A ratio and the LV MPI had returned to control levels, while the ejection fraction and fractional shortening of both control and STZ-treated mice were significantly lower than those detected in sham-operated mice (Fig 2.5A and B), suggesting the presence of systolic dysfunction in hearts subjected to I/R injury.

Group 1: One week after STZ treatment

Group	Before surgery		Five weeks after surgery			
	Blood glucose (mM)	Body weight (g)	Blood glucose (mM)	Body weight (g)	Heart weight (mg)	Heart/Body weight ratio
Sham	9.4 ± 1.0	38.9 ± 0.9	7.8 ± 0.5	41.2 ± 0.3	225.0 ± 5.5	5.5 ± 0.2
Ctrl IR	9.1 ± 0.7	38.0 ± 2.1	7.1 ± 0.7	42.6 ± 1.9	237.5 ± 10.3	5.6 ± 0.1
STZ+IR	11.9 ± 0.9	39.3 ± 1.1	23.0 ± 3.9[a]	39.5 ± 0.8	215.3 ± 14.5	5.4 ± 0.3

Group 2: Three weeks after STZ treatment

Group	Before surgery		Five weeks after surgery			
	Blood glucose (mM)	Body weight (g)	Blood glucose (mM)	Body weight (g)	Heart weight (mg)	Heart/Body weight ratio
Sham	7.9 ± 0.2	42.8 ± 2.2	8.8 ± 0.3	45.4 ± 3.1	220.8 ± 6.8	4.9 ± 0.3
Ctrl IR	7.9 ± 0.3	43.8 ± 1.7	7.5 ± 0.4	44.2 ± 1.4	248.9 ± 14.3[b]	5.6 ± 0.2[b]
STZ+IR	20.8 ± 2.8[a]	38.7 ± 0.7	30.4 ± 2.2[a]	39.8 ± 0.5	198.7 ± 2.5	5.0 ± 0.1

Table 2.1 Characteristics of CD-1 mice subjected to myocardial I/R injury 1 or 3 weeks after STZ treatment.

Blood glucose and body weight were measured before surgery. Five weeks after inducing I/R, blood glucose and body weight were measured again, and heart weight and heart/body weight ratio were recorded. Sham: sham-operated control mice, Ctrl IR: control mice subjected to I/R injury, STZ+IR: STZ-treated mice subjected to I/R injury. (n=3-4 for group 1, and n=4-7 for group 2; a: $p<0.05$ compared to Sham and Ctrl IR mice, b: $p<0.05$ vs. sham and STZ+IR mice).

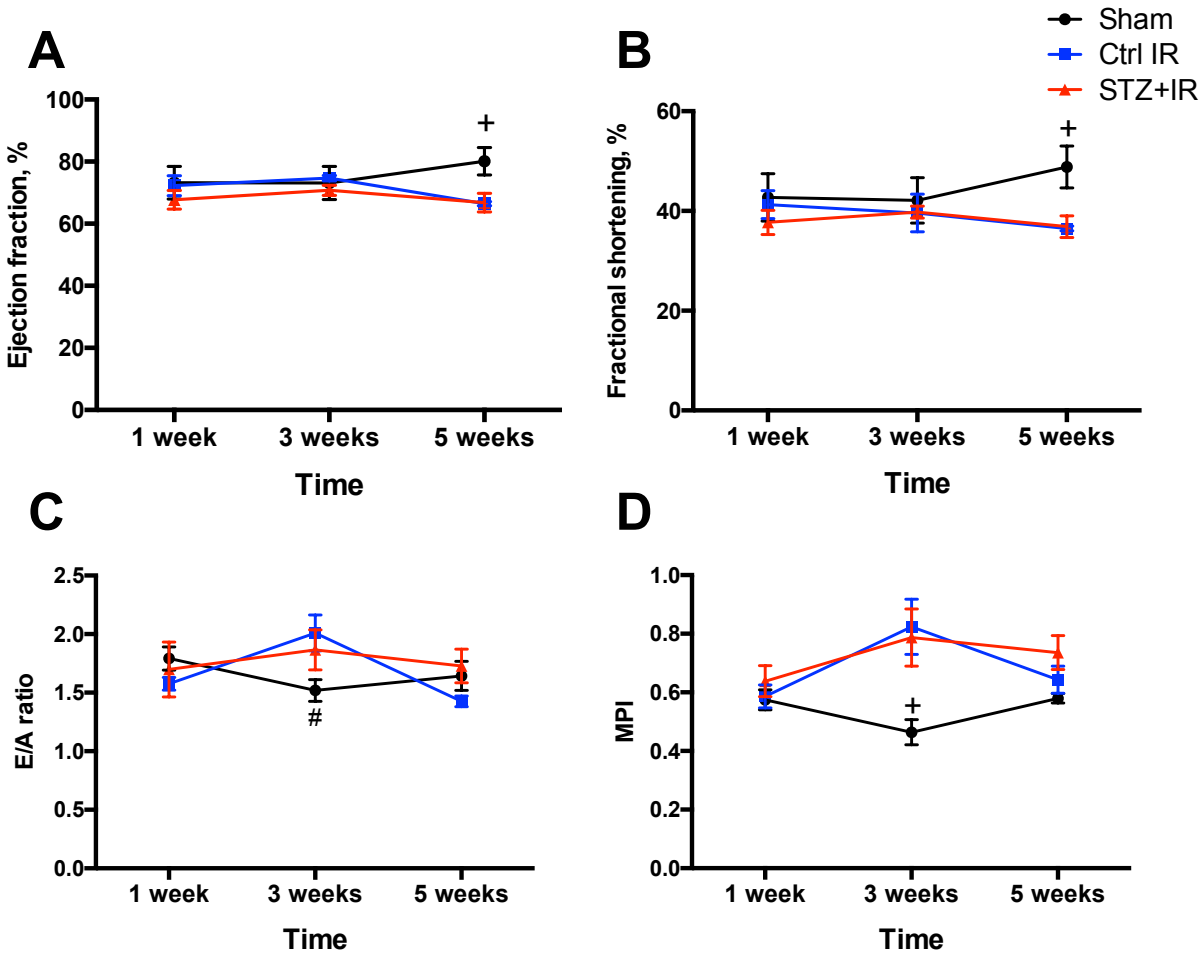

Figure 2.5 Systolic and diastolic cardiac function values of mice subjected to myocardial I/R injury after 1 week of STZ treatment.

Ejection fraction (A) and fractional shortening (B), were used to evaluate systolic cardiac function, and the E/A ratio (C) was used to evaluate diastolic cardiac function. The LV MPI is an indicator of both systolic and diastolic cardiac function (D). Sham: sham-operated control mice, Ctrl IR: control mice subjected to I/R injury, STZ+IR: STZ-treated mice subjected to I/R injury. (n=3-4, +=$p<0.05$ sham vs. Ctrl IR and STZ+IR, #=$p<0.05$ Sham vs. control I/R injury).

Nonetheless, no significant differences in systolic or diastolic cardiac function were detected between control and STZ-treated mice subjected to myocardial I/R injury at any point of the study. It also should be noted that by 5 weeks after surgery, the non-fasting blood glucose levels of STZ-treated mice had increased, and were now significantly higher than those of untreated mice (Table 2.1). However, no significant differences in body weight, heart weight or the heart/body weight ratio were detected.

Before inducing myocardial I/R injury, CD-1 mice that were treated with STZ 3 weeks before surgery had significantly higher non-fasting glucose levels than their control counterparts (Table 2.1). However, no differences in body weight were detected (Table 2.1). One and three weeks after the induction of myocardial I/R injury, there were no significant differences in either systolic or diastolic cardiac function among groups (Fig 2.6). However, five weeks after surgery, fractional shortening and ejection fraction were significantly lower in control I/R mice compared to their sham counterparts and to the STZ-treated mice subjected to I/R injury (Fig 2.6A and B). Also at this point, STZ-treated mice subjected to I/R injury had a significantly higher E/A ratio compared to their untreated counterparts (Fig 2.6C), suggesting restrictive LV filling patterns (182). There were no significant differences in LV MPI at any point of the study. Heart weight was significantly higher in control mice subjected to I/R injury than in their sham counterparts and the STZ-treated mice, and the increase was preserved even after standardizing to body weight (Table 2.1). Altogether, these results suggest that although CD-1 mice subjected to I/R injury develop cardiac dysfunction, mice with STZ-induced diabetes have a similar or better performance than their non-diabetic counterparts.

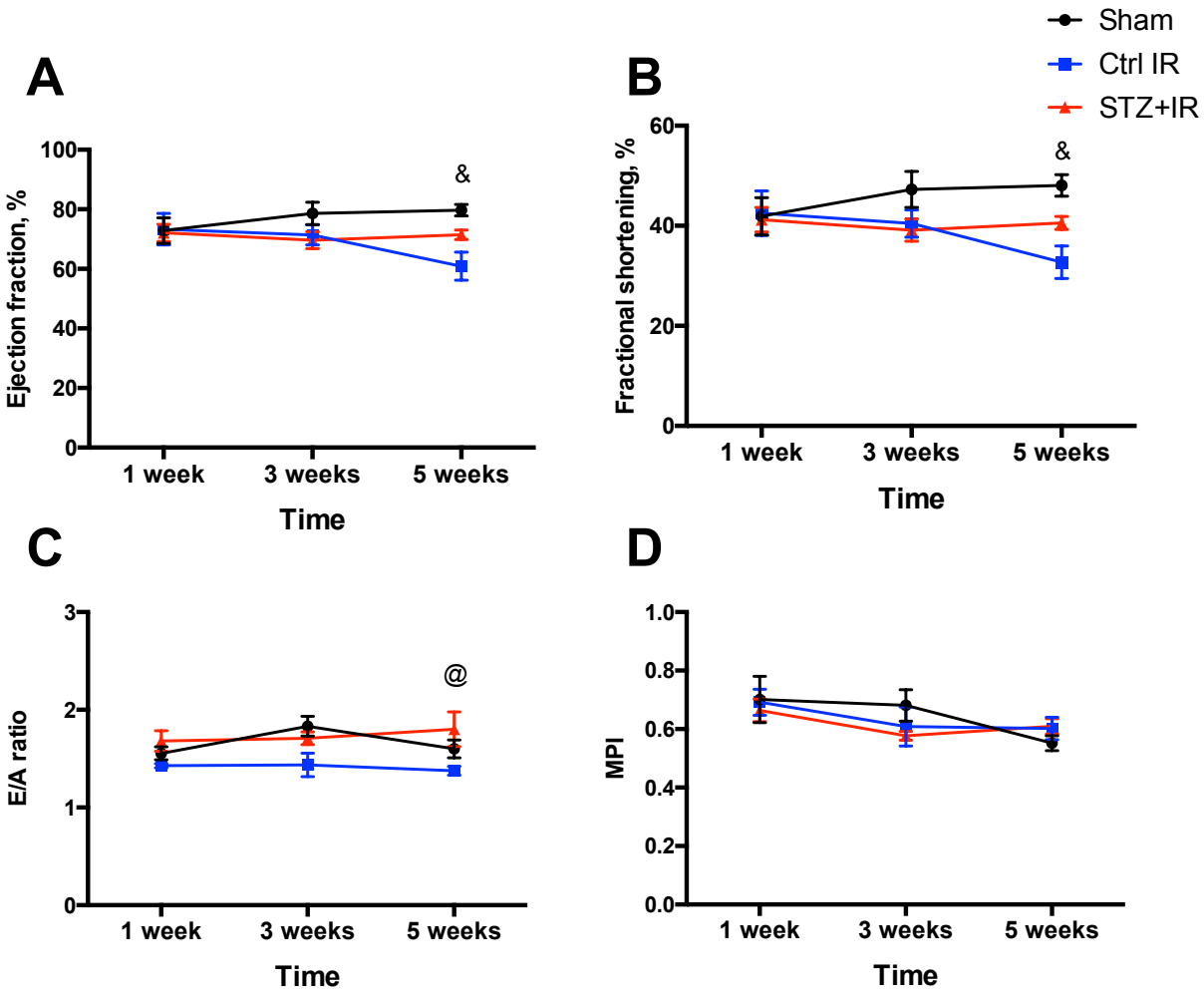

Figure 2.6 Systolic and diastolic cardiac function values of mice subjected to myocardial I/R injury 3 weeks after STZ treatment.

Ejection fraction (A) and fractional shortening (B), were used to evaluate systolic cardiac function, and the E/A ratio (C) was used to evaluate diastolic cardiac function. The LV MPI is an indicator of both systolic and diastolic cardiac function (D). Sham: sham-operated control mice, Ctrl IR: control mice subjected to I/R injury, STZ+IR: STZ-treated mice subjected to I/R injury. (n=4-7, &=$p<0.05$ Ctrl IR vs. sham and STZ+IR, @=$p<0.05$ Ctrl IR vs. STZ+IR).

2.3.4 Discussion

The ligation of the LAD coronary artery is a highly invasive surgery. The literature reports that the induction of myocardial I/R injury by LAD ligation has mortality rates as high as 30 and 50% (179, 184); however, in our hands the overall mortality rate was much lower. This observation, along with the fact that non-diabetic mice subjected to this procedure had impaired cardiac function compared to their sham-operated counterparts, supports the suggestion that the protocol here developed was effective at inducing myocardial I/R injury. Nonetheless, the cardiac function of diabetic mice was similar, and in some cases better than that detected in non-diabetic mice.

Clinical studies clearly demonstrate that diabetic hearts are more susceptible to myocardial I/R injury; however, experimental models have shown conflicting results. Literature reports suggest that diabetic mouse hearts may have higher, lower, or equal susceptibility to I/R injury (185), and these differences seem to be mainly due to the experimental conditions used in each of them, such as the length of diabetes, the length of ischemia and reperfusion, and the mouse strain used. The fact that we were unable to detect an effect of diabetes on the development of myocardial I/R injury even in overtly diabetic mice, suggests that CD-1 mice are not only more resistant to the development of diabetic cardiomyopathy, but also to the cardiac dysfunction associated with myocardial I/R injury in diabetic conditions.

Other strains of mice have shown more susceptibility to the deleterious effects of the combination of diabetes and myocardial I/R injury. For instance, Rui et al. (186) reported that diabetic C57BL/6 mice subjected to myocardial I/R injury have larger infarct sizes than their non-diabetic counterparts. Moreover, the induction of diabetes in

this strain of mice also translates in further cardiac dysfunction after inducing I/R injury (187).

The results obtained in this study suggest that, due to their CD-1 background, ROCK2+/- mice are not an appropriate model for determining the role of ROCK2 in the development of myocardial I/R injury during diabetes. However, the presence of cardiac dysfunction in non-diabetic mice subjected to I/R injury suggested that these mice would be useful to assess the effect of whole-body ROCK2 partial deletion on the development of myocardial I/R injury in non-diabetic conditions.

2.4 Summary and conclusions

The two preliminary studies reported above support the following conclusions:

- In non-diabetic conditions, both WT and ROCK2+/- mice had similar systolic cardiac function, suggesting that the partial deletion of this ROCK isoform does not impair systolic cardiac function. On the other hand, diabetic WT mice failed to develop systolic cardiac dysfunction, even though they had an increase in ROCK2 expression, probably due to their CD-1 background. Therefore, it was not possible to evaluate the role of ROCK2 on the development of diabetes-induced cardiac dysfunction in these mice.

- The induction of myocardial I/R injury caused a significant decrease of cardiac function in non-diabetic CD-1 mice; however, their diabetic counterparts had a similar or better performance. It is not clear why diabetic CD-1 mice did not develop further cardiac dysfunction, but in accordance with the results obtained in the first preliminary study, this may have been related to the mouse strain. Alternatively, even though non-fasting blood

glucose was elevated in CD-1 mice treated with STZ, it is possible that a higher dose of STZ would have produced a more rapid and intense response. Unlike ROCK2+/- mice, cardiac-specific ROCK2 knockout mice have a C57BL/6J background. Since diabetic C57BL/6J mice have shown to be susceptible to the deleterious effects of myocardial I/R injury (175, 176), this animal model was used instead to evaluate the effects of cardiomyocyte-ROCK2 on the development of myocardial I/R injury during diabetes.

As mentioned in chapter 1, ROCK inhibition has shown cardioprotective activity against the development of myocardial I/R injury via activation of the RISK pathway and reduced inflammation (158-160). Since both of these mechanisms take place at a relatively early stage of reperfusion (33, 47), we decided that in our further studies, we would evaluate the consequences of I/R injury at short times of reperfusion in order to monitor the effects of ROCK2 deletion on these early responses to myocardial I/R injury. The evaluation of cardiac function at later times of reperfusion involves different responses, such as the development of hypertrophy and fibrosis, both outside the scope of the present thesis.

Chapter 3: Contribution of ROCK2 to myocardial I/R injury

3.1 Introduction

In the United States, close to 1 million cases of new and recurrent myocardial infarction are reported every year (188). In order to avoid the adverse effects of ischemia, reperfusion must be instituted. However, the prompt normalization of ischemic conditions during reperfusion triggers a deleterious mechanism known as myocardial I/R injury. This type of injury is characterized by many detrimental changes such as ion accumulation, elevated ROS production, autophagy, apoptosis and necrosis, which ultimately lead to cardiac tissue death (12). Myocardial I/R injury represents a major health burden, since it can lead to the development of reperfusion arrhythmias, microvascular dysfunction, and myocardial stunning (7). Several types of pharmacologic interventions focused on attenuating the effects of myocardial I/R injury have been proposed, but no definite solution has been found.

The over-activation of ROCK, a serine/threonine kinase activated by the small G-protein RhoA, has been implicated in the development of a number of different cardiovascular diseases and pathologies, including myocardial I/R injury. Bao et al. (158) were the first to suggest that increased activation of ROCK had a significant role during the development of no-flow myocardial I/R injury *in vivo*. Subsequently it was reported that the over-activation of ROCK occurs specifically during myocardial reperfusion (160). While initial studies suggested that the cardioprotective mechanisms triggered by ROCK inhibition include activation of the RISK pathway (159, 161), more recently it has

been suggested that the inhibition of ROCK activation in neutrophils leading to reduced leukocyte infiltration and inflammatory cytokine production plays a major role (162).

ROCK is expressed as two different isoforms, ROCK1 and ROCK2. These isoforms share an overall amino acid identity of 65%, and have 92% homology in the kinase domain. While ROCK1 is widely expressed in all human tissues except brain and muscle, ROCK2 is mainly found in brain, muscle, heart, lungs and placenta (127). Previous reports that have analyzed the effect of ROCK inhibition on myocardial I/R injury employed only non-isoform selective inhibitors, so it is unclear whether ROCK1, ROCK2 or both isoforms contribute to the development of this condition. In the present study, we investigated the specific contribution of the ROCK2 isoform, and examined the underlying mechanisms. Our results indicate that mice with whole-body partial deletion of ROCK2 are protected against the development of myocardial I/R injury. This was associated with activation of the RISK pathway at an early stage of reperfusion and with reduced production of inflammatory cytokines but not with reduced neutrophil infiltration. Furthermore, a cardioprotective effect was also seen in hearts from mice with cardiomyocyte-specific deletion of ROCK2, indicating that the adverse effects of ROCK2 activation arise at least in part from actions within the cardiomyocyte compartment.

3.2 Materials and methods

3.2.1 Animals

ROCK2+/- mice were generated as described by Zhou et al. (171), and were backcrossed for 7 generations on a CD-1 background. Complete knockout of ROCK2 is

highly lethal in utero (171); therefore, only ROCK2+/- mice were employed. Male ROCK2+/- mice and their WT littermates were used in experiments. ROCK2$^{flox/flox}$ mice were generated as described by Okamoto et al. (142) and in order to obtain cardiac-specific ROCK2 knockouts, these mice were crossed with alpha-myosin heavy chain (α-MHC) Cre recombinase (α-MHC-*MerCreMer*) mice. After 4 generations, ROCK2$^{flox/flox}$-α-MHC-*MerCreMer* and ROCK2$^{flox/flox}$-non-α-MHC-*MerCreMer* mice were obtained. At 8 weeks of age, ROCK2$^{flox/flox}$-α-MHC-*MerCreMer* and ROCK2$^{flox/flox}$-non-α-MHC-*MerCreMer* mice were treated for 5 consecutive days with 20 mg/kg/day of tamoxifen diluted in corn oil, in order to generate cardiac-specific ROCK2 knockout mice (cROCK2-/-) and their ROCK2 expressing littermates (cROCK2+/+) (189). Male cROCK2-/- and cROCK2+/+ mice were used in experiments. This investigation conforms to the Canadian Council on Animal Care Guidelines on the Care and Use of Experimental Animals and the Guide for Care and Use of Laboratory Animals published by the United States National Institutes of Health (NIH publication no. 85–23, revised 1996). All protocols were approved by the University of British Columbia Animal Care Committee.

3.2.2 *In vivo* myocardial I/R injury and echocardiography measurements

At 11 weeks of age, the basal cardiac function, cardiac dimensions and myocardial wall deformation of ROCK2+/- mice and their WT counterparts were evaluated using the Vevo 2100 echocardiography system (Fujifilm VisualSonics, ON, Canada). In brief, mice were anesthetized with 4-4.5% isoflurane and then maintained at 1% isoflurane. Body temperature was kept constant at 37±0.5°C and all measurements

were done at a heart rate of 500±30 bpm. Fractional shortening, ejection fraction and cardiac dimensions were obtained from 2-D M-mode imaging from a parasternal short-axis view. B-mode long-axis view images were used to calculate radial and longitudinal endocardial strain, strain rate and velocity using Speckle tracking with VevoStrain software (Fujifilm VisualSonics, ON, Canada). Two days later, mice were subjected to myocardial I/R injury by transient ligation of the LAD coronary artery using a modification of the method of Eguchi et al. (190). Briefly, mice were anesthetized with a subcutaneous injection of ketamine/xylazine (80 and 5 mg/kg, respectively) and intubated with a 22G catheter. They were ventilated using a mixture of oxygen and isoflurane (1-2%), and a subcutaneous injection of bupivacaine (0.25%, 30-60 µl) was administered at the incision site. Pre-operative buprenorphine (0.05 mg/kg, subcutaneous) was also provided. A left side thoracotomy between the 3th and 4th rib was performed, and the LAD coronary artery was ligated for 40 min using 8-0 Vicryl suture. Blanching of the myocardium indicated a successful ligation. In sham-operated mice, suture was passed underneath the LAD coronary artery, but no ligation was performed. At the end of the ischemic period, the knot was carefully removed in order to restore blood flow and the chest was closed using 6-0 Vicryl suture. This same procedure was performed in cROCK2-/- and cROCK2+/+ mice 8 weeks after tamoxifen treatment. No significant differences were found in body weight before or after surgery. Mortality rates were similar between genotypes after inducing myocardial I/R injury (approximately 20% for ROCK2+/- and WT mice, and 10% for cROCK2-/- and cROCK2+/+ mice), and all deaths occurred during the first 45 minutes of reperfusion, most likely due to pneumothorax or arrhythmia (191, 192). After 24 hours of reperfusion, surviving mice

were subjected to the echocardiography procedure described above. Mice were then euthanized and hearts quickly removed and snap frozen in liquid nitrogen. Tissues were stored at -80°C until further analysis. A second set of mice was exposed to LAD coronary artery or sham ligation and 2 hours of reperfusion, following which hearts were removed and stored as described above.

3.2.3 Measurement of infarct size

Infarct size was measured employing a modified version of the protocol of Bohl et al. (193). Briefly, mice subjected to LAD ligation and 24 hours of reperfusion as described above were anesthetized using 4-4.5% of isoflurane, hearts were quickly excised, and the aorta cannulated using a 20G blunted needle. The hearts were then perfused with Krebs-Henseleit buffer until all residual blood was removed. The LAD coronary artery was re-ligated at the same position as before, and a 1.5% solution of Evans blue dye was used to perfuse the remote myocardium. The whole heart was then semi-frozen at -20°C for 15 min and cut into 6 thin short-axis slices. The slices were rinsed in PBS, thawed, and incubated in a 1% solution of triphenyltetrazolium chloride (TTC) at 37°C for 20 min. They were then blotted and placed in 10% formalin for 20 min at room temperature, following which they were weighed and placed between glass slides. The heart slices were photographed under a stereomicroscope and the area of necrosis (AON) and the area at risk (AAR) were measured using ImageJ v1.46 r (NIH, Bethesda, MD). Infarct size was calculated as the percentage of AON relative to the AAR.

3.2.4 H&E staining and neutrophil infiltration

After 24 hours of reperfusion, hearts were quickly excised and fixed in 10% formalin for 48 hours. The tissues were then washed and stored in PBS buffer. The segments between the LAD coronary artery ligation and 2 mm above the apex were paraffin embedded. Two sets of sections (5 μm thickness) were prepared; one was subjected to hematoxylin and eosin (H&E) staining and the other one to immunohistochemical (IHC) staining, in order to determine the extent of Ly6G+ neutrophil infiltration. Briefly, paraffin-embedded sections were deparaffinized with xylene, and re-hydrated with a series of graded concentrations of ethanol. Antigen retrieval was performed by placing the sections in citrate buffer (pH 6), and heating them in a microwave (2 minutes at high power and 20 minutes at 20% power). Endogenous peroxidase activity was blocked using a 0.6% peroxide solution in methanol for 15 minutes. Blocking buffer (1% BSA in PBS) was added to each section and incubated for 25 minutes. They were then incubated in anti-mouse Ly-6G primary antibody (Clone 1A8, BioLegend, San Diego, CA) overnight at 4°C, followed by an Ig biotinylated antibody (SouthernBiotech, Birmingham, AL) for 45 minutes at room temperature. Sections were then covered with streptavidin poly-HRP (Pierce-Thermo Fisher Scientific, Waltham, MA) and incubated for 45 minutes at room temperature. A 3,3' diaminobenzidine color development solution was added, and sections were counterstained with hematoxylin. Neutrophil infiltration was determined by counting the number of neutrophils in 6 randomly selected fields using a microscope at 20x magnification.

3.2.5 Extraction of mRNA and RT-PCR

Total RNA was isolated from 30-50 mg of frozen heart tissue subjected to 24 hours of reperfusion using TRIzol (Invitrogen, Carlsbad, CA) as described by the manufacturer. Reverse transcription was done using the SuperScript VILO cDNA Synthesis kit (Invitrogen, Carlsbad, CA) and 1 μg of total RNA. RT-PCR was performed using SYBR Select Master Mix (Applied Biosystems, Foster City, CA) on an Applied Biosystems StepOnePlus machine. The endogenous control was 36B4, and the primer sequences were the following: IL-6 (F): GAGGATACCACTCCCAACAGACC, IL-6 (R): AAGTGCATCATCGTTGTTCATACA (194), IL-1β (F): AGATGAAGGGCTGCTTCC, IL-1β (R): CTGCCTGAAGCTCTTGTTG (designed using AutoPrime 1.0 software, www.autoprime.de), TNFα (F): AGGTTCTCTTCAAGGGACAAG, TNFα (R): GCAGAGAGGAGGTTGACTTT, MCP-1 (F): TAGGCTGGAGAGCTACAAGAGGAT, MCP-1 (R): AGACCTCTCTCTTGAGCTTGGTGA, 36B4 (F): AGATGCAGCAGATCCGCAT, 36B4 (R): GTTCTTGCCCATCAGCACC (195). Relative mRNA expression was calculated using the 2-ΔΔCT method.

3.2.6 Western blot analysis

Frozen hearts subjected to 2 and 24 hours of reperfusion were homogenized in RIPA buffer (Tris HCl 50 mM pH 7.4, NP-40 1%, SDS 0.1%, sodium deoxycholate 0.5%, NaCl 150 mM, EDTA 2 mM and protease and phosphatase inhibitor). Proteins from each sample were separated using 8–10% SDS-PAGE gels and immunoblotted using primary antibodies against ROCK2 (Santa Cruz Biotechnology, Santa Cruz, CA),

ROCK1 (BD Biosciences, Franklin Lakes, NJ), ^{Ser473}p-Akt, Akt, ^{Ser9}p-GSK-3β, GSK-3β, ^{Ser1177}p-eNOS, eNOS, $^{Ser380/Thr382/383}$PTEN, and PTEN (Cell Signaling, Danvers, MA). Band density was measured by densitometry using ImageJ v1.46 r (NIH, Bethesda, MD), and protein expression was normalized to GAPDH (Santa Cruz Biotechnology, Santa Cruz, CA), Ponceau staining, or the corresponding total protein.

3.2.7 ROCK activity assay

To determine ROCK activity, frozen heart tissue samples were homogenized in a non-denaturing lysis buffer (50 mM Tris-HCl, 150 mM NaCl, 1mM EDTA, 1mM EGTA, 1mM Na_3VO_4, 1mM 2-glycerolphosphate, 1% Non-Idet P-40, 1x protease inhibitors, pH 7.5). A 10x concentration of assay buffer (250 mM Tris-HCl, 100 mM $MgCl_2$, 50 mM glycerol-2-phosphate, 1 mM Na_3VO_4, 10 mM 1,4-dithiothreitol (DTT), 5 mM ATP, 0.2 μg/ml truncated MYPT1 $^{(654-880)}$, pH 7.5) was added to the homogenates, and the mixture was incubated at 30ºC for 30 minutes with gentle agitation. To stop the reaction, Laemli buffer was added and samples were incubated at 90ºC for 5 minutes. The extent of phosphorylation of ^{Thr853}MYPT1, an indicator of ROCK activity, was determined by Western blotting. The ROCK inhibitor H1152 (1 μM) was used to confirm that MYPT1 phosphorylation at this site was specific for ROCK.

3.2.8 PTEN activity assay

In order to evaluate PTEN activity, phosphate release from phosphatidylinositol 3,4,5-trisphosphate (PIP_3) diC_8 was measured using a Malachite Green assay kit (both Echelon, Biosciences, Salt Lake City, UT) as described by Soliman el al. (196). Briefly,

frozen heart tissue samples were homogenized in a non-denaturing lysis buffer (25 mM Tris, pH 8.0, 150 mM NaCl, 1% Non-Idet P-40, 1 mM EDTA, and 5% glycerol), and prepared at the same concentration. PTEN was immunoprecipitated overnight at 4°C using anti-PTEN-Sepharose bead conjugate (Cell Signaling, Beverly, MA). Then, samples were centrifuged for 30 seconds and washed five times with non-denaturing lysis buffer. The pellets were collected and resuspended in enzyme reaction buffer (50 mM Tris-HCl, pH 8.0, 50 mM NaCl, 10 mM dithiothreitol, and 10 mM $MgCl_2$) and the reaction was carried out following manufacturer's instructions. PTEN activity was expressed as the percent conversion of PIP_3.

3.2.9 Statistical analysis

All values are expressed as means ± SE; n denotes the number of animals in each group. Results were analyzed for statistical significance using GraphPad Prism version 5.00 for Mac (GraphPad Software, San Diego, CA). All data were analyzed by one-way ANOVA followed by the Neuman-Keuls test. Where only two groups were analyzed, an unpaired t-test was performed. Results were considered statistically significant at $p<0.05$.

3.3 Results

3.3.1 Infarct size in hearts from ROCK2+/- mice

To determine if partial deletion of ROCK2 influences the extent of myocardial I/R injury, infarct size was evaluated. At the end of 24 hours of reperfusion, there were no significant differences in the AAR of WT and ROCK2+/- mice hearts, suggesting that the size of the ischemic area induced by LAD ligation was similar in all hearts (Fig. 3.1 A

and B). However, myocardial infarct size, calculated as the AON/AAR, was significantly lower in ROCK2+/- mice than in their WT counterparts (Fig. 3.1 A and C), suggesting that this ROCK isoform is involved in the development of myocardial I/R injury. Furthermore, the H&E staining of post-I/R hearts showed that, in the vicinity of the LAD, ROCK2+/- mice had less cardiomyocyte disruption than their WT counterparts (Fig. 3.1 D).

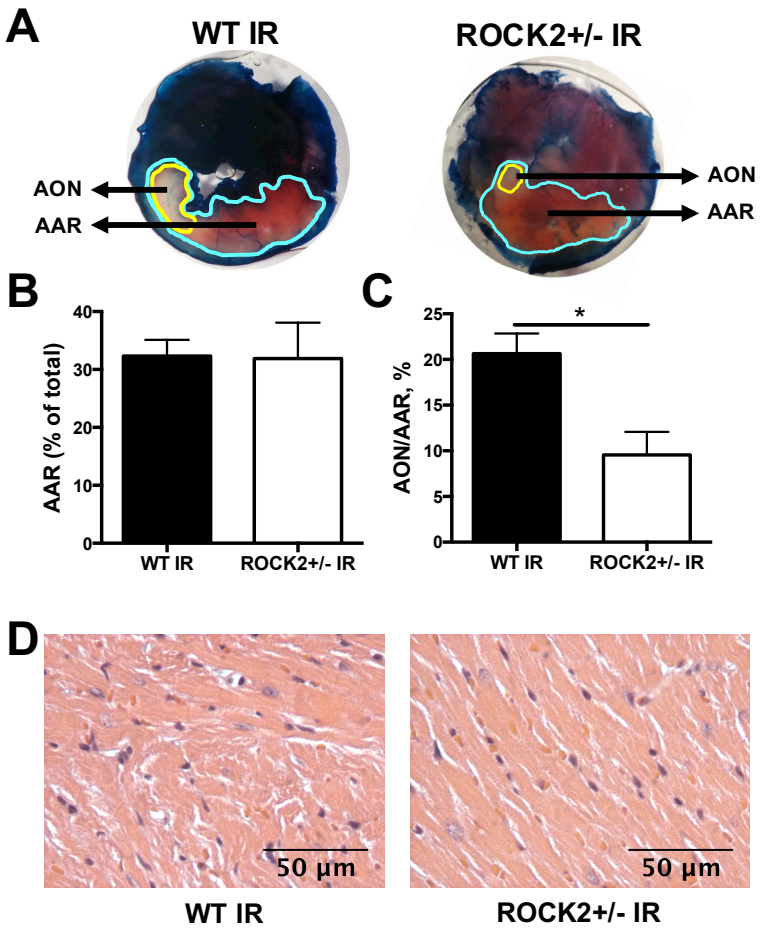

Figure 3.1 Infarct size in WT and ROCK2+/- mice hearts after 24 hours of reperfusion.

Representative images showing the AAR and AON following 40 min of ischemia and 24 hours of reperfusion in hearts from WT and ROCK2+/- mice (A). Mean AAR (B) and mean infarct size (C), calculated as the ratio of AON to AAR in WT and ROCK2+/- hearts (n=4-5, *$p<0.05$). Representative images of H&E stained sections (40x) of WT and ROCK2+/- mice hearts after 24 hours of reperfusion (D).

3.3.2 Basal and post-I/R cardiac function and parameters

In order to further assess the role of ROCK2 during myocardial I/R injury, cardiac function before and after surgery was evaluated. At 11 weeks of age, basal cardiac function (Fig. 3.2) and cardiac parameters (Table 3.1) of ROCK2+/- mice and their WT counterparts were not significantly different, consistent with our previous observations (196). Cardiac strain, a measure of tissue deformation, and strain rate, a measure of the time-course of deformation, were also evaluated, and no significant differences were found between the two genotypes at baseline (Table 3.2).

Following LAD ligation and 24 hours of reperfusion, cardiac function was significantly impaired in WT mice. Fractional shortening and ejection fraction decreased by 44% and 36% compared to the basal levels, respectively (Fig. 3.2 B and C), and these changes were associated with a significant increase in systolic left ventricular internal diameter (Table 3.1). End diastolic and systolic volumes also tended to be higher in WT mice following I/R injury, although these differences were not statistically significant (Table 3.1). Similarly, both radial and longitudinal endocardial strain were significantly reduced compared to baseline (Table 3.2), consistent with the development of myocardial I/R injury (190).

In contrast, fractional shortening and ejection fraction following induction of I/R injury in ROCK2+/- mice (Fig. 3.2 B and C), were not significantly different from those observed at baseline (53.0 ± 3.5% basal vs. 48.1 ± 4.1% post-I/R and 83.9 ± 3.2% basal vs. 79.5 ± 4.3% post-I/R, respectively). Consistent with this, there was no significant change in systolic left ventricular internal diameter following I/R injury in ROCK2+/- mice, nor were there changes in end diastolic and systolic volumes. Furthermore, radial

and longitudinal endocardial cardiac strain and strain rates in post-I/R ROCK2+/- mice were similar to the values observed at baseline (Table 3.2). Taken together, these results indicate that partial deletion of ROCK2 prevents the development of cardiac contractile dysfunction 24 hours after I/R injury.

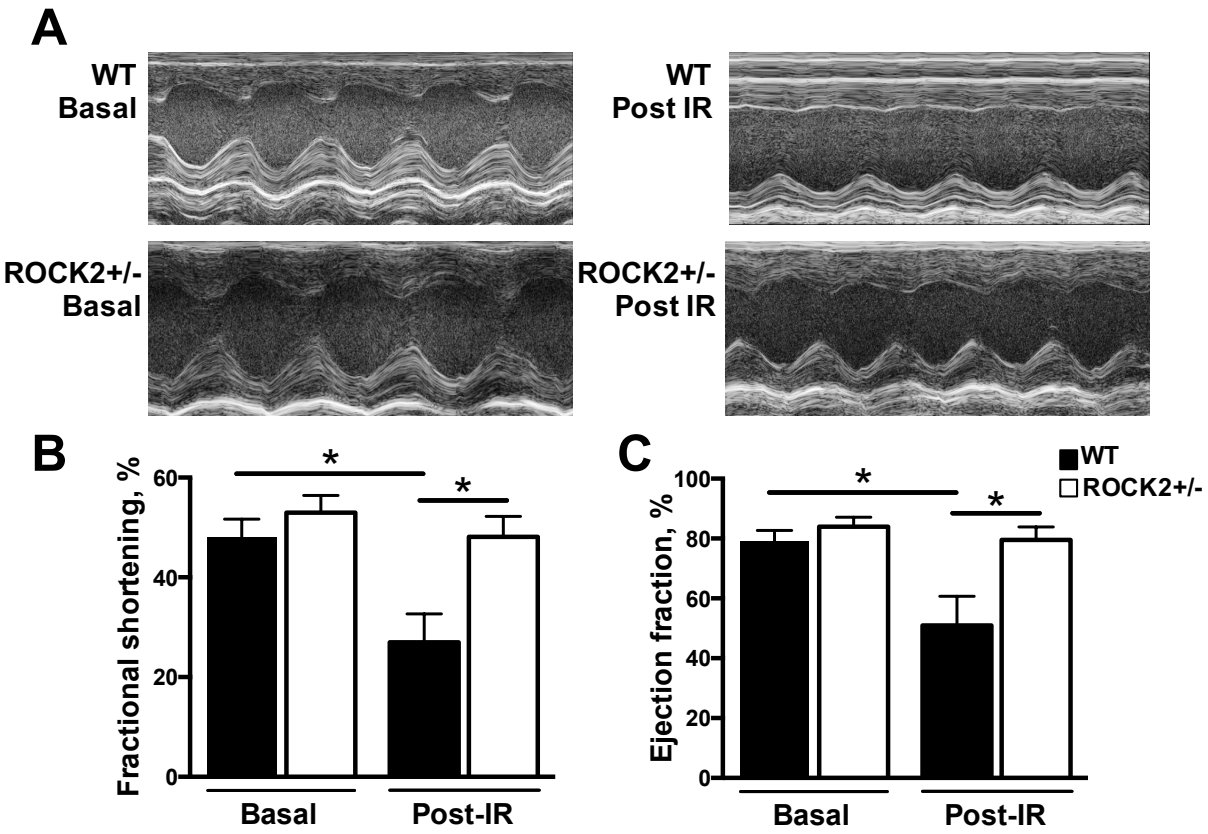

Figure 3.2 Cardiac function in WT and ROCK2+/- mice after myocardial I/R injury.

Representative images of the M-mode parasternal short-axis view of WT and ROCK2+/- mice measured before (basal) and after (post-I/R) myocardial I/R injury (A). Fractional shortening (B), and ejection fraction (C) of basal and post-I/R WT and ROCK2+/- mice (n=4-5, *p<0.05).

	Basal level		Post-I/R injury	
	WT	**ROCK2+/-**	**WT**	**ROCK2+/-**
HR (bpm)	506.8 ± 18.1	491.0 ± 18.7	496.1 ± 25.3	522.1 ± 11.7
SV (µl)	59.1 ± 5.7	56.3 ± 4.2	46.5 ± 3.1	46.7 ± 3.2
EDV (µl)	74.6 ± 5.2	68.0 ± 7.9	90.3 ± 11.7	59.7 ± 6.7
ESV (µl)	15.6 ± 2.6	11.7 ± 3.8	48.8 ± 16.2	13.0 ± 4.0
LVID, d (mm)	4.0 ± 0.4	3.9 ± 0.4	4.4 ± 0.5	3.7 ± 0.3
LVID, s (mm)	2.2 ± 0.2	1.9 ± 0.5	3.2 ± 1.0[a]	1.9 ± 0.5[b]

Table 3.1 Echocardiographic assessment of cardiac parameters before and after ischemia and 24 hours of reperfusion in WT and ROCK2+/- mice.

HR, heart rate; LV, left ventricular; SV, stroke volume; EDV, end-diastolic volume; ESV, end-systolic volume; LVID, left ventricular internal diameter; d, diastole; s, systole (n=4-5, a: $p<0.05$ compared to the corresponding basal level, b: $p<0.05$ compared to the other genotype).

	Basal level		Post-I/R injury	
	WT	**ROCK2+/-**	**WT**	**ROCK2+/-**
RADIAL				
Strain, %	26.7 ± 2.1	21.8 ± 1.4	11.8 ± 2.1[a]	23.4 ± 5.4[b]
Strain rate, 1/s	5.7 ± 0.5	5.0 ± 0.7	3.3 ± 0.5	4.7 ± 0.7
LONGITUDINAL				
Strain, %	-13.9 ± 2.1	-17.1 ± 1.9	-7.4 ± 1.2[a]	-14.1 ± 2.0[b]
Strain rate, 1/s	-4.2 ± 0.7	-5.1 ± 0.8	-2.3 ± 0.4	-4.7 ± 1.3

Table 3.2 Cardiac strain and strain rate before and after ischemia and 24 hours of reperfusion.

Radial and longitudinal measurements of endocardial strain and strain rate (n=4-5, a: $p<0.05$ compared to the corresponding basal level, b: $p<0.05$ compared to the other genotype).

3.3.3 ROCK expression and activity

As expected, total ROCK2 expression in sham-operated hearts from ROCK2+/- mice was significantly lower than their WT counterparts, but no differences in ROCK1 expression were detected, suggesting that the knockdown of ROCK2 did not cause a compensatory up-regulation of the other isoform (Fig. 3.3). Neither 2 nor 24 hours of reperfusion after ischemia had an effect on the expression of ROCK1 or ROCK2 in either WT or ROCK2+/- mice hearts (Fig. 3.3). Furthermore, despite the difference in ROCK2 expression, no significant differences in total ROCK activity were detected between sham-operated WT and ROCK2+/- hearts (Fig. 3.3 C, F). However, following ischemia and both 2 and 24 hours of reperfusion, total ROCK activity was significantly higher in

hearts from WT mice, and this increase was prevented in their ROCK2+/- counterparts (Fig. 3.3 C, F).

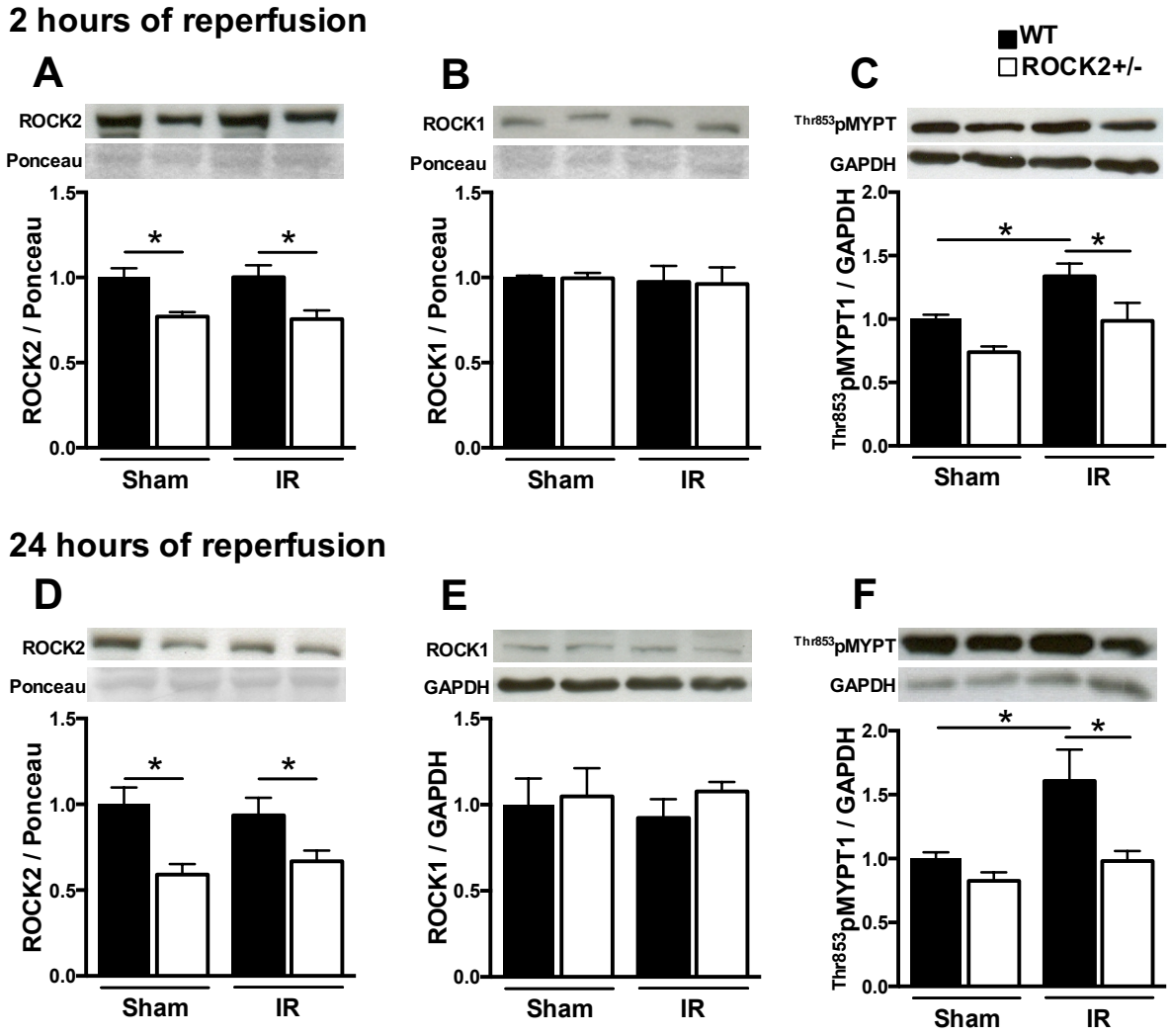

Figure 3.3 ROCK isoforms expression and ROCK activity in WT and ROCK2+/- mice hearts following I/R injury.

ROCK2 (A) and ROCK1 (B) protein expression (n=3-4, * $p<0.05$), and ROCK activity measured by MYPT phosphorylation (C) (n=4-6, * $p<0.05$) in sham and post-I/R WT and ROCK2+/- mice after 2 hours of reperfusion with western blot representative images. ROCK2 (D) and ROCK1 (E) protein expression, and ROCK activity measured by MYPT phosphorylation (F) in sham and post-I/R WT and ROCK2+/- mice after 24 hours of reperfusion (n=5-7, * $p<0.05$) with western blot representative images.

3.3.4 Activation of the RISK pathway

Since the cardioprotective effect of ROCK inhibition during I/R injury has been associated with activation of the RISK pathway, we assessed whether this pathway was activated in hearts from ROCK2+/- mice. To this end, we evaluated the phosphorylation of Akt at Ser473, which leads to its activation, as well as that of its downstream targets GSK-3β at Ser9 (leading to its inactivation), and eNOS at Ser1177 (promoting its activation). The activation of the RISK pathway occurs at the onset of reperfusion (161, 197); therefore, phosphorylation levels were evaluated after 2 hours of reperfusion.

Compared to their sham-operated controls, no changes in the levels of ^{Ser473}pAkt, ^{Ser9}pGSK-3β, or ^{Ser1177}peNOS were detected in WT hearts after myocardial I/R injury (Fig. 3.4 A, B, C). However, the levels of ^{Ser473}pAkt and ^{Ser9}pGSK-3β were significantly higher in ROCK2+/- hearts subjected to I/R than in their WT counterparts (Fig. 3.4 A, B), although no significant difference in ^{Ser1177}peNOS levels was found (Fig. 3.4 C). No significant differences in the total expression of these proteins were detected. These data suggest that at an early stage of reperfusion, the activation of the RISK pathway is at least partially responsible for the cardioprotection observed in ROCK2+/- mice subjected to I/R injury.

It has been reported that ROCK phosphorylates and activates PTEN (198), a phosphatase that acts as a negative regulator of PI3K/Akt signaling. Hence, we evaluated whether partial deletion of ROCK2 activates the RISK pathway via PTEN inactivation. However, no changes in the levels of $^{Ser380/Thr382/383}$PTEN, total PTEN or PTEN activity were detected between groups (Fig. 3.4 D, E, F) after 2 hours of reperfusion, suggesting

that the activation of the RISK pathway in ROCK2+/- hearts was not mediated via decreased PTEN activity.

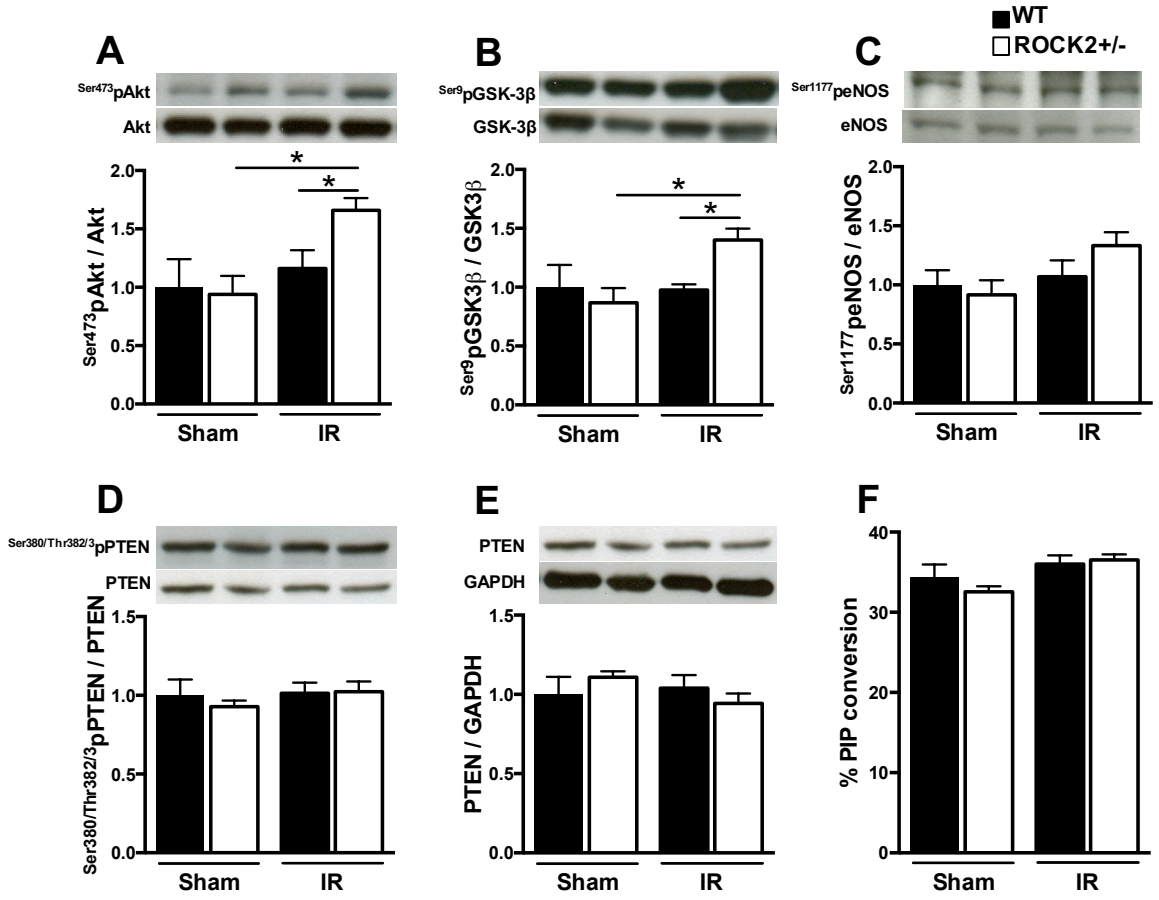

Figure 3.4 Akt and GSK-3β phosphorylation in post-I/R WT and ROCK2+/- hearts as an index of activation of the RISK pathway.

Phosphorylation levels of Akt (A), GSK-3β (B), and eNOS (C) in sham and post-I/R WT and ROCK2+/- mice after 2 hours of reperfusion (n=3-4, * $p<0.05$) with western blot representative images. Phosphorylation levels of PTEN (D), total PTEN expression (E), and PTEN activity (F) in sham and post-I/R WT and ROCK2+/- mice after 2 hours of reperfusion (n=4-6, * $p<0.05$) with western blot representative images.

3.3.5 Neutrophil infiltration and production of inflammatory mediators

Inflammation is an important mechanism involved in the development and pathophysiology of myocardial I/R injury, and one of its main characteristics is the increased production of pro-inflammatory mediators such as cytokines and chemokines. Consistent with this, in WT mice hearts subjected to I/R injury, the mRNA expression of the pro-inflammatory cytokines TNFα and IL-1β, and the chemokine MCP-1, was significantly higher than in the corresponding sham-operated WT mice hearts (Fig. 3.5 A, C and D). The mRNA expression of IL-6 had a tendency to be higher in WT mice after myocardial I/R injury, but due to high variability, no significant differences were found between the groups (Fig. 3.5 B).

Conversely, the induction of myocardial I/R injury in ROCK2+/- mice did not increase the mRNA expression of either IL-1β or IL-6, and the expression of IL-1β in post-I/R ROCK2+/- hearts was significantly decreased compared to their WT counterparts (Fig. 3.5 B and C). Furthermore, although mRNA expression of TNFα in post-I/R ROCK2+/- hearts was increased compared to their sham-operated controls, the levels were significantly lower than in post-I/R WT hearts (Fig. 3.5 A). In contrast, the mRNA expression of MCP1 was not significantly different in ROCK2+/- mice hearts subjected to I/R injury than in either their sham-operated controls or post-I/R WT hearts (Fig. 3.5 D). These data suggest that the production of pro-inflammatory cytokines induced by myocardial I/R injury is at least partially regulated by ROCK2.

It has been demonstrated that during reperfusion, neutrophils are one of the first leukocytes attracted to the myocardium, and that their levels remain elevated for at least 24 hours (41). Therefore, we evaluated whether there was a difference in neutrophil

infiltration between hearts from WT and ROCK2+/- mice 24 hours after reperfusion (Fig. 3.6). However, the number of Ly6G+ neutrophils in post-I/R ROCK2+/- hearts was not significantly different from their WT counterparts (Fig. 3.6 D). No significant neutrophil infiltration was detected in sham-operated hearts (Fig. 3.6 A).

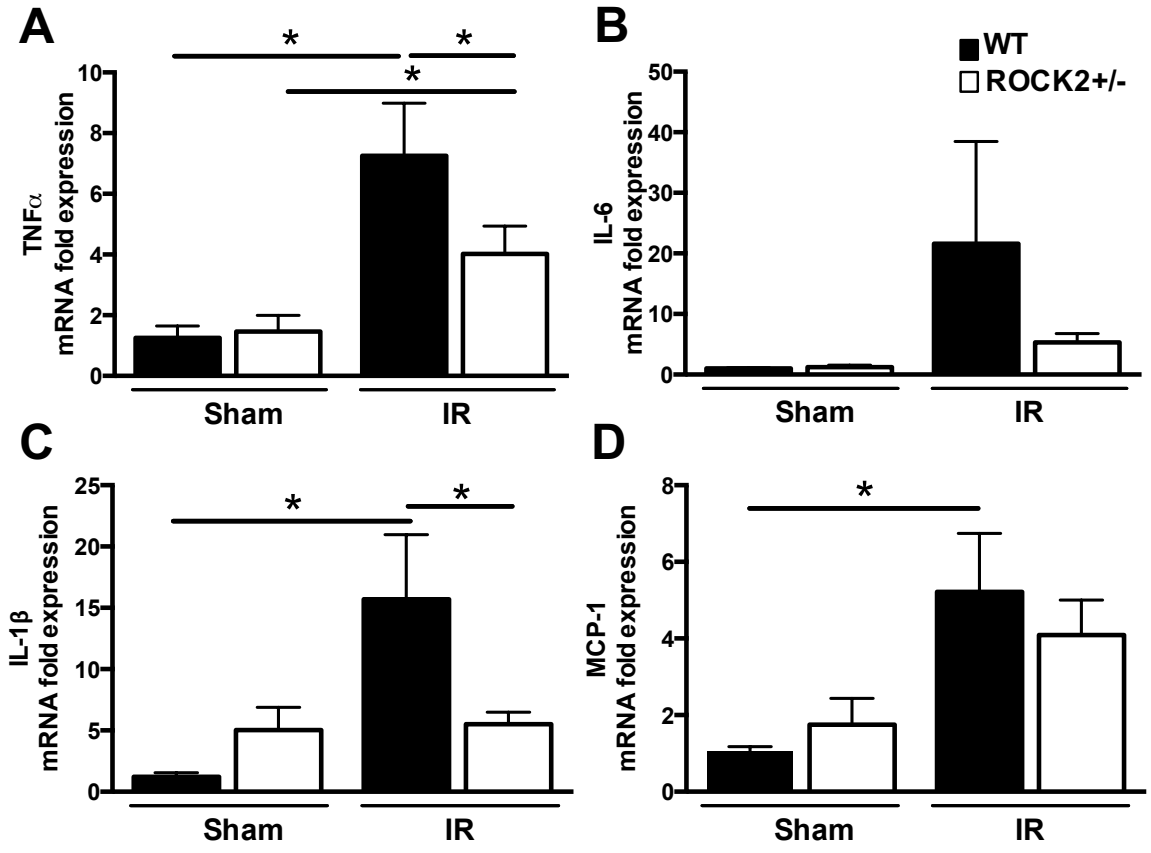

Figure 3.5 The mRNA expression of inflammatory chemokines and cytokines in post-I/R WT and ROCK2+/- hearts.

TNFα (A), IL-6 (B), IL-1β (C) and MCP-1 (D) mRNA expression of sham and post-I/R WT and ROCK2+/- hearts subjected to 24 hours of reperfusion (n=5-7, *p<0.05).

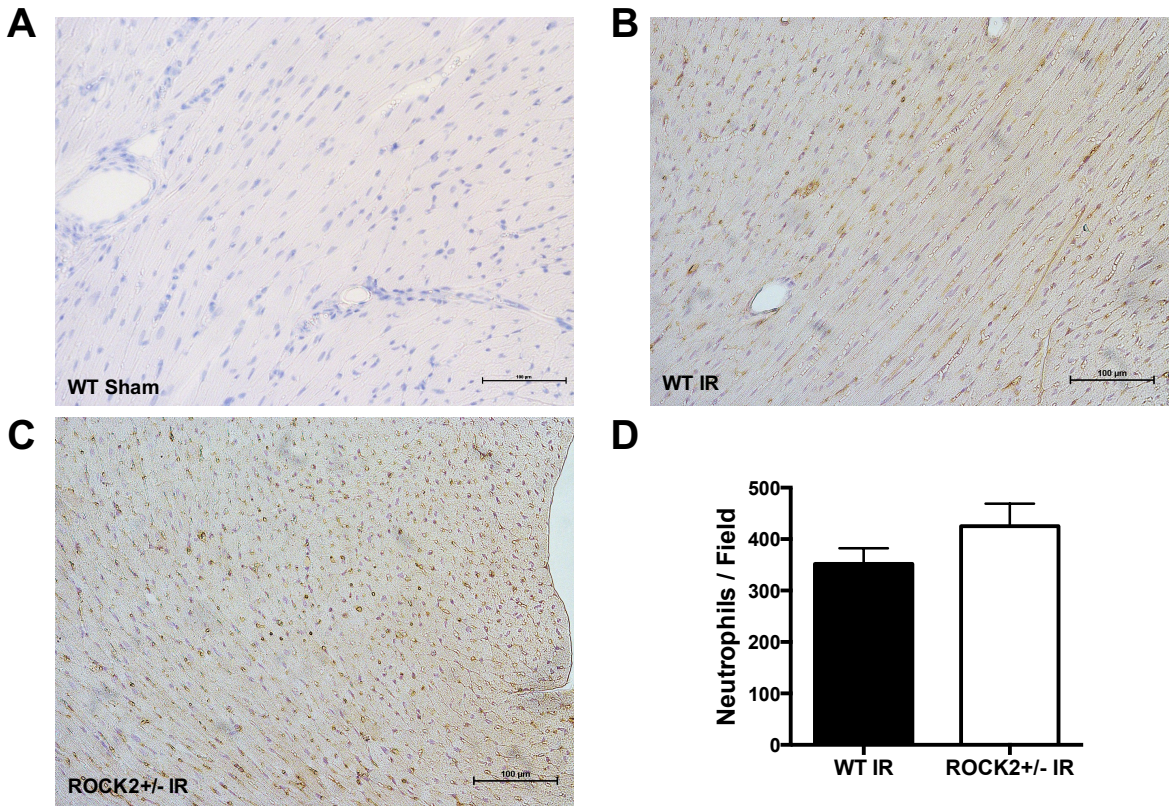

Figure 3.6 Ly6G+ neutrophil infiltration was similar in WT and ROCK2+/- hearts subjected to myocardial I/R injury.

Representative images (20x) of the Ly6G immunohistochemical staining of WT Sham (A), WT post-I/R (B), and ROCK2+/- post-I/R mice hearts (C) after 24 hours of reperfusion. Quantification of infiltrated neutrophils per field (n=3, 6 random fields per sample, $p>0.05$) (C).

3.3.6 Infarct size and RISK pathway activation in hearts from cROCK2-/- mice

In order to determine whether cardiomyocyte-specific ROCK2 expression contributes to I/R injury, we evaluated infarct size in hearts of mice with inducible cardiomyocyte deletion of ROCK2 following 40 min of ischemia and 24 hours of reperfusion. Cardiac-specific deletion of ROCK2 was confirmed by comparing the levels of expression of this protein in heart and skeletal muscle following tamoxifen treatment.

A decrease in ROCK2 expression was detected in cROCK2-/- hearts but not in cROCK2-/- skeletal muscle, where the level of expression was the same as that observed in cROCK2+/+ mice (Fig. 3.7 A). There was no significant difference between the two genotypes in the AAR following 24 hours of reperfusion. However, infarct size was 40% smaller in hearts from cROCK2-/- than from cROCK2+/+ mice, indicating that activation of ROCK2 within the cardiomyocyte compartment is sufficient to induce I/R injury (Fig. 3.7 B, C). ROCK2 expression levels of cROCK2-/- hearts were significantly lower (approximately 40%) than those observed in cROCK2+/+ hearts (Fig. 3.7 D). The remaining ROCK2 protein detected in cROCK2-/- hearts is likely due to a combination of incomplete excision from cardiomyocytes (tamoxifen knockout efficiency is 80% at most (189)), and its expression in other cardiac cells, such as fibroblasts, vascular smooth muscle cells and endothelial cells. No significant differences in ROCK2 expression were detected after inducing I/R injury (Fig. 3.7 D), consistent with the observations made in ROCK2+/- mice. Furthermore, as was also found in hearts from ROCK2+/- mice, the level of ^{Ser473}pAkt was significantly higher in cROCK2-/- than in cROCK2+/+ hearts subjected to I/R injury (Fig. 3.7 E), Altogether, these data show that the deleterious role of ROCK2 in myocardial I/R injury takes place primarily in the cardiomyocyte, and that the protection achieved by reducing the expression of this isoform is at least partially mediated by the activation of Akt.

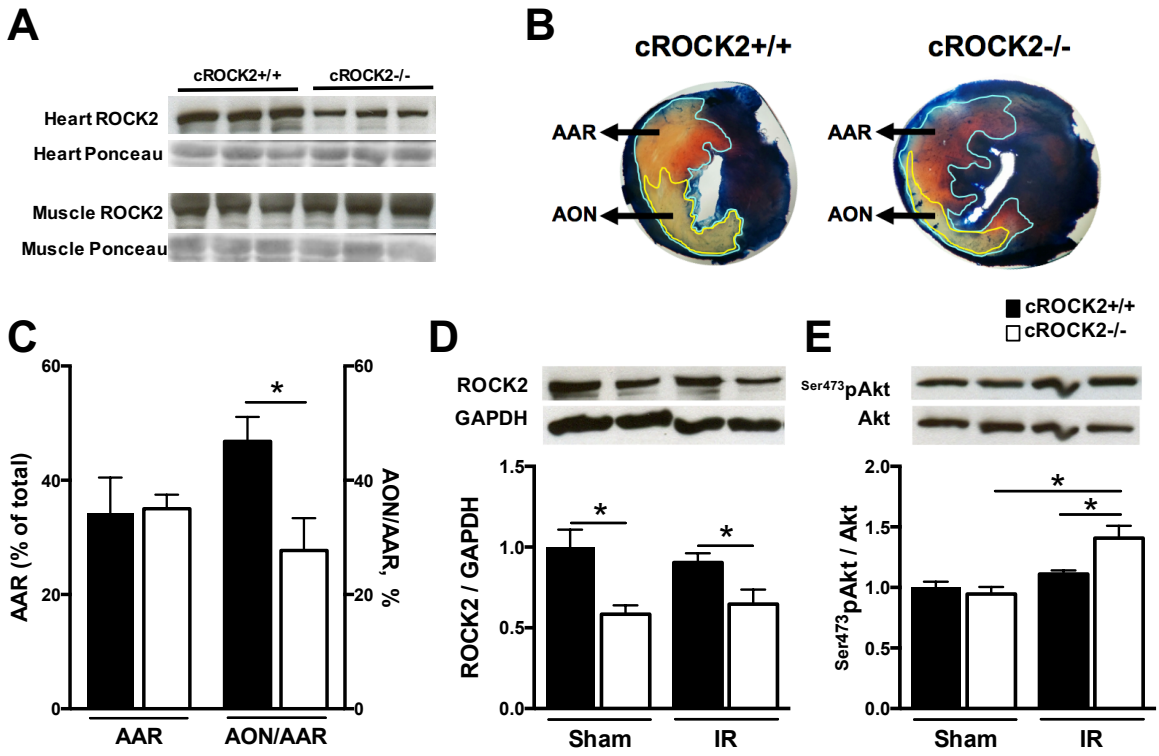

Figure 3.7 Infarct size and Akt activity in cROCK2-/- and cROCK2+/+ mice subjected to I/R injury. Western blot representative images showing that tamoxifen-induced ROCK2 knockout was specific to cardiac tissue (A). Representative images showing the AAR and AON following 40 min of ischemia and 24 hours of reperfusion in cROCK2+/+ and cROCK2-/- hearts (B). Mean AAR and infarct size (AON/AAR) (C) in cROCK2+/+ and cROCK2-/- hearts (n=6-8, *p<0.05). ROCK2 expression (D) and Akt phosphorylation (E) levels measured in sham and post-I/R cROCK2+/+ and cROCK2-/- mice after 2 hours of reperfusion (n=5-6, * p<0.05) with western blot representative images.

3.4 Discussion

In the present study, we evaluated the role of ROCK2 in the development of myocardial I/R injury. Our main findings were that decreasing the expression of ROCK2, either globally or specifically within cardiomyocytes, produced a marked and significant

reduction in infarct size. This was associated with normalized post-I/R cardiac function and less cardiomyocyte disruption in hearts from ROCK2+/- mice. Furthermore, ROCK activation induced by myocardial I/R injury was prevented in ROCK2+/- mice, leading to higher levels of Akt and GSK-3β phosphorylation at an early stage of reperfusion and to decreased production of inflammatory cytokines but not decreased neutrophil infiltration. These data suggest that activation of ROCK2, specifically in the cardiomyocyte compartment, plays an important role in promoting I/R injury in the heart by suppressing activation of cardioprotective Akt signaling and promoting an inflammatory response.

To our knowledge, this is the first time that the contribution of a specific ROCK isoform to myocardial I/R injury has been demonstrated. Although there is a high degree of similarity between the two ROCK isoforms, each of them has been shown to have non-redundant roles (126, 128). For example, it has been demonstrated that ROCK2 binds directly to and phosphorylates MYPT1 (134), that ROCK1 does the same with Rho-GTPase RhoE (199), and that each isoform appears to have specific roles in the regulation of insulin signaling (195, 196, 200). The differences between these two isoforms could be due to alternate mechanisms by which they are activated in different situations, as well as cell-specific variations in their expression levels and protein interactions (128).

Both ROCK1 and ROCK2 have been shown to be expressed in the heart (201), although their relative contribution to total ROCK activity has not been elucidated. In the present study, a similar level of ROCK activity was observed in sham-operated hearts from WT and ROCK2+/- mice despite the lower level of ROCK2 expression in the latter. This suggests that under normal conditions, ROCK1 may contribute to a greater extent

than ROCK2 to basal ROCK activity. On the other hand, the increase in ROCK activity detected in hearts from WT but not ROCK2+/- mice subjected to I/R injury suggests that ROCK2 may be activated to a greater extent than ROCK1 following I/R injury. The reason why ROCK activation was completely prevented following I/R injury in hearts from mice with only a partial decrease in ROCK2 expression is not clear. However, these data are consistent with the results of our recent study, in which the increase in ROCK2 activity seen in hearts of WT mice fed a high fat diet was completely prevented in hearts from ROCK2+/- mice (196). In contrast to our data showing that ROCK isoform expression was unchanged following 40 min of ischemia, Zhang et al. (202) reported that the expression of both isoforms increased in rat hearts subjected to 30 min of ischemia and 3 hours of reperfusion, suggesting that there may be species-related differences in the effect of I/R on ROCK isoform expression in the heart.

That ROCK2 is the isoform responsible for promoting the deleterious cardiac effects of myocardial I/R injury is supported by our observations that infarct size and reduced cardiac strain were attenuated in hearts from ROCK2+/- mice, and cardiac function was preserved. On the other hand, very little is known about the role of ROCK1 in myocardial I/R injury. Haudek et al. (203) reported that ROCK1-/- mice hearts subjected to repeated periods of occlusion and reperfusion over a week did not develop the fibrosis characteristic of this model, consistent with a role for ROCK1 in promoting cardiac fibrosis in pathological conditions (144). Also, Zhang et al. (202) suggested that the extracellular signal-regulated kinase/mitogen-activated protein kinase pathway opposes ROCK1 during ischemic preconditioning. However, whether ROCK1 inhibition is cardioprotective during the development of I/R injury remains to be investigated.

The activation of cardioprotective signaling pathways at the onset of reperfusion reduces the extent of cell death caused by myocardial I/R injury (47). The RISK pathway, one of the first signaling pathways shown to antagonize I/R injury, can be activated by a variety of endogenous and external signals that bind to receptors such as G-protein coupled receptors and growth factor receptors. This pathway involves a series of pro-survival kinases that ultimately lead to the reduction of cardiac damage (47). In the present study, increased phosphorylation of Akt and its downstream target GSK-3β were detected after 2 hours of reperfusion in hearts from ROCK2+/- mice, although there was no change in phosphorylation of either kinase in hearts from WT mice. This suggests that decreasing ROCK2 expression, which prevented the I/R-induced increase in ROCK activity, permitted an increase in phosphorylation and activation of Akt. One possible explanation for this is that in WT hearts, an I/R-induced increase in ROCK2 activity opposes activation of intrinsic cardioprotective signaling through Akt. Furthermore, it is possible that the activation of this cardioprotective pathway might begin at an even earlier stage, given that we were unable to detect evidence of eNOS activation at this time point. Previous studies that evaluated the cardioprotective activity of ROCK inhibitors against the development of myocardial I/R injury have found a significant increase in Ser 1177 phosphorylation of eNOS only at very short times of reperfusion (7-10 minutes) (160, 204). Altogether, these results suggest that the reduction of myocardial infarct size observed in ROCK2+/- mice hearts was at least partly due to the prompt activation of the RISK pathway.

It has been reported that ROCK is capable of phosphorylating and activating PTEN, leading to decreased activation of Akt (198), while genetic deletion of PTEN has

been shown to decrease the extent of myocardial I/R injury (205). Therefore, we hypothesized that the activation of the RISK pathway induced by the partial deletion of ROCK2 was mediated by a decrease in PTEN activity. However, no changes in the activity of PTEN, or in its expression or phosphorylation could be detected in hearts from ROCK2+/- mice following I/R, suggesting that ROCK2 does not suppress Akt activation by modulating PTEN activity in I/R injury. PI3K/Akt signaling can be activated by a myriad of mediators, and it is possible that the activation of this pathway via ROCK2 partial deletion is modulated by a less direct mechanism.

I/R injury elicits an inflammatory response that, although necessary for cardiac repair, has been shown to contribute to the pathophysiology of this condition. Hypoxia, increased ROS production, mechanical stretch, and other stress signals that are characteristic of myocardial I/R injury, stimulate toll-like receptors that subsequently activate NFκB, a redox-sensitive transcription factor that promotes the production of pro-inflammatory cytokines and chemokines in resident cardiac cells, such as cardiomyocytes, fibroblasts, endothelial cells, adipocytes and inflammatory cells (206). These cytokines and chemokines then stimulate the recruitment of circulating inflammatory cells such as neutrophils and monocytes/macrophages that further amplify the production of these pro-inflammatory elements (206). The decreased production of TNFα, IL-1β and IL-6 found following I/R injury in hearts from ROCK2+/- mice suggests that the inflammatory response is reduced in hearts from these animals, and is consistent with previous studies showing a decrease in I/R-induced inflammatory cytokine production following pre-treatment with non-isoform selective ROCK inhibitors (162). This could be the indirect result of activation of the RISK pathway, since this is

associated with decreased opening of the MPTP, reducing the increase in ROS production (12) and the subsequent inflammatory response. However, it is also possible that ROCK2 activation results in direct stimulation of NFκB, promoting mRNA expression of inflammatory cytokines, since a role for ROCK2 in activating NFκB has been reported (207).

Interestingly, the decrease in cytokine production following induction of I/R injury in hearts from ROCK2+/- mice was not associated with a decrease in neutrophil infiltration after 24 hours, since we did not observe a significant difference in neutrophil count between post-IR ROCK2+/- and WT mice hearts. This is in contrast with previous studies in which non-selective ROCK inhibitors were shown to reduce neutrophil infiltration (158, 162). Leukocyte infiltration is initiated by the chemoattraction promoted by pro-inflammatory cytokines, but in order to move from the circulation into the affected tissue, leukocytes must undergo transendothelium migration (208). It is possible that ROCK2 has a greater role in activating the pathways that lead to the transcription of pro-inflammatory cytokines, while ROCK1 has a more downstream role in leukocyte recruitment. This is supported by studies in a vascular injury model induced by carotid artery ligation, in which ROCK1+/- but not ROCK2+/- mice showed lower leukocyte migration due to the reduced induction of endothelial adhesion molecules (209).

Nevertheless, it is important to highlight that despite the failure to reduce leukocyte infiltration in the present study, the partial deletion of ROCK2 was able to successfully lower infarct size and preserve cardiac function. Our observation that the latter was also found in hearts from mice with cardiomyocyte-specific loss of ROCK2 is consistent with a lesser role for immune cells in the cardioprotection offered by reduced

expression of ROCK2. This is supported by the finding that the activation of Akt was also observed in cROCK2-/- hearts subjected to I/R injury, suggesting that the activation of Akt signaling is the primary mechanism by which ROCK2 inhibition counteracts the development of myocardial I/R injury.

In conclusion, the results of the present study implicate ROCK2 as an important contributor to I/R injury in the heart, through suppression of cardioprotective Akt signaling and inflammation. Although we did not investigate the potential contribution of ROCK1 to I/R injury, the observation that lowering ROCK2 expression both globally and specifically within cardiomyocytes produced a significant reduction in infarct size and preserved cardiac function in ROCK2+/- mice, suggests that the selective inhibition of the ROCK2 isoform could represent a new form of treatment against myocardial I/R injury. Given that a selective ROCK2 inhibitor is now in clinical trials (210), this has potentially important translational implications.

Chapter 4: Diabetes impairs the cardioprotective effect of cardiomyocyte-specific ROCK2 deletion in myocardial I/R injury

4.1 Introduction

Every year, more than 55,000 people in Canada suffer a myocardial infarction for the first time (211). Moreover, it has been estimated that 20% of these patients will suffer a second infarct after only three years (4). When a myocardial infarction occurs, reperfusion must be promptly instituted in order to avoid cell death due to myocardial ischemia (5). However, the sudden return of oxygen and nutrients to the myocardium induces a type of myocardial damage known as I/R injury.

Compared to non-diabetics, patients with diabetes are more likely to suffer a myocardial infarction. For instance, their risk of suffering a myocardial infarction for the first time is as high as the one non-diabetic patients with a previous myocardial infarction have (80). Because of this, those with diabetes are also more susceptible to myocardial I/R injury, and more sensitive to its deleterious effects, with larger infarcts, lower ejection fraction after I/R, and greater mortality (84, 85).

ROCK is a serine/threonine kinase involved in many physiological functions, such as, cell migration, adhesion and motility, as well as smooth muscle contraction (125). However, its overactivation has been implicated in the development of many pathological conditions. In myocardial I/R injury, the administration of ROCK inhibitors, before or at the time of reperfusion, has been described as a cardioprotective (158-161). There are two isoforms of ROCK: ROCK1, which is expressed in all human tissues except brain and muscle, and ROCK2, which is mostly expressed in brain, muscle, heart,

lungs and placenta (127). In the previous study of this thesis (Chapter 3), we found that the over-activation of ROCK2 was involved in the development of myocardial I/R injury, and that the cardiomyocyte was at least partly responsible for this response.

Given the prevalence of myocardial I/R injury among diabetic patients, it is important that cardioprotection against the development of I/R is also evaluated under diabetic conditions. Previous studies from our lab have demonstrated that ROCK plays an important role in the development of diabetic cardiomyopathy, a condition defined as ventricular dysfunction that occurs independently of changes in vascular function, coronary artery disease or hypertension (155). Moreover, further research has shown that in diabetic rat hearts, ROCK2 expression is increased, while the expression levels of ROCK1 are similar at both diabetic and non-diabetic conditions, suggesting that this isoform is the one involved in the development of diabetic cardiomyopathy (157). Therefore, the main objective of the present study was to evaluate the role of cardiomyocyte-ROCK2 in the development of myocardial I/R injury during diabetes.

4.2 Materials and methods

4.2.1 Animals

ROCK2$^{flox/flox}$ mice were generated as described by Okamoto et al. (142). In order to obtain cardiac-specific ROCK2 knockouts, these mice were crossed with mice expressing the αMHC-*MerCreMer* transgene. After 4 generations, ROCK2$^{flox/flox}$-α-MHC-*MerCreMer* and ROCK2$^{flox/flox}$-non-α-MHC-*MerCreMer* mice were obtained. At 8 weeks of age, male ROCK2$^{flox/flox}$-αMHC-*MerCreMer* mice and their ROCK2$^{flox/flox}$ non-αMHC-*MerCreMer* littermate controls were treated with 20 mg/kg of tamoxifen diluted

in corn oil by intraperitoneal injection for 5 consecutive days in order to generate cROCK2-/- and cROCK2+/+ mice (189). At 12 weeks of age, mice were treated for 5 consecutive days with 50 mg/kg/day of streptozotocin (STZ) or its citrate buffer (0.1 M, pH 4.5) vehicle. Male cROCK2-/- and ROCK2 cROCK2+/+ mice were used in all experiments.

This investigation conforms to the Canadian Council on Animal Care Guidelines on the Care and Use of Experimental Animals and the Guide for Care and Use of Laboratory Animals published by the United States National Institutes of Health (NIH publication no. 85–23, revised 1996). All protocols were approved by the University of British Columbia Animal Care Committee.

4.2.2 *In vivo* myocardial I/R injury and echocardiography measurements

Using One Touch Ultra test strips and the One Touch Ultra 2 glucometer (LifeScan, Burnaby, BC, Canada), non-fasting blood glucose levels were measured 4 weeks after STZ treatment. Mice were considered diabetic if non-fasting blood glucose levels were at 18 mM or higher. Basal cardiac function, cardiac dimensions, and cardiac strain were then determined using the Vevo 2100 echocardiography system (Fujifilm VisualSonics, ON, Canada). Briefly, mice were anesthetized with 4-4.5% isoflurane, and then maintained at 1% isoflurane for the remainder of the procedure. Body temperature was maintained at 37±0.5°C, and all echocardiographic measurements were done at a heart rate of 475±25 bpm. Mice were positioned at a parasternal short-axis view, and using scans obtained by 2-D M-mode, fractional shortening, ejection fraction, and cardiac dimensions were calculated. B-mode long-axis view images were then used to calculate

radial and longitudinal endocardial strain and strain rate using Speckle tracking with VevoStrain software (Fujifilm VisualSonics, ON, Canada).

Myocardial I/R injury was induced *in vivo* 48 hours later, by transient ligation of the LAD coronary artery. In brief, mice were anesthetized using a ketamine/xylazine mixture. Non-diabetic mice received 80 and 5 mg/kg of ketamine and xylazine, respectively; while diabetic mice received 40 and 1.25 mg/kg. If diabetic mice were still active after 10 minutes, the ketamine/xylazine mixture was administered a second time. Mice were then intubated using a 22G catheter, and ventilated with a mixture of oxygen and isoflurane (1-2%). Bupivacaine (0.25%, subcutaneous) was injected at the incision site, and pre-operative buprenorphine (0.05 mg/kg for control mice and 0.025 mg/kg diabetic mice, subcutaneous) was provided.

A left side thoracotomy was performed between the 3rd and 4th rib, and the LAD coronary artery was ligated with 8-0 Vicryl suture. Blanching of the surrounding tissue was considered evidence that the ligation was successful. In sham-operated mice, the suture was passed under the LAD coronary artery, but the ligation was not performed. After 40 minutes of ischemia, reperfusion was instituted by carefully removing the knot, and the chest was then closed using 6-0 Vicryl suture. No significant differences were found in the mortality rates of cROCK2+/+ and cROCK2-/- mice (9.7% vs. 5.4%, respectively, p=0.28), or non-diabetic and diabetic mice (6.8% vs. 8.3%, respectively, p=0.92). All deaths occurred in the first 40 minutes of reperfusion, possibly due to pneumothorax or arrhythmia (191, 192).

After 24 hours of reperfusion, cardiac function, cardiac dimensions and cardiac strain were re-evaluated by echocardiography as described above. Mice were then

euthanized. Blood was collected and serum was separated centrifuging at 3000 rpm for 15 minutes, while hearts and skeletal muscles were quickly excised and snap frozen with liquid nitrogen. Tissues were stored at -80°C until further analysis. Another set of mice hearts were subjected to 40 min of ischemia and 2 hours of reperfusion, and tissues were collected and stored as previously described.

4.2.3 Infarct size measurement

Using a modified version of the protocol proposed by Bohl et al. (193), we measured infarct size in mice subjected to 24 hours of reperfusion. Briefly, mice were anesthetized with 4-4.5% isoflurane, and hearts were quickly excised and placed in ice-cold Krebs-Henseleit buffer. The aorta was cannulated using a 20G blunted needle, and the heart was then perfused in order to remove residual blood. The LAD coronary artery was re-ligated at the same position, and the remote myocardium was stained by perfusing 1.5% Evans blue dye solution. Hearts were semi-frozen by placing them at -20°C for 15 minutes, and then cut into 6 thin short-axis slices. The heart slices were thawed and washed in PBS. Afterwards, they were incubated in a 1% solution of TTC at 37°C for 20 min. Heart slices were blotted and placed in 10% formalin for 20 minutes at room temperature. Finally, they were weighed, placed between glass slides, and photographed under a stereomicroscope. Infarct size was calculated as the percentage of AON relative to AAR; these measurements were made using ImageJ v1.46 r (NIH, Bethesda, MD).

4.2.4 Serum lactate dehydrogenase levels

Levels of lactate dehydrogenase (LDH) were measured in serum of mice subjected to ischemia and 2 hours of reperfusion using the QuantiChrom™ Lactate Dehydrogenase Kit (BioAssay Systems, Hayward, CA). The protocol provided by the manufacturer was followed.

4.2.5 Neutrophil infiltration

The apex of mouse hearts subjected to 24 hours of reperfusion was fixed in 10% formalin for 48 hours. At the end of this fixing period, tissues were washed with PBS buffer, and embedded in paraffin. Sections of 5μm thickness were prepared, in order to evaluate Ly6G+ neutrophil infiltration by IHC staining. Paraffin-embedded sections were deparaffinized using xylene, and then re-hydrated with a series of graded concentrations of ethanol. Sections were placed in citrate buffer (pH 6), and heated using a microwave (2 minutes at high power and 20 minutes at 20% power) in order to perform antigen retrieval. Sections were then placed in a 0.6% peroxide solution in methanol for 15 min to block endogenous peroxidase activity. Sections were blocked for 25 minutes with 1% BSA in PBS, and then incubated in anti-mouse Ly-6G primary antibody (Clone 1A8, BioLegend, San Diego, CA) overnight at 4°C. The following day, sections were incubated in Ig biotinylated antibody (SouthernBiotech, Birmingham, AL) for 45 minutes at room temperature. Incubation with streptavidin poly-HRP (Pierce-Thermo Fisher Scientific, Waltham, MA) for 45 minutes at room temperature was then performed. Finally, a 3,3' diaminobenzidine color development solution was added, and hematoxylin was used as a counterstain. Neutrophil infiltration was determined by counting the

number of neutrophils in 3 randomly selected fields using a microscope at 20x magnification.

4.2.6 Extraction of mRNA and RT-PCR

Total RNA was extracted from both diabetic and non-diabetic mouse hearts subjected to 24 hours of reperfusion. Frozen heart tissue (30 to 50 mg) was homogenized in TRIzol (Invitrogen, Carlsbad, CA), and the isolation was performed as described by the manufacturer. The SuperScript VILO cDNA Synthesis kit (Invitrogen, Carlsbad, CA) was then used to perform reverse transcription of 1 μg of total RNA to cDNA. Afterwards, RT-PCR was performed on an Applied Biosystems StepOnePlus system, using SYBR Select Master Mix (Applied Biosystems, Foster City, CA). The sequences of each primer were the following: IL-1β (F): AGATGAAGGGCTGCTTCC, IL-1β (R): CTGCCTGAAGCTCTTGTTG (designed using AutoPrime 1.0 software, www.autoprime.de), TNFα (F): AGGTTCTCTTCAAGGGACAAG, TNFα (R): GCAGAGAGGAGGTTGACTTT, 36B4 (F): AGATGCAGCAGATCCGCAT, 36B4 (R): GTTCTTGCCCATCAGCACC (195). The concentration of mRNA in each heart was quantified using the 2-ΔΔCT method.

4.2.7 Western blot analysis

Protein expression and phosphorylation of mouse hearts subjected to 2 and 24 hours of reperfusion were measured by western blot. Frozen heart tissue samples were homogenized in RIPA buffer (Tris HCl 50 mM pH 7.4, NP-40 1%, SDS 0.1%, sodium deoxycholate 0.5%, NaCl 150 mM, EDTA 2 mM and protease and phosphatase

inhibitor). The proteins in each sample were separated on 8-10% SDS-PAGE gels, and transferred to PVDF membranes. Proteins were then immunoblotted with antibodies to ROCK2 (Santa Cruz Biotechnology, Santa Cruz, CA), ROCK1 (BD Biosciences, Franklin Lakes, NJ), ^{Tyr612}p-IRS-1 (Thermo Fisher Scientific, Waltham, MA), IRS-1, ^{Ser473}p-Akt, Akt, ^{Ser9}p-GSK-3β, GSK-3β, ^{Ser1177}p-eNOS, eNOS, $^{Ser380/Thr382/383}$p-PTEN, PTEN, ^{Tyr458}p85 p-PI3K, p85 PI3K, ^{Ser536}p65 p-NFκB, and p65 NFκB (Cell Signaling, Danvers, MA), then incubated in secondary anti-mouse or anti-rabbit antibody. ImageJ v1.46 r (NIH, Bethesda, MD) was used to perform densitometry and measure band density. GAPDH (Santa Cruz Biotechnology, Santa Cruz, CA), Ponceau staining, or the corresponding total protein, were used to normalize protein expression.

4.2.8 ROCK activity assay

In order to measure the level of ROCK activity in diabetic and non-diabetic mice hearts subjected to 2 and 24 hours of reperfusion, a ROCK activity assay was performed. Frozen heart tissue was homogenized in non-denaturing lysis buffer (50 mM Tris-HCl, 150 mM NaCl, 1mM EDTA, 1mM EGTA, 1mM Na_3VO_4, 1mM 2-glycerolphosphate, 1% Non-Idet P-40, 1x protease inhibitors, pH 7.5). A 10x concentration of assay buffer (250 mM Tris-HCl, 100 mM $MgCl_2$, 50 mM glycerol-2-phosphate, 1 mM Na_3VO_4, 10 mM DTT, 5 mM ATP, 0.2 μg/ml truncated MYPT1 $^{(654-880)}$, pH 7.5) was added to each sample, and they were then incubated for 30 minutes at constant agitation at 30ºC. At the end of this incubation period, Laemli buffer was added and samples were heated at 90ºC for 5 minutes. In order to measure ROCK activity, the phosphorylation level of ^{Thr853}MYPT1 was evaluated using western blotting. Protein phosphorylation was

normalized against GAPDH (Santa Cruz Biotechnology, Santa Cruz, CA) and quantified by densitometry as mentioned above.

4.2.9 Statistical analysis

Data are expressed as means ± SE, and n refers to the number of mice in each group. GraphPad Prism version 5.00 for Mac (GraphPad Software, San Diego, CA) was used to analyze all results, and one-way ANOVA followed by the Neuman-Keuls test was used to determine statistical significance. Results were considered statistically significant at a value of $p<0.05$.

4.3 Results

4.3.1 General characteristics of diabetic cROCK2+/+ and cROCK2-/- mice

Four weeks after STZ treatment, both cROCK2+/+ and cROCK2-/- mice had significantly higher levels of non-fasting blood glucose than those injected with citrate buffer vehicle (Table 4.1). In the group of mice subjected to 24 hours of reperfusion, the levels of non-fasting blood glucose were similar for both genotypes; however, in those subjected to 2 hours of reperfusion, the blood glucose of diabetic cROCK2-/- mice was slightly higher than the one detected in diabetic cROCK2+/+ mice (Table 4.1). Similarly, in mice subjected to 24 hours of reperfusion, the body weight of diabetic cROCK2+/+ and cROCK2-/- mice were significantly lower than those detected in their non-diabetic counterparts. In mice subjected to 2 hours of reperfusion, the weight of diabetic cROCK2-/- mice was significantly lower compared to mice injected with vehicle (Table 4.1). In mice subjected to either 2 or 24 hours of reperfusion, no significant differences

on heart weight or heart to body weight ratio were detected among groups (Table 4.1). Altogether, these results demonstrate that mice were rendered diabetic four weeks after STZ treatment.

	Group	Blood glucose (mM)	Body weight (g)	Heart weight (mg)	Heart/Body weight ratio
2 hours of reperfusion	Sham cROCK2+/+	9.2 ± 0.8	30.8 ± 0.4	154.1 ± 3.8	5.0 ± 0.2
	Sham cROCK2-/-	8.7 ± 0.5	30.8 ± 1.3	159.4 ± 7.9	5.0 ± 0.3
	IR-Cit cROCK2+/+	8.7 ± 0.3	31.0 ± 0.8	148.6 ± 8.2	4.9 ± 0.2
	IR-Cit cROCK2-/-	9.2 ± 0.1	33.0 ± 1.2	163.8 ± 7.3	5.0 ± 0.2
	IR-STZ cROCK2+/+	27.2 ± 1.9[a]	28.0 ± 0.7	135.0 ± 3.0	4.9 ± 0.1
	IR-STZ cROCK2-/-	31.9 ± 0.9[ab]	26.2 ± 0.7[a]	140.5 ± 8.0	5.4 ± 0.2
24 hours of reperfusion	Sham cROCK2+/+	10.1 ± 0.8	32.0 ± 1.1	168.9 ± 13.6	5.2 ± 0.2
	Sham cROCK2-/-	9.6 ± 0.9	30.8 ± 0.2	155.3 ± 8.7	5.1 ± 0.3
	IR-Cit cROCK2+/+	8.9 ± 0.2	30.6 ± 0.6	169.3 ± 11.1	5.5 ± 0.4
	IR-Cit cROCK2-/-	8.8 ± 0.4	30.0 ± 0.8	169.2 ± 6.7	5.7 ± 0.2
	IR-STZ cROCK2+/+	28.5 ± 1.7[a]	27.0 ± 0.7[a]	145.7 ± 7.8	5.4 ± 0.3
	IR-STZ cROCK2-/-	29.7 ± 0.9[a]	26.0 ± 1.5[a]	138.5 ± 6.8	5.5 ± 0.4

Table 4.1 Characteristics of non-diabetic and diabetic cROCK2-/- and cROCK2+/+ mice subjected to ischemia and 2 or 24 hours of reperfusion.

Blood glucose and body weight were measured before surgery, while heart weight and heart/body weight ratio were recorded at the end of the reperfusion period. Sham: sham-operated non-diabetic mice, IR-Cit: non-diabetic mice subjected to I/R injury, IR-STZ: diabetic mice subjected to I/R injury (n=5-6 for both times of reperfusion; a: $p<0.05$ compared to Sham and IR-Cit mice, b: $p<0.05$ vs. their cROCK2+/+ counterparts).

4.3.2 Infarct size and the extent of I/R injury in diabetic cROCK2-/- mice

In order to evaluate the effect of cardiomyocyte-specific ROCK2 deletion on the development of myocardial I/R injury under diabetic conditions, we measured the infarct size of diabetic cROCK2-/- mice subjected to 40 minutes of ischemia and 24 hours of reperfusion. There were no significant differences in the AAR of cROCK2+/+ and cROCK2-/- mice, whether non-diabetic or diabetic, suggesting that the LAD ligation was similar in all hearts (Fig. 4.1 A, B). As reported in the previous chapter, infarct size, measured as the ratio of AON to AAR, was significantly lower in non-diabetic-cROCK2-/- mice than in their ROCK2 expressing counterparts, consistent with a cardioprotective effect of cardiomyocyte ROCK2 deletion. In contrast, infarct size was significantly greater in diabetic than non-diabetic cROCK2-/- mice while there were no significant differences in infarct size between diabetic cROCK2-/- and cROCK2+/+ mice (Fig. 4.1 A, C), suggesting that the cardioprotection provided by the cardiac-specific knockout of ROCK2 is abolished under diabetic conditions.

Levels of LDH in serum were evaluated after ischemia and 2 hours of reperfusion, as an additional measure of cardiac injury and necrosis. Serum LDH tended to be higher in non-diabetic cROCK2+/+ mice, while there was no detectable elevation in serum LDH levels in non-diabetic cROCK2-/- mice, compared to sham-operated mice (Fig. 4.1 D). However, in contrast to both their sham-operated and post-I/R non-diabetic counterparts, diabetic cROCK2-/- mice subjected to myocardial I/R injury had significantly higher serum LDH levels (Fig. 4.1 D). These results are consistent with those of the infarct size measurement, since they suggest that cROCK2-/- mice are more susceptible to the deleterious effects of myocardial I/R injury under diabetic than non-diabetic conditions.

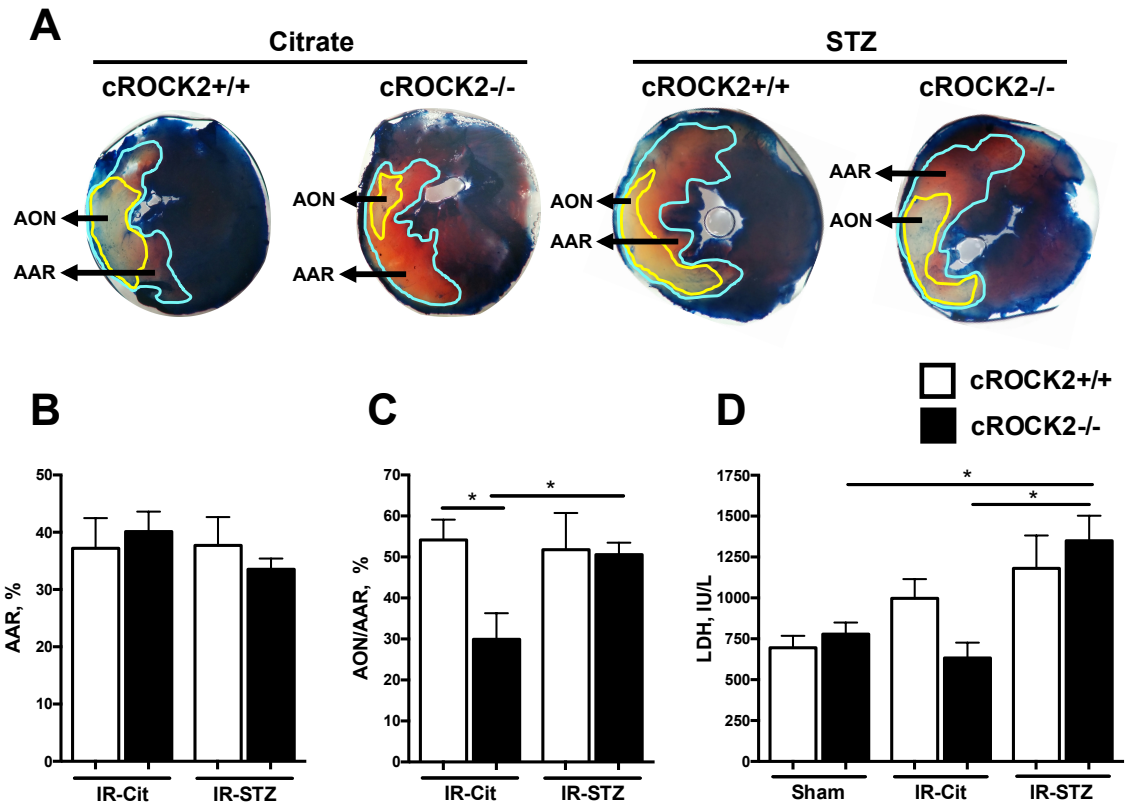

Figure 4.1 Effects of STZ-diabetes on infarct size in hearts from cROCK2-/- and cROCK2+/+ mice. Representative images showing the AAR and AON following 40 min of ischemia and 24 hours of reperfusion in non-diabetic and diabetic cROCK2+/+ and cROCK2-/- hearts (A). Mean AAR (B) and mean infarct size (C), calculated as the ratio of AON to AAR in non-diabetic (Cit) and diabetic (STZ) cROCK2+/+ and cROCK2-/- hearts (n=6-8, *p<0.05). LDH levels after inducing ischemia and 2 hours of reperfusion (D) (n=5-6, *p<0.05).

4.3.3 Cardiac function and cardiac strain before and after myocardial I/R injury

Cardiac function and cardiac dimensions, as well as cardiac strain, were also evaluated by echocardiography prior to, and 24 hours after the induction of I/R injury in non-diabetic and diabetic cROCK2+/+ and cROCK2-/- mice. No differences in basal

cardiac function or dimensions could be detected between any of the groups prior to induction of I/R injury. Furthermore, although hearts in all groups had a tendency to perform worse after I/R injury, no significant differences in fractional shortening or ejection fraction could be detected between basal and post-I/R mice (Table 4.2). Likewise, cardiac strain, a measure of tissue deformation, and strain rate, a measure of the time-course of deformation, were similar in all groups both basally and post/I-R (Table 4.3).

Parameter (units)	Non-diabetic				Diabetic			
	cROCK2+/+		cROCK2-/-		cROCK2+/+		cROCK2-/-	
	Basal	Post-I/R	Basal	Post-I/R	Basal	Post-I/R	Basal	Post-I/R
HR (bpm)	508.0 ± 21.4	472.7 ± 10.8	501.3 ± 6.9	490.2 ± 4.2	484.4 ± 5.6	461.0 ± 11.7	495.9 ± 5.8	468.1 ± 8.9
CO (mL/min)	19.7 ± 1.6	16.3 ± 1.6	17.5 ± 1.4	17.1 ± 0.7	18.4 ± 0.9	14.7 ± 0.3	18.3 ± 0.8	15.7 ± 1.1
SV (µl)	38.7 ± 2.3	34.4 ± 2.9	34.9 ± 2.7	34.9 ± 1.4	38.0 ± 1.8	32.1 ± 0.9	36.9 ± 1.5	33.5 ± 2.2
EDV (µl)	45.0 ± 3.2	42.8 ± 2.8	38.9 ± 3.2	51.8 ± 6.7	45.6 ± 2.9	37.5 ± 0.8	44.0 ± 2.5	37.6 ± 1.0
ESV (µl)	5.2 ± 0.4	5.6 ± 0.5	4.0 ± 0.8	10.3 ± 4.0	7.6 ± 1.5	6.0 ± 0.8	7.1 ± 1.8	8.7 ± 2.1
LV Mass, (mg)	107.5 ± 5.9	118.7 ± 5.7	111.5 ± 6.8	114.4 ± 8.7	103.8 ± 4.8	102.7 ± 4.2	93.5 ± 2.8	102.0 ± 3.5
LVID, s (mm)	1.5 ± 0.1	1.7 ± 0.2	1.3 ± 0.1	2.0 ± 0.4	1.6 ± 0.1	1.8 ± 0.2	1.5 ± 0.2	1.9 ± 0.2
LVID, d (mm)	3.2 ± 0.1	3.2 ± 0.1	3.1 ± 0.1	3.5 ± 0.2	3.2 ± 0.1	3.2 ± 0.1	3.2 ± 0.1	3.3 ± 0.2
FS (%)	55.2 ± 1.7	49.6 ± 6.5	60.7 ± 2.0	49.6 ± 6.5	52.7 ± 3.4	44.1 ± 6.0	54.3 ± 3.7	43.1 ± 4.1
EF (%)	86.4 ± 1.5	81 ± 5.5	90.2 ± 1.3	79.4 ± 6.7	83.9 ± 2.6	76.3 ± 6.1	84.8 ± 3.0	74.1 ± 4.8

Table 4.2 Echocardiographic assessment of cardiac function and parameters before and after myocardial I/R injury in non-diabetic and diabetic cROCK2+/+ and cROCK2-/- mice.

HR, heart rate; CO, cardiac output; SV, stroke volume; EDV, end-diastolic volume; ESV, end-systolic volume; LV, left ventricular; LVID, left ventricular internal diameter; d, diastole; s, systole; FS, fractional shortening; EF, ejection fraction (n=5-7, $p>0.05$).

Parameter (units)	Non-diabetic				Diabetic			
	cROCK2+/+		cROCK2-/-		cROCK2+/+		cROCK2-/-	
	Basal	Post-I/R	Basal	Post-I/R	Basal	Post-I/R	Basal	Post-I/R
Radial strain, %	27.8 ± 2.3	27.6 ± 2.4	32.9 ± 1.5	33.2 ± 1.8	22.3 ± 1.8	18.6 ± 3.6	17.6 ± 4.3	20.3 ± 3.0
Radial strain rate, 1/s	6.7 ± 0.5	6.8 ± 0.5	6.2 ± 0.3	6.9 ± 0.6	5.4 ± 0.3	4.9 ± 0.4	4.5 ± 0.8	4.9 ± 0.6
Longitudinal strain, %	-19.4 ± 1.6	-19.0 ± 2.4	-22.6 ± 0.9	-23.6 ± 2.1	-12.3 ± 2.3	-13.3 ± 2.4	-14.5 ± 2.5	-13.6 ± 3.0
Longitudinal strain rate, 1/s	-6.1 ± 0.5	-6.6 ± 1.0	-5.9 ± 0.7	-6.6 ± 0.3	-4.1 ± 0.7	-5.1 ± 1.0	-3.7 ± 0.4	-4.4 ± 0.9

Table 4.3 Cardiac strain and strain rate before and after myocardial I/R injury in non-diabetic and diabetic cROCK2+/+ and cROCK2-/- mice.

Radial and longitudinal endocardial strain and strain rate were evaluated before ischemia (basal) and after 24 hours of reperfusion (post-I/R) (n=8-5, $p>0.05$).

4.3.4 ROCK expression and activity

ROCK2 expression in sham-operated cROCK2-/- mice hearts was approximately 50% lower than that detected in their ROCK2 expressing counterparts (Fig 4.2 A and D). The remaining ROCK2 expressed in cROCK2-/- mice hearts can be attributed to both the recombination efficiency of tamoxifen, which is approximately 80% in αMHC-MerCreMer mice (189), and the expression of ROCK2 in other cardiac cells, such as fibroblasts, endothelial cells and vascular smooth muscle cells. Following ischemia and both 2 and 24 hours of reperfusion, there was no change in ROCK2 expression in either non-diabetic or diabetic cROCK2-/- and cROCK2+/+ mice compared to their corresponding sham-operated mice (Fig 4.2 A and D), indicating a lack of effect of myocardial I/R injury on ROCK2 expression. ROCK1 expression was similar in sham-operated cROCK2-/- mice and their ROCK2 expressing counterparts, and was also unchanged following induction of I/R injury in either non-diabetic or diabetic mice, suggesting that the cardiomyocyte-specific knockout of ROCK2 does not cause a compensatory up-regulation of this other isoform under any of these conditions (Fig 4.2 B and E).

There was no difference in total ROCK activity, measured as the level of ^{Thr853}MYPT1 phosphorylation, between sham-operated cROCK2+/+ and cROCK2-/- hearts in the 2 hour reperfusion group (Fig. 4C). However, following induction of ischemia and 2 hours of reperfusion, ROCK activity was significantly lower in non-diabetic cROCK2-/- hearts than in their cROCK2+/+ counterparts, suggesting that an increase in ROCK activity induced by myocardial I/R injury was prevented in these hearts. No significant differences were detected between non-diabetic and diabetic cROCK2+/+ hearts subjected to ischemia and 2 hours of reperfusion (Fig 4.2 C), indicating that diabetes did not potentiate any I/R-induced increase in ROCK activity. Furthermore, after 2 hours of reperfusion, diabetic cROCK2-/- hearts also

exhibited levels of phosphorylated ^{Thr853}MYPT1 similar to those detected in their non-diabetic counterparts (Fig 4.2 C). In the group of mice subjected to 24 hours of reperfusion, the level of ^{Thr853}MYPT1 phosphorylation was significantly lower in sham-operated cROCK2-/- mice hearts than in their cROCK2+/+ counterparts (Fig 4.2 F). Similarly, both non-diabetic and diabetic cROCK2-/- mice hearts subjected to ischemia and 24 hours of reperfusion exhibited significantly lower levels of ROCK activity than their ROCK2 expressing counterparts (Fig 4.2 F).

4.3.5 Inactivation of the RISK pathway under diabetic conditions

In order to assess whether the loss of cardioprotection observed in diabetic cROCK2-/- mice hearts subjected to I/R injury was related to changes in the activation of the RISK pathway, we evaluated the phosphorylation levels of Akt at Ser473, which leads to its activation, as well as those of its downstream targets GSK-3β at Ser9 (leading to its inactivation), and eNOS at Ser1177 (promoting its activation). Since the RISK pathway is known to be activated at an early stage of reperfusion, the phosphorylation levels of these proteins were evaluated in mice hearts subjected to ischemia and 2 hours of reperfusion.

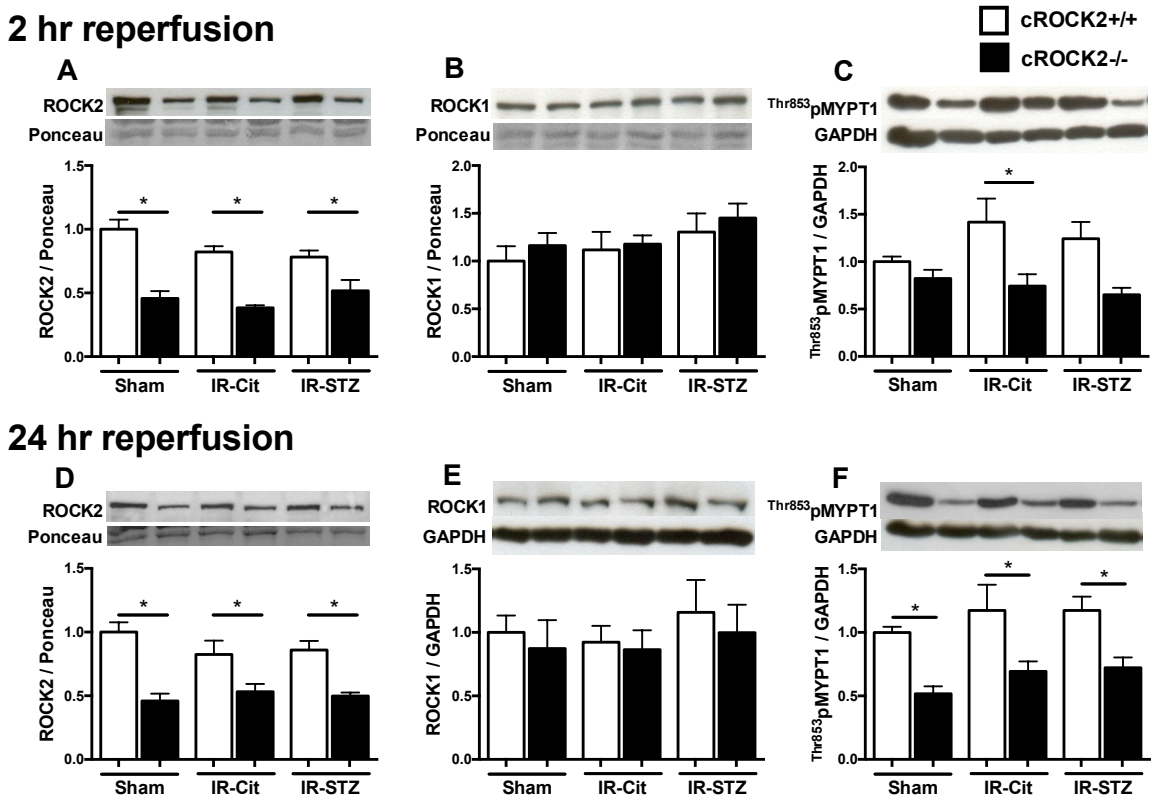

Figure 4.2 Effects of STZ-diabetes on ROCK isoform expression and ROCK activity in post-I/R cROCK2-/- and cROCK2+/+ mice hearts following 2 or 24 hours of reperfusion.

ROCK2 (A) and ROCK1 (B) protein expression and ROCK activity measured by MYPT phosphorylation (C) in sham, non-diabetic (Cit) and diabetic (STZ) cROCK2+/+ and cROCK2-/- hearts after 2 hours of reperfusion with western blot representative images (n=5-6, * $p<0.05$). ROCK2 (D) and ROCK1 (E) protein expression and ROCK activity measured by MYPT phosphorylation (F) sham, non-diabetic (Cit) and diabetic (STZ) cROCK2+/+ and cROCK2-/- hearts after 24 hours of reperfusion with western blot representative images (n=5-6, * $p<0.05$).

As described in Chapter 3 of this thesis, following induction of I/R injury, non-diabetic cROCK2+/+ hearts had a ^{Ser473}pAkt level similar to that observed in sham-operated cROCK2+/+ hearts, while non-diabetic cROCK2-/- hearts had a significantly higher level of ^{Ser473}pAkt than their sham-operated counterparts (Fig 4.3 A). However, compared to the non-diabetics, diabetic

cROCK2-/- mouse hearts subjected to I/R injury had a significantly lower level of Akt phosphorylation, similar to that observed in diabetic cROCK2+/+ hearts (Fig 4.3 A). The phosphorylation of GSK-3β followed a similar tendency. No significant differences in ^{Ser9}pGSK-3β levels were detected between I/R-induced non-diabetic cROCK2+/+ mice hearts and their sham-operated counterparts, while the induction of I/R injury in non-diabetic cROCK2-/- mice hearts was associated with a significantly higher level of ^{Ser9}pGSK-3β (Fig 4.3 B). However, this increase was not detected in diabetic cROCK2-/- mice hearts subjected to I/R injury (Fig 4.3 B). Although ^{Ser1177}peNOS levels tended to be higher in both non-diabetic and diabetic hearts subjected to I/R injury, no significant differences were found among groups (Fig. 4.3 C). Since eNOS is only active at very short times of reperfusion (7-10 minutes) (160, 204), it is possible that by 2 hours of reperfusion, ^{Ser1177}peNOS levels had returned to baseline levels. No differences in the total expression of Akt, GSK-3β or eNOS were detected between any of the groups.

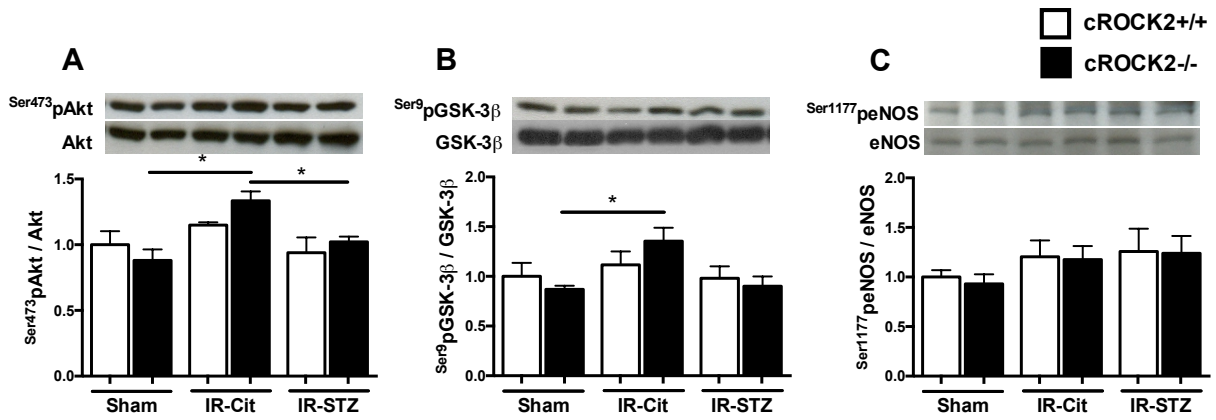

Figure 4.3 Effects of STZ-diabetes on Akt and GSK-3β phosphorylation in cROCK2-/- and cROCK2+/+ mice hearts subjected to ischemia and 2 hours of reperfusion.

Phosphorylation levels of Akt (A), GSK-3β (B), and eNOS (C) in sham, non-diabetic (Cit) and diabetic (STZ) cROCK2+/+ and cROCK2-/- hearts after 2 hours of reperfusion with western blot representative images (n=5-6, * $p<0.05$).

4.3.6 Modulation the RISK pathway under diabetic conditions

In order to understand how the I/R-induced activation of Akt in cROCK2-/- mice hearts is abrogated under diabetic conditions, we first evaluated whether there was a diabetes-induced increase in PTEN expression or phosphorylation given that this protein is a negative regulator of Akt. However, after ischemia and 2 hours of reperfusion, no changes in PTEN phosphorylation (Fig 4.4 A) or expression (Fig 4.4 B) were detected among groups.

Insulin signaling is also known to influence the activity of the PI3K/Akt pathway. When insulin binds to and stimulates the autophosphorylation of the insulin receptor, tyrosine phosphorylation and activation of IRS-1 is promoted. Activated IRS-1 recruits and activates PI3K, which then leads to Akt activation. Therefore, we evaluated the phosphorylation level of IRS-1 at Tyr612, as well as its total expression. No significant differences were detected between non-diabetic cROCK2-/- and cROCK2+/+ mice subjected to ischemia and 2 hours of reperfusion and their respective sham-operated counterparts (Fig 4.5 A). However, diabetic cROCK2-/- and cROCK2+/+ mice hearts had significantly lower levels of ^{Tyr612}pIRS-1 to total IRS-1 compared to non-diabetic cROCK2-/- mice hearts following I/R injury (Fig 4.5 A). Nonetheless, this appeared to be largely due to an increase in total IRS-1 expression, which was significantly higher in diabetic cROCK2-/- and cROCK2+/+ mice hearts than in their sham-operated and I/R-induced non-diabetic counterparts (Fig 4.5 B). Furthermore, no significant differences were detected in the absolute levels of ^{Tyr612}pIRS-1 (figure not shown).

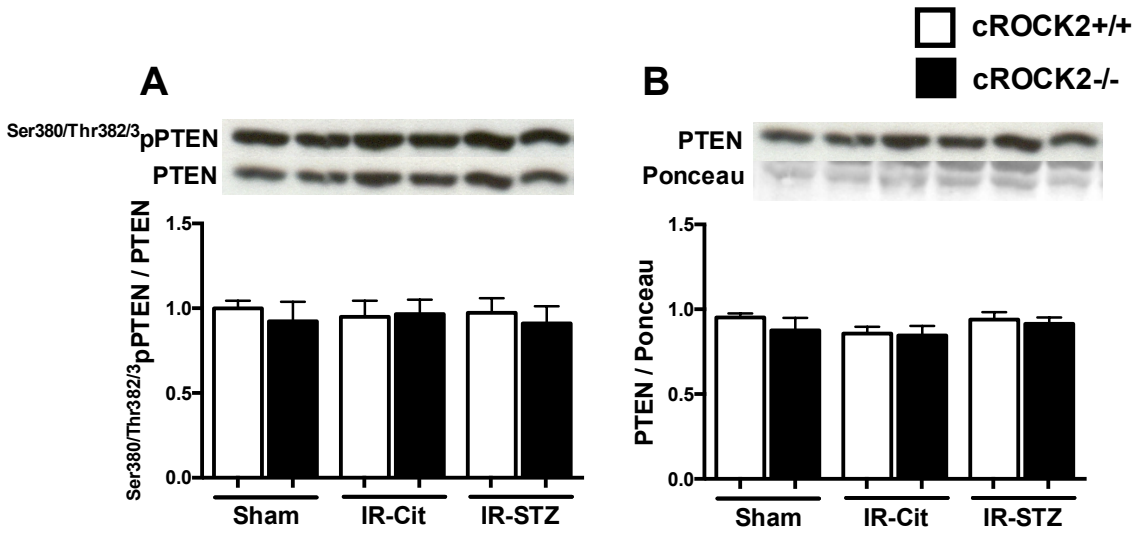

Figure 4.4 Effects of STZ-diabetes on PTEN phosphorylation and expression in hearts of cROCK2-/- and cROCK2+/+ mice subjected to ischemia and 2 hours of reperfusion.

Phosphorylation levels of PTEN (A), and PTEN total expression (B) in sham, non-diabetic (Cit) and diabetic (STZ) cROCK2+/+ and cROCK2-/- hearts after 2 hours of reperfusion with western blot representative images (n=5-6, $p>0.05$).

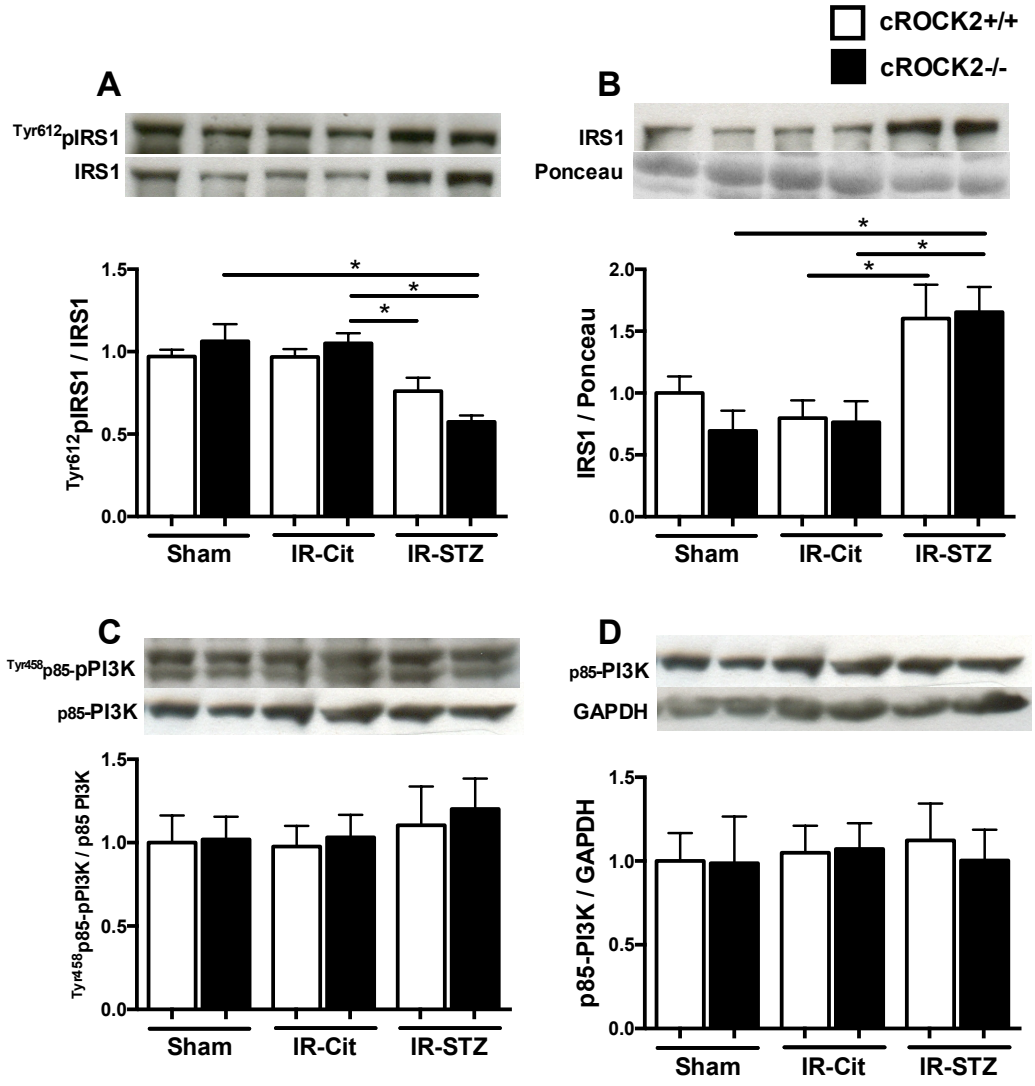

Figure 4.5 Effects of STZ-diabetes on IRS-1 and PI3K phosphorylation and expression in cROCK2-/- and cROCK2+/+ mice hearts subjected to ischemia and 2 hours of reperfusion.

Phosphorylation levels of IRS-1 (A), IRS-1 total expression (B), phosphorylation levels of PI3K (C) and PI3K total expression (D), in sham, non-diabetic (Cit) and diabetic (STZ) cROCK2+/+ and cROCK2-/- hearts after 2 hours of reperfusion with western blot representative images (n=5-6, * $p<0.05$).

At this same time of reperfusion, we also assessed the expression of PI3K and its phosphorylation at Tyr458, a site known to reflect the activation of this kinase (212). However, no differences in ^{Tyr458}pPI3K levels (Fig 4.5 C) or PI3K expression (Fig 4.5 D) were detected between cROCK2-/- and cROCK2+/+ mice hearts subjected to I/R injury under either diabetic or non-diabetic conditions.

4.3.7 Neutrophil infiltration and the mRNA production of inflammatory cytokines

The induction of myocardial I/R injury initiates an inflammatory response that promotes the production of pro-inflammatory cytokines and the accumulation of inflammatory cells. In our previous study (Chapter 3), we found that in hearts from ROCK2+/- mice subjected to I/R injury, pro-inflammatory cytokines were reduced although neutrophil infiltration was unaffected. Here, we evaluated the role of cardiomyocyte ROCK2 in these responses under both non-diabetic and diabetic conditions. Although non-diabetic cROCK2+/+ mice hearts subjected to I/R had a tendency to produce more IL-1β mRNA (Fig 4.6 A) than their sham-operated counterparts, this increase was not statistically significant. But compared to both sham-operated mice and to non-diabetic cROCK2+/+ mice subjected to I/R injury, non-diabetic cROCK2-/- mice hearts produced much greater levels of IL-1β mRNA (Fig 4.6 A). Interestingly, this difference was abolished under diabetic conditions, where the mRNA production of IL-1β in cROCK2-/- mice hearts subjected to I/R was significantly lower, and comparable to the one detected in their sham-operated counterparts (Fig 4.6 A).

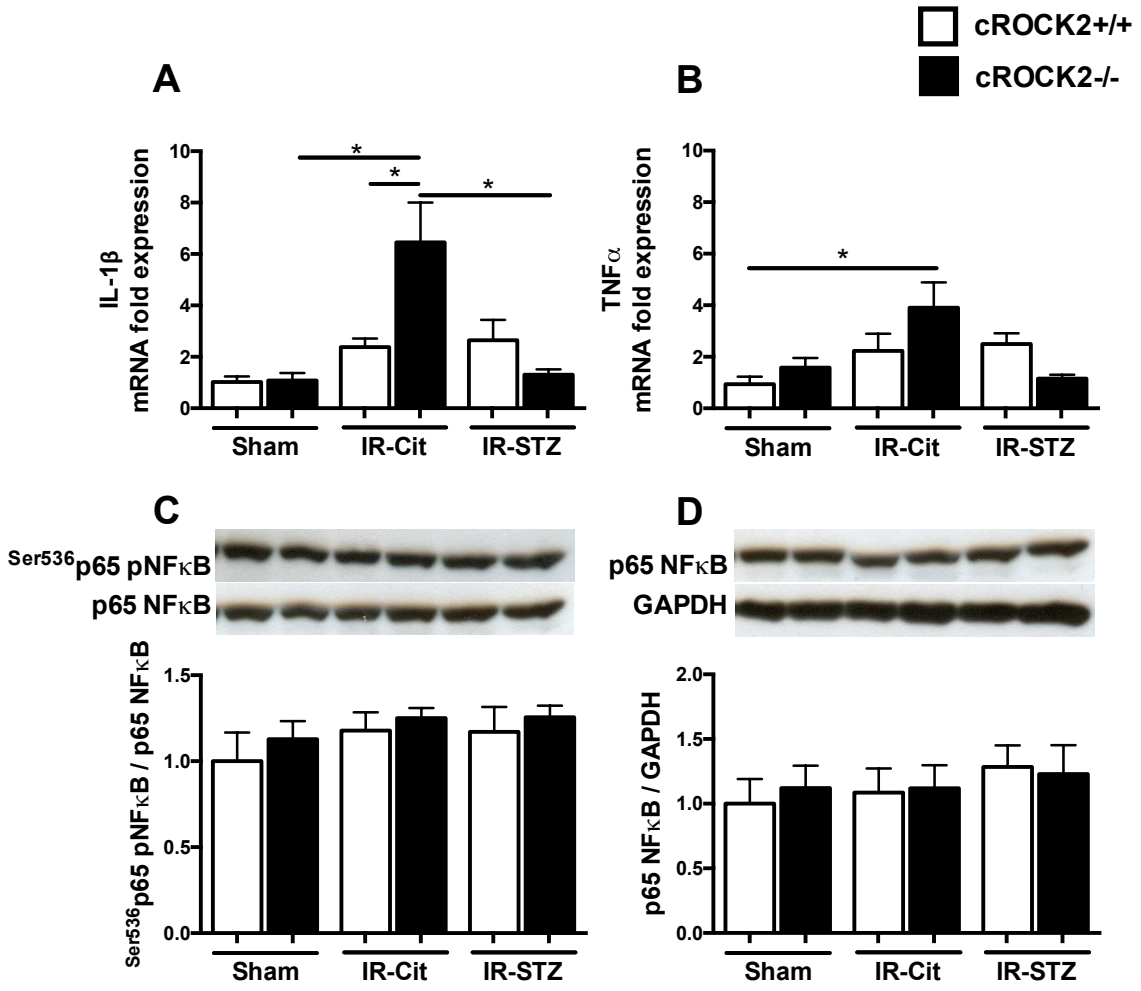

Figure 4.6 Effects of STZ-diabetes on the mRNA expression of pro-inflammatory cytokines, NFκB phosphorylation and NFκB expression in cROCK2-/- and ROCK2+/+ hearts subjected to I/R.

IL-1β (A) and TNFα (B) mRNA expression of sham, non-diabetic (Cit) and diabetic (STZ) cROCK2+/+ and cROCK2-/- hearts subjected to ischemia and 24 hours of reperfusion (n=5-6, *p<0.05). Phosphorylation levels of NFκB (C), and NFκB total expression (D) in sham, non-diabetic (Cit) and diabetic (STZ) cROCK2+/+ and cROCK2-/- hearts subjected to ischemia and 24 hours of reperfusion with western blot representative images (n=5-6, * p<0.05).

A similar trend was observed with the production of TNFα mRNA, in that the mRNA production of this cytokine was significantly higher in non-diabetic cROCK2-/- mice hearts subjected to I/R than in sham-operated hearts, and this increase was no longer noticeable under diabetic conditions (Fig 4.6 B), although the differences were not as marked as those of IL-1β. These results suggest that in non-diabetic conditions, the cardiac-specific knockout of ROCK2 promotes the I/R-induced mRNA production of pro-inflammatory cytokines, and that under diabetic conditions this increase is abrogated. In an effort to understand how cytokine mRNA production was regulated in these hearts, we evaluated the expression levels of NFκB, as well as its phosphorylation at Ser536, a site known to be correlated with its activation (213). However, after ischemia and 2 hours of reperfusion, no changes in ^{Ser536}pNFκB (Fig 4.6 C) or NFκB expression (Fig 4.6 D) were detected under either non-diabetic or diabetic conditions.

Neutrophils are one of the first inflammatory cells that are attracted to the site of injury after I/R takes place. Both cROCK2-/- and cROCK2+/+ mice hearts subjected to I/R injury showed a higher level of Ly6G+ neutrophil infiltration compared to their sham-counterparts; however, this difference was significant only cROCK2-/- mice hearts. Under diabetic conditions, this increase was no longer as pronounced, and no significant differences were detected between diabetic cROCK2-/- and cROCK2+/+ mice hearts subjected to I/R.

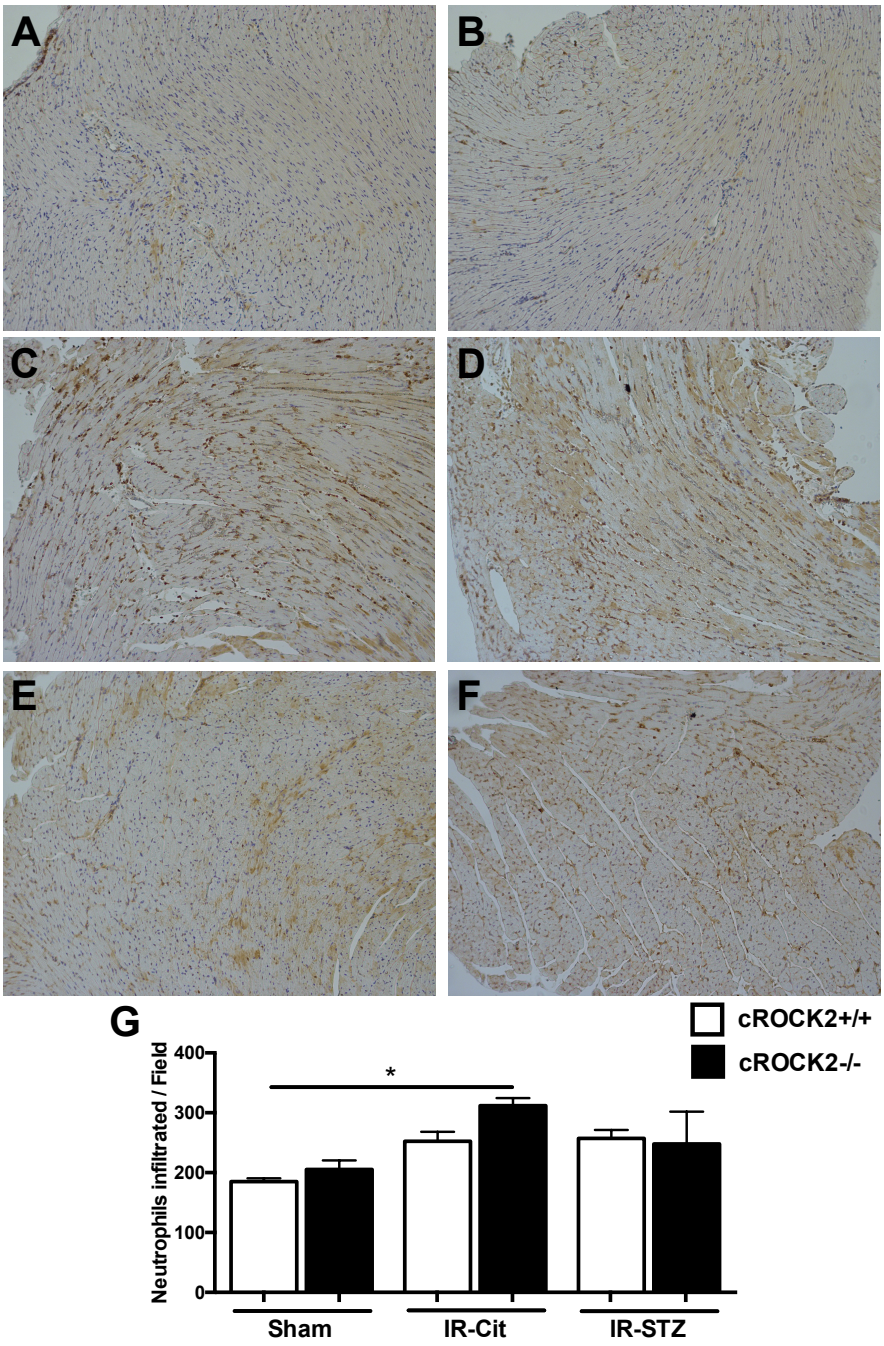

Figure 4.7 Ly6G+ neutrophil infiltration in diabetic and non-diabetic cROCK2+/+ and cROCK2-/- hearts subjected to I/R injury.

Representative images (20x) of the Ly6G+ immunohistochemical staining of sham cROCK2+/+ (A), sham cROCK2-/- (B), post-I/R non-diabetic cROCK2+/+ (C), post-I/R non-diabetic cROCK2-/- (D), post-I/R diabetic cROCK2+/+ (E) and post-I/R diabetic cROCK2-/- (F) mice hearts after 24 hours of reperfusion. Quantification of infiltrated neutrophils per field (G) (n=3, 3 random fields per sample, * $p<0.05$).

4.4 Discussion

Patients with diabetes are not only more susceptible to myocardial infarction, but also more sensitive to the deleterious effects of myocardial I/R injury. Therefore, it is very important to evaluate the effectiveness of therapeutic interventions targeting I/R injury under these conditions. Previously we had reported that the over-activation of ROCK2 is involved in the development of myocardial I/R injury, and that the cardiomyocyte-specific deletion of this ROCK isoform was at least partially responsible for the cardioprotection observed in mice with a whole-body partial deletion of ROCK2. In the present study, we investigated whether the cardioprotection against I/R injury observed in cROCK2-/- mice is maintained during diabetes. Our main findings were: 1) in diabetic mice, the cardiomyocyte-specific knockout of ROCK2 no longer decreases infarct size, and this loss of cardioprotection is associated with an increase in serum LDH in diabetic cROCK2-/- mice subjected to I/R, 2) the activation of Akt and the inactivation of its downstream target GSK-3β stimulated by cardiomyocyte-specific ROCK2 knockout is abrogated under diabetic conditions and 3) cardiomyocyte ROCK2 appears to exert a regulatory effect on the inflammatory response to I/R injury that is also attenuated in diabetes.

Previous work from our lab has demonstrated that the RhoA-ROCK pathway is involved in the development of diabetic cardiomyopathy (155), and has suggested that ROCK2 is the isoform involved in this process (157). Therefore, when we detected the cardioprotective activity of ROCK2 knockdown in the development of myocardial I/R injury, we hypothesized that this cardioprotection would be maintained under diabetic conditions. However, diabetic cROCK2-/- mice hearts subjected to I/R injury no longer presented the decrease in infarct size found in their non-diabetic counterparts. The increased susceptibility to I/R injury of diabetic compared to non-diabetic cROCK2-/- mice hearts was corroborated by the increase in serum LDH detected in

these mice. Unlike infarct size and serum LDH release, cardiac function and cardiac strain did not reflect these changes in cardioprotection. The data obtained with non-diabetic cROCK2+/+ and cROCK2-/- mice were different than those detected in WT and ROCK2+/- mice, since no clear cardiac dysfunction was detected after inducing myocardial I/R injury. Furthermore, the induction of diabetes did not have an effect on cardiac function or cardiac strain, suggesting that the induction of I/R injury 4 weeks after STZ treatment is enough to impair cardioprotection but not the contractile function of the heart. Since all STZ-treated mice were overtly diabetic, we believe that the lack of differences might have been related to this mouse strain being more resistant to the development of post-I/R cardiac dysfunction.

The cardiomyocyte-specific deletion of ROCK2 prevented the increase of ROCK activity after 2 hours of reperfusion. However, it seems that by 24 hours of reperfusion, ROCK activity was mostly driven by the amount of ROCK2 present in cardiomyocytes rather than the induction of myocardial I/R injury at both diabetic and non-diabetic conditions. These data differ from what we observed in our previous study, where sham-operated ROCK2+/- and WT mice had no differences in ROCK activity at either point of reperfusion. As was previously stated in Chapter 3, it is possible that in ROCK2+/- mice hearts, ROCK1 contributes to a greater extent to basal ROCK activity, in order to compensate for the loss of this other ROCK isoform. However, this compensation might not take place in cardiomyocytes given that this response was not detected in sham-operated cROCK2-/- mice hearts at 24 hours of reperfusion.

The loss of infarct size reduction and the increase of LDH release in diabetic cROCK2-/- mice hearts subjected to I/R were concomitant with the fact that, under diabetic conditions, ROCK2 cardiomyocyte-specific knockout no longer promoted the phosphorylation of Akt and GSK-3β. A loss of cardioprotection under type 1 diabetic conditions has been previously

reported. For instance, Ghaboura et al. (214) showed that erythropoietin-induced cardioprotection against I/R injury was maintained in rats made insulin resistant with a high fat diet. However, in rats with type 1 diabetes induced by STZ treatment, this cardioprotection was lost. Erythropoietin treatment promoted an increase in Akt, GSK-3β, and Erk1/2 phosphorylation in control and insulin-resistant rats, but not in diabetic rats. Therefore, it was suggested that a hyperglycemia-induced alteration of the RISK pathway was responsible for the loss of erythropoietin-induced cardioprotection (214). Similarly, Whittington et al. (215) reported that in aging rat hearts subjected to I/R injury, the phosphorylation of Akt, GSK-3β, and STAT-3, a component of the SAFE pathway, are significantly lower under diabetic than non-diabetic conditions.

Evidence has been presented suggesting that over-activation of PTEN is responsible for the impairment of the PI3K/Akt pathway in diabetic rat hearts subjected to I/R injury (121). However, we were unable to detect diabetes-induced changes in PTEN expression or phosphorylation following I/R injury in either cROCK2+/+ or cROCK2-/- hearts, suggesting that this mechanism is not universal for all models of type 1 diabetes. It has also been reported that decreases in the tyrosine-phosphorylation of IRS-1 are related to the hyperglycemic-induced loss of cardioprotection detected in cardiomyocytes subjected to hypoxia-reperfusion (216). However, although we observed that compared to their non-diabetic counterparts, diabetic cROCK2-/- and cROCK2+/+ mice hearts subjected to I/R have a significantly lower level of ^{Tyr612}pIRS-1, this appeared to be largely due to a diabetes-induced increase in total expression of IRS-1. The low levels of circulating insulin in diabetic cROCK2-/- and cROCK2+/+ mice may promote the upregulation of IRS-1 expression in an effort to stimulate insulin signaling. As a result, although relative levels of ^{Tyr612}pIRS-1 to total IRS-1 were lower in diabetic hearts, the

absolute levels of tyrosine phosphorylated IRS-1 were not significantly different than those in non-diabetic hearts, suggesting that IRS signaling may be unchanged in these hearts. This is supported by our observation that PI3K activity, measured as the phosphorylation of this protein at Tyr458, also appeared to be unchanged in diabetic compared to non-diabetic hearts.

Unexpectedly and in contrast to the results previously obtained with ROCK2+/- mice, where the mRNA expression of pro-inflammatory cytokines induced by myocardial I/R injury was significantly lower, non-diabetic cROCK2-/- mice hearts subjected to I/R exhibited a higher production of IL-1β and to a lesser extent, TNFα mRNA, compared to their cROCK2+/+ counterparts. Furthermore, the presence of diabetes in cROCK2-/- mice hearts subjected to I/R injury was sufficient to lower cytokine mRNA levels to baseline levels, although cytokine mRNA production in diabetic cROCK2+/+ hearts remained unchanged from that in non-diabetic hearts. Since no differences were observed between sham-operated cROCK2-/- and cROCK2+/+ mice hearts, we do not believe this was a consequence of the surgical procedure. Neutrophil infiltration followed very similar trends to the changes in inflammatory cytokine mRNA production, suggesting that cytokine mRNA translated to functional cytokines that promoted the infiltration of these inflammatory cells. These results suggest that in non-diabetic conditions, the cardiac-specific knockout of ROCK2 promotes the I/R-induced mRNA production of pro-inflammatory cytokines, and that under diabetic conditions this increase is abrogated.

This discrepancy between results obtained in the whole-body ROCK2+/- mice and the cardiac-specific cROCK2-/- mice suggests that the role of ROCK2 in the inflammatory response in cardiomyocytes is different from that in other cells. It is well known that when necrosis takes place, the release of intracellular components initiates an inflammatory response. Therefore, less necrosis in cardiac tissue should translate into less inflammation, and since infarct size reflects

the extent of cardiac necrosis, it is possible that the reduction of pro-inflammatory cytokine mRNA detected in ROCK2+/- mice is secondary to the reduction of infarct size also achieved in these mice. On the other hand, the increase in cytokine mRNA found in cROCK2-/- hearts suggests that ROCK2 may actually suppress cardiomyocyte cytokine mRNA production during I/R injury. Although most reports focus on the adverse effects of pro-inflammatory cytokines during myocardial I/R injury, there are also studies suggesting that cytokines may be protective against the development of this condition (217). However, this is only true when cytokine concentrations are low. Since protein levels of pro-inflammatory cytokines were not measured in these hearts, it is not clear whether this increase in mRNA production was translating into protein or not. Nonetheless, this increase of pro-inflammatory cytokine mRNA in non-diabetic cROCK2-/- mice hearts subjected to I/R injury was not associated with any damaging effects such as an increase of infarct size or serum LDH.

One of the limitations of the present study was that although protection from the development of I/R injury provided by cardiomyocyte-specific ROCK2 knockout is lost in diabetic hearts, it is not clear if ROCK2 inhibition in other types of cells would prevent the deleterious effects of myocardial I/R injury under diabetic conditions. Therefore, a subsequent study that evaluates this would give a fuller picture of the role of ROCK2 in the development of myocardial I/R injury during hyperglycemia.

In conclusion, the results of the present study suggest that despite our previous studies implicating ROCK2 in the deleterious effects of diabetes on the heart, reduction of its expression in cardiomyocytes is not sufficient to protect against I/R injury in diabetes. The impairment of the cardioprotective activity of cardiomyocyte-ROCK2 deletion demonstrates the importance of

evaluating the effectiveness of therapeutic targets against myocardial I/R injury in the presence of comorbidities such as diabetes.

Chapter 5: Conclusion

5.1 Summary and conclusions

During a myocardial infarction, the occluded region of the heart enters into an ischemic state that, if untreated, will lead to cell death. Timely reperfusion must be instituted in order to avoid this; however, this procedure leads to a type of cardiac damage known as myocardial I/R injury (5). Patients who are susceptible to myocardial infarction often have comorbidities, such as diabetes, that worsen the outcome of I/R injury (84, 85); therefore, it is of great importance to also consider the effects that this disease has on the development of myocardial I/R injury. It has been reported that ROCK is overactivated in animal models of myocardial I/R injury (158-160), however, it was unknown whether ROCK1, ROCK2 or both isoforms, is/are responsible for this effect. Furthermore, none of the previous reports had evaluated whether diabetes had an effect on the cardioprotective role of ROCK inhibition against I/R injury. Here, we proposed to evaluate whether the overactivation of ROCK2 contributes to I/R injury in the normal and diabetic heart.

The first aim of the present thesis was to establish an *in vivo* model of myocardial I/R injury in non-diabetic and diabetic conditions. Since we planned on using ROCK2+/- mice that were bred on a CD-1 background to evaluate the role of ROCK2 on the development of myocardial I/R, we first evaluated the basal cardiac function of these mice under non-diabetic and diabetic conditions. In non-diabetic mice, the partial deletion of ROCK2 does not affect systolic cardiac function. However, no significant differences in systolic cardiac function were detected between diabetic and non-diabetic WT mice at 8 or 11 weeks after STZ treatment, suggesting that this strain of mice requires a longer time to develop diabetes-induced cardiac dysfunction. Nonetheless, since the induction of I/R injury may induce a different response than

the one obtained at basal conditions, we decided to evaluate the cardiac function of non-diabetic and diabetic CD-1 mice subjected to *in vivo* myocardial I/R injury by transient ligation of the LAD coronary artery. Non-diabetic mouse hearts subjected to I/R had impaired cardiac function, but their diabetic counterparts had a similar or better performance, suggesting that ROCK2+/- mice, due to their CD-1 background, are not an appropriate model to study the effects of diabetes on the development of myocardial I/R injury. Since cROCK2-/- mice have a C57BL/6 background, the effects of diabetes on I/R injury were evaluated in these mice in the third aim of this work.

The second aim of the thesis was to investigate the whole-body and cardiomyocyte-specific contribution of ROCK2 in myocardial I/R injury. After ischemia and 24 hours of reperfusion, the infarct size of ROCK2+/- mice hearts was much lower than the one developed by their WT counterparts. Similarly, a post-I/R reduction in cardiac function was detected in WT mice, while in ROCK2+/- mice, cardiac function was conserved. The induction of I/R injury prompted a significant increase in ROCK activity in WT hearts, but in ROCK2+/- mouse hearts this was prevented. After 2 hours of reperfusion, the phosphorylation levels of Akt and GSK-3β, both elements of the RISK pathway, were significantly higher in ROCK2+/- hearts than in their WT counterparts, implying that cardioprotective signaling pathways are activated by the knockdown of ROCK2. Furthermore, the I/R-induced increase of pro-inflammatory cytokine mRNA was attenuated in ROCK2+/- mice. However, no significant differences on Ly6G+ neutrophil infiltration were found between ROCK2+/- and WT mice hearts. These results suggest that although ROCK2 partial deletion prevents the production of pro-inflammatory cytokines, this ROCK isoform is not as involved in the more downstream inflammatory responses. By specifically deleting ROCK2 in cardiomyocytes, we observed that the reduction of

infarct size previously detected in ROCK2+/- mice subjected to I/R injury was maintained. Furthermore, this decrease in infarct size was also associated with an increase in Akt activity. Altogether, the results of this study indicate that ROCK2, specifically that in cardiomyocytes, plays an important role in the development of myocardial I/R injury, and that the cardioprotection achieved by knocking out ROCK2 is associated with activation of the RISK pathway.

The third aim of the present thesis was to evaluate the role of cardiomyocyte ROCK2 in the development of myocardial I/R injury in diabetic hearts. Our results indicate that the reduction of infarct size previously achieved in non-diabetic cROCK2-/- mice subjected to myocardial I/R injury is abrogated under diabetic conditions. Although no significant differences in cardiac function were detected before or after myocardial I/R injury, the increase of serum LDH in diabetic cROCK2-/- mice subjected to I/R injury confirmed these observations.–No increase in ROCK expression was detected in either cROCK2+/+ or cROCK2-/- mice hearts under diabetic conditions, suggesting that the loss of cardioprotection in diabetic hearts was not triggered by an increase in ROCK activity. At 2 hours of reperfusion, hearts from non-diabetic cROCK2-/- mice subjected to I/R had a significant increase in Akt and GSK-3β phosphorylation compared to their ROCK2 expressing counterparts, suggesting the activation of the RISK pathway. However, under diabetic conditions, this increase was no longer detected. These observations suggest that the lack of cardioprotection detected in diabetic cROCK2-/- mice subjected to I/R is at least partially regulated by a diabetes-induced impairment of prosurvival pathways. The activation of proteins known to modulate Akt signaling was also evaluated; however, the loss of Akt activity in diabetic hearts could not be explained by changes in PTEN, IRS or PI3K. Unexpectedly and in contrast to the results obtained with ROCK2+/- mice, non-

diabetic cROCK2-/- mice hearts subjected to I/R exhibited an increase in pro-inflammatory cytokine mRNA production compared to their cROCK2+/+ counterparts. Furthermore, this increase was no longer detected under diabetic conditions. Additionally, this higher level of pro-inflammatory cytokine mRNA production was associated with greater neutrophil infiltration.

Taken together, the results of these 3 studies suggest that ROCK2 plays an important role in the development of myocardial I/R injury, and that the cardioprotective effect provided by its inhibition or genetic deletion is likely mediated at least in part by the activation of Akt and the inactivation of its downstream target GSK-3β in the cardiomyocyte. However, this cardioprotection is abrogated under diabetic conditions, possibly due to impaired Akt signaling. Unfortunately, the effects on I/R-induced inflammation are not as clear. However, the differences between whole-body ROCK2+/- mice and cardiac-specific cROCK2-/- mice suggest that in cardiomyocytes, the role of ROCK2 in I/R-induced inflammation is different from that in other cells. These findings are summarized in Fig. 5.1.

One of the greatest strengths of the work presented in this thesis was the use of an *in vivo* model to evaluate the role of ROCK2 in the development of myocardial I/R injury under both non-diabetic and diabetic conditions. Unlike *in vitro* models, that can only simulate the conditions present during myocardial I/R injury, or *ex vivo* models, that isolate the heart from all the physiological changes that occur in response to I/R injury, an *in vivo* model allows us to evaluate this condition as a whole, and gives us the most comprehensive understanding of the development of myocardial I/R injury. Furthermore, the fact that we employed both ROCK2+/- and cROCK2-/- mice, allowed us to effectively isolate the effects of this isoform. Even though a selective ROCK2 inhibitor was developed while the present thesis was conducted,

pharmacological inhibitors may not achieve the same degree of specificity that a genetic model offers (218).

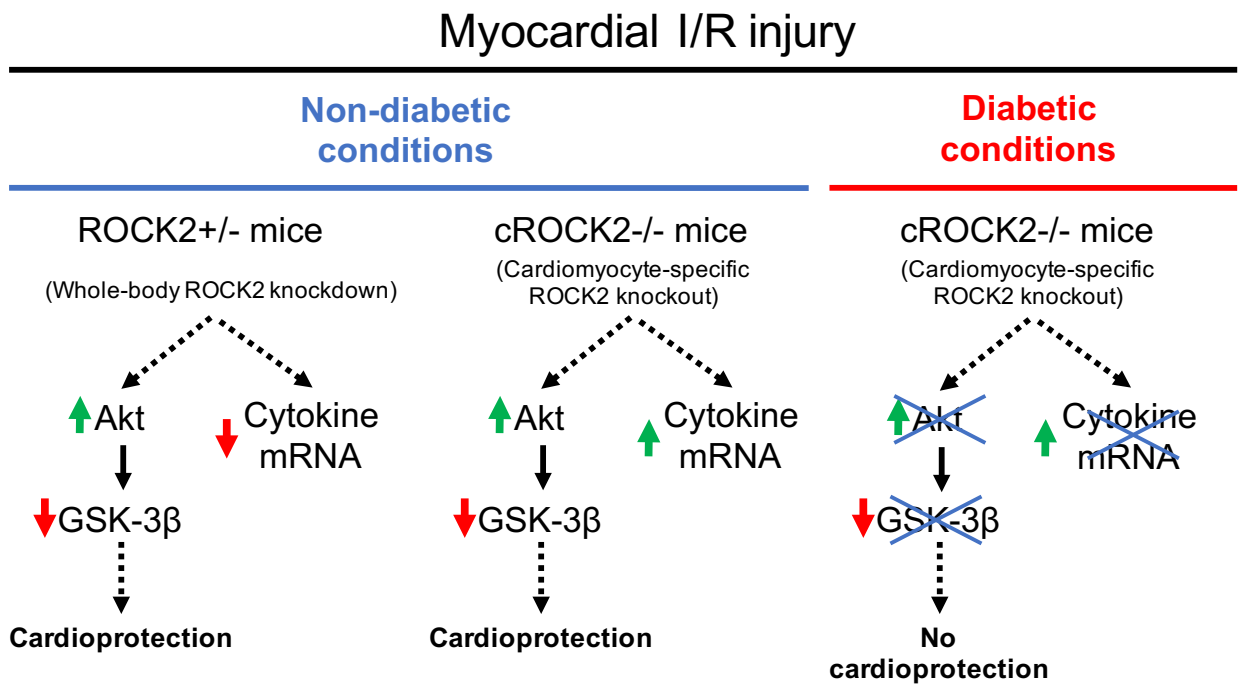

Figure 5.1 Summary figure with the principal findings of the present thesis.

By using ROCK2+/- and cROCK2-/- mice, we were able to evaluate the role of ROCK2 in the development of I/R injury at both diabetic and non-diabetic conditions. The cardioprotection achieved by the whole-body knockdown and the cardiomyocyte-specific knockout of ROCK2 in non-diabetic conditions was mediated via Akt signaling, however this mechanism was abrogated by the presence of diabetes.

On the other hand, one of the limitations of the present thesis was the fact that we only evaluated the role of ROCK2 in the short-term responses to myocardial I/R injury. We decided to concentrate our efforts on these since previous studies that evaluated the cardioprotective role of non-isoform specific ROCK inhibition had also focused on the first 24 hours of reperfusion, and showed that ROCK inhibition was involved in the activation of the RISK pathway, a cardioprotective pathway activated at the onset of reperfusion (158-160). Nonetheless, it is

important to assess the consequences of ROCK2 deletion on the long-term responses to I/R injury in both non-diabetic and diabetic conditions before a more elaborate clinical study is conducted. Another limitation relates to the differences detected in the mRNA production of pro-inflammatory mediators in non-diabetic hearts. While the whole-body partial deletion of ROCK2 inhibited the I/R-induced mRNA production of TNFα and IL-1β, the cardiomyocyte-specific deletion of this isoform promoted it. As previously mentioned, the reasons for this are not clear, and more research is necessary in order to fully understand the role of ROCK2 in the development of the I/R-induced inflammatory response. Lastly, even though the model here used has been shown to be one of the most comprehensive in the development of myocardial I/R injury, it should be pointed out that there are clear differences between mice subjected to I/R injury and patients who suffer a myocardial infarction and are subjected to reperfusion. In mice, a healthy artery is ligated to simulate ischemia, and this ligature is then removed to promote reperfusion. However, patients who suffer a myocardial infarction usually have atherosclerosis and other conditions that affect arterial condition and function. Therefore, the basal conditions in each case are significantly different. One way to circumvent this would be to breed ROCK2+/- and cROCK2-/- mice with mice that are known to develop atherosclerosis, such as ApoE knockout mice.

In conclusion, both whole-body partial deletion and cardiomyocyte-specific deletion of ROCK2 have a cardioprotective effect against the development of myocardial I/R injury in non-diabetic conditions. This cardioprotection is likely mediated by the activation of Akt and the inactivation of its downstream target GSK-3β. However, the cardioprotection conferred by cardiomyocyte-specific ROCK2 deletion is lost under diabetic conditions, possibly due to the abrogation of cardioprotective signaling pathways.

5.2 Therapeutic implications

In the present thesis, we were able to describe the role of ROCK2 in the development of myocardial I/R injury, and our results suggest that the isoform-selective inhibition of this protein represents a feasible form of therapy against the development of myocardial I/R in non-diabetic patients. As mentioned above, a ROCK2 isoform selective inhibitor has recently been developed by Kadmon Corporation, and its application for the treatment of autoimmune diseases such as psoriasis is currently being investigated (210). This inhibitor could potentially be tested along with non-isoform specific ROCK inhibitors in a clinical trial, so that the responses obtained with each of these drugs are compared. Additionally, compared to inhibitors that are non-isoform specific, isoform-selective inhibitors should display a better toxicity profile since fewer proteins are being targeted. Therefore, this may be another advantage of using an isoform-selective ROCK2 inhibitor for the treatment of myocardial I/R injury.

Our results suggest that the cardioprotection achieved by knocking out ROCK2 from cardiomyocytes is lost under diabetic conditions; however, it would still be necessary to evaluate whether ROCK2 inhibition in other types of cells reduces the cardiac damage induced by I/R injury in diabetes. Only after this it will be possible to determine whether treatment with an isoform-selective ROCK2 inhibitor would benefit diabetic patients.

5.3 Main findings

- Systolic cardiac function in non-diabetic WT and ROCK2+/- mice was similar, suggesting that ROCK2 partial deletion does not have an effect on systolic cardiac function. However, WT mice did not develop diabetes-induced systolic cardiac

dysfunction within the time period examined, even though ROCK2 expression was significantly higher, possibly due to their CD-1 background. Therefore, ROCK2+/- mice were not employed to evaluate the role of ROCK2 on the development of myocardial I/R injury under diabetic conditions.

- In hearts from non-diabetic CD-1 mice, the induction of myocardial I/R injury decreased cardiac function. However, the cardiac function of hearts from diabetic CD-1 mice was similar or better than that detected in their non-diabetic counterparts. The reasons for this are unclear, although we believe this may also be related to mouse strain. Therefore, only cROCK2-/-, which have a C57BL/6J background, were used to evaluate the role of ROCK2 in the development of myocardial I/R injury under diabetic conditions.
- ROCK overactivation has been related to the development of myocardial I/R injury. However, it was not known whether ROCK1, ROCK2, or both isoforms were responsible for this pathological response. Here, we observed that ROCK2+/- mice had smaller infarct sizes compared to their WT counterparts, and this was associated with preserved cardiac function, activation of the RISK pathway and reduced production of pro-inflammatory cytokines.
- In mice with a cardiomyocyte-specific ROCK2 knockout, cardioprotection against I/R injury is maintained, suggesting that at least part of the I/R-induced overactivation of ROCK2 takes place in the cardiomyocyte. Furthermore, since our data showed that Akt was activated and GSK-3β was inactivated in these hearts, it is likely that the activation of the RISK pathway takes place at the cardiomyocyte.
- Under diabetic conditions, the cardioprotection provided by cardiomyocyte-specific ROCK2 deletion is abrogated, possibly due to impaired in the activation of Akt and

GSK-3β. Neither PTEN, a negative regulator of Akt, nor defective IRS-1-PI3K signaling appear to be involved in this process.

- In contrast to the effects observed in hearts from ROCK2+/- mice, the cardiomyocyte-specific deletion of ROCK2, caused a significant increase in I/R induced pro-inflammatory cytokine mRNA production under non-diabetic conditions. This was also related to a significant increase in Ly6G+ neutrophil infiltration.

5.4 Future research directions

- *Assessing the role of ROCK2 in isolated cardiomyocytes subjected to hypoxia/reperfusion under both hyperglycemic and non-hyperglycemic conditions*:

  By evaluating the expression and phosphorylation levels of Akt, GSK-3β and IRS in cardiomyocytes isolated from cROCK2-/- and cROCK2+/+ mice under normoglycemic conditions, we will be able to corroborate that this is the pathway leading to the cardioprotection found in non-diabetic cROCK2-/- hearts. Furthermore, measuring cytokine mRNA production in an *in vitro* model of hypoxia/reperfusion would allow us to isolate cardiomyocytes from other cells that are also subjected to the deleterious effects of myocardial injury. If an increase in cytokine mRNA production is still detected in cROCK2-/- mice cardiomyocytes subjected to hypoxia/reperfusion, this would indicate that ROCK2 plays a role in controlling the expression of these inflammatory mediators in cardiomyocytes.

- *Evaluating the role of ROCK2 in the long-term consequences of myocardial I/R injury under both non-diabetic and diabetic conditions*:

Even though the induction of I/R injury had no detectable effect on cardiac function or cardiac strain after 24 hours of hours of reperfusion, an echocardiographic follow up of 6 weeks would allow us to determine whether over the longer term, cardiac function is impaired in these mice (190). Furthermore, hearts subjected to ischemia and a long period of reperfusion develop fibrosis and cardiac hypertrophy (219). By having this follow up, we will be able to see if the activation of cardioprotective pathways at the onset of reperfusion translates into a reduction in cardiac remodeling. At the point of termination, we would be able to assess the extent of fibrosis by Masson's trichrome staining and by measuring the mRNA and protein expression of collagen type I and III; while cardiac hypertrophy can be evaluated by measuring cardiomyocyte size.

- *Evaluating the role of ROCK1 in the development of myocardial I/R injury under both non-diabetic and diabetic conditions*:

  The work presented in this thesis provides strong support for the concept that in non-diabetic conditions, ROCK2 deletion has a cardioprotective effect against the development of myocardial I/R injury. Although knocking out ROCK2 does not promote the upregulation of ROCK1, whether this isoform has a role in the development of myocardial I/R injury is not understood. We unfortunately do not have access to a model of either whole-body knockdown or cardiomyocyte-specific ROCK1 knockout; however, we believe that using one or both of these two mouse models would provide great insight.

- *Evaluate the role of ROCK2 in myocardial I/R injury using human induced pluripotent stem cell-derived cardiomyocytes:*

In this study, a mouse model was used to determine the role of ROCK2 in the development of I/R injury in both non-diabetic and diabetic hearts. However, by using human induced pluripotent stem cell-derived cardiomyocytes subjected to conditions of hypoxia-reperfusion, we would be able to test whether the results obtained here are applicable to patients who have suffered myocardial I/R injury. A genome-editing technique such as the CRISPR/Cas9 system could potentially be used to selectively induce the knockout of ROCK2 in these cells (220).

Bibliography

1. World Health Organization. Cardiovascular diseases (CVDs) 2017. Available from: http://www.who.int/mediacentre/factsheets/fs317/en/. Accessed on: June 20, 2017.
2. Public Health Agency of Canada. Tracking heart disease and stroke in Canada. 2009. Available from: https://www.canada.ca/en/public-health/services/reports-publications/2009-tracking-heart-disease-stroke-canada.html. Accessed on: August 28, 2017.
3. Mayo Clinic. Heart disease. 2017. Available from: http://www.mayoclinic.org/diseases-conditions/heart-disease/symptoms-causes/dxc-20341558. Accessed on: July 10, 2017.
4. Stone GW, Maehara A, Lansky AJ, de Bruyne B, Cristea E, Mintz GS, et al. A prospective natural-history study of coronary atherosclerosis. N Engl J Med. 2011;364(3):226-35.
5. Yellon DM, Hausenloy DJ. Myocardial reperfusion injury. N Engl J Med. 2007;357(11):1121-35.
6. Hausenloy DJ, Yellon DM. Ischaemic conditioning and reperfusion injury. Nat Rev Cardiol. 2016;13(4):193-209.
7. Verma S, Fedak PW, Weisel RD, Butany J, Rao V, Maitland A, et al. Fundamentals of reperfusion injury for the clinical cardiologist. Circulation. 2002;105(20):2332-6.
8. Hausenloy DJ, Yellon DM. Myocardial ischemia-reperfusion injury: a neglected therapeutic target. J Clin Invest. 2013;123(1):92-100.
9. Ferdinandy P, Schulz R, Baxter GF. Interaction of cardiovascular risk factors with myocardial ischemia/reperfusion injury, preconditioning, and postconditioning. Pharmacol Rev. 2007;59(4):418-58.
10. Ibanez B, Heusch G, Ovize M, Van de Werf F. Evolving therapies for myocardial ischemia/reperfusion injury. J Am Coll Cardiol. 2015;65(14):1454-71.
11. Hahn JY, Song YB, Kim EK, Yu CW, Bae JW, Chung WY, et al. Ischemic postconditioning during primary percutaneous coronary intervention: the effects of postconditioning on myocardial reperfusion in patients with ST-segment elevation myocardial infarction (POST) randomized trial. Circulation. 2013;128(17):1889-96.
12. Murphy E, Steenbergen C. Mechanisms underlying acute protection from cardiac ischemia-reperfusion injury. Physiol Rev. 2008;88(2):581-609.
13. Sanada S, Komuro I, Kitakaze M. Pathophysiology of myocardial reperfusion injury: preconditioning, postconditioning, and translational aspects of protective measures. Am J Physiol Heart Circ Physiol. 2011;301(5):H1723-41.
14. Chen S, Li S. The Na(+)/Ca(2+) exchanger in cardiac ischemia/reperfusion injury. Med Sci Monit. 182012. p. Ra161-5.
15. Becker LB. New concepts in reactive oxygen species and cardiovascular reperfusion physiology. Cardiovasc Res. 2004;61(3):461-70.
16. Hess ML, Manson NH. Molecular oxygen: friend and foe. The role of the oxygen free radical system in the calcium paradox, the oxygen paradox and ischemia/reperfusion injury. J Mol Cell Cardiol. 1984;16(11):969-85.
17. Baines CP. The mitochondrial permeability transition pore and ischemia-reperfusion injury. Basic Res Cardiol. 2009;104(2):181-8.
18. Halestrap AP, McStay GP, Clarke SJ. The permeability transition pore complex: another view. Biochimie. 2002;84(2-3):153-66.

19. Di Lisa F, Carpi A, Giorgio V, Bernardi P. The mitochondrial permeability transition pore and cyclophilin D in cardioprotection. Biochim Biophys Acta. 2011;1813(7):1316-22.
20. Kalogeris T, Baines CP, Krenz M, Korthuis RJ. Cell biology of ischemia/reperfusion injury. Int Rev Cell Mol Biol. 2012;298:229-317.
21. Alberts B, Johnson A, Lewis J, Raff M, Roberts K, Walter P. Programmed cell death (apoptosis). Molecular Biology of the Cell. 4th Edition ed. New York: Garland Science; 2002.
22. Lopez-Neblina F, Toledo AH, Toledo-Pereyra LH. Molecular biology of apoptosis in ischemia and reperfusion. J Invest Surg. 2005;18(6):335-50.
23. Jagtap P, Szabo C. Poly(ADP-ribose) polymerase and the therapeutic effects of its inhibitors. Nat Rev Drug Discov. 2005;4(5):421-40.
24. Hochhauser E, Kivity S, Offen D, Maulik N, Otani H, Barhum Y, et al. Bax ablation protects against myocardial ischemia-reperfusion injury in transgenic mice. Am J Physiol Heart Circ Physiol. 2003;284(6):H2351-9.
25. Grunenfelder J, Miniati DN, Murata S, Falk V, Hoyt EG, Kown M, et al. Upregulation of Bcl-2 through caspase-3 inhibition ameliorates ischemia/reperfusion injury in rat cardiac allografts. Circulation. 2001;104(12 Suppl 1):I202-6.
26. Magistrelli P, Coppola R, Tonini G, Vincenzi B, Santini D, Borzomati D, et al. Apoptotic index or a combination of Bax/Bcl-2 expression correlate with survival after resection of pancreatic adenocarcinoma. J Cell Biochem. 2006;97(1):98-108.
27. Vanden Hoek TL, Qin Y, Wojcik K, Li CQ, Shao ZH, Anderson T, et al. Reperfusion, not simulated ischemia, initiates intrinsic apoptosis injury in chick cardiomyocytes. Am J Physiol Heart Circ Physiol. 2003;284(1):H141-50.
28. Inserte J, Hernando V, Garcia-Dorado D. Contribution of calpains to myocardial ischaemia/reperfusion injury. Cardiovasc Res. 2012;96(1):23-31.
29. Galluzzi L, Kroemer G. Secondary Necrosis: Accidental No More. Trends Cancer. 2017;3(1):1-2.
30. Zhang S, Wang J, Du Y, Shang J, Wang L, Wang J, et al. Chapter 9: Cell autophagy and myocardial ischemia/reperfusion injury. Ischemic Heart Disease. Rijekam Croatia: InTech; 2013.
31. Matsui Y, Takagi H, Qu X, Abdellatif M, Sakoda H, Asano T, et al. Distinct roles of autophagy in the heart during ischemia and reperfusion: roles of AMP-activated protein kinase and Beclin 1 in mediating autophagy. Circ Res. 2007;100(6):914-22.
32. Epelman S, Liu PP, Mann DL. Role of innate and adaptive immune mechanisms in cardiac injury and repair. Nat Rev Immunol. 2015;15(2):117-29.
33. Liu J, Wang H, Li J. Inflammation and Inflammatory Cells in Myocardial Infarction and Reperfusion Injury: A Double-Edged Sword. Clin Med Insights Cardiol. 2016;10:79-84.
34. Eltzschig HK, Eckle T. Ischemia and reperfusion--from mechanism to translation. Nat Med. 2011;17(11):1391-401.
35. Zuidema MY, Zhang C. Ischemia/reperfusion injury: The role of immune cells. World J Cardiol. 2010;2(10):325-32.
36. Hua F, Ha T, Ma J, Li Y, Kelley J, Gao X, et al. Protection against myocardial ischemia/reperfusion injury in TLR4-deficient mice is mediated through a phosphoinositide 3-kinase-dependent mechanism. J Immunol. 2007;178(11):7317-24.

37. Arslan F, Smeets MB, O'Neill LA, Keogh B, McGuirk P, Timmers L, et al. Myocardial ischemia/reperfusion injury is mediated by leukocytic toll-like receptor-2 and reduced by systemic administration of a novel anti-toll-like receptor-2 antibody. Circulation. 2010;121(1):80-90.
38. Sawa Y, Ichikawa H, Kagisaki K, Ohata T, Matsuda H. Interleukin-6 derived from hypoxic myocytes promotes neutrophil-mediated reperfusion injury in myocardium. J Thorac Cardiovasc Surg. 1998;116(3):511-7.
39. Chandrasekar B, Smith JB, Freeman GL. Ischemia-reperfusion of rat myocardium activates nuclear factor-KappaB and induces neutrophil infiltration via lipopolysaccharide-induced CXC chemokine. Circulation. 2001;103(18):2296-302.
40. Gao X, Zhang H, Belmadani S, Wu J, Xu X, Elford H, et al. Role of TNF-alpha-induced reactive oxygen species in endothelial dysfunction during reperfusion injury. Am J Physiol Heart Circ Physiol. 2008;295(6):H2242-9.
41. Jordan JE, Zhao ZQ, Vinten-Johansen J. The role of neutrophils in myocardial ischemia-reperfusion injury. Cardiovasc Res. 1999;43(4):860-78.
42. Kin H, Wang NP, Halkos ME, Kerendi F, Guyton RA, Zhao ZQ. Neutrophil depletion reduces myocardial apoptosis and attenuates NFkappaB activation/TNFalpha release after ischemia and reperfusion. J Surg Res. 2006;135(1):170-8.
43. Palatianos GM, Balentine G, Papadakis EG, Triantafillou CD, Vassili MI, Lidoriki A, et al. Neutrophil depletion reduces myocardial reperfusion morbidity. Ann Thorac Surg. 2004;77(3):956-61.
44. Schulz R, Heusch G. Tumor necrosis factor-alpha and its receptors 1 and 2: Yin and Yang in myocardial infarction? Circulation. 119. United States2009. p. 1355-7.
45. Lecour S, Smith RM, Woodward B, Opie LH, Rochette L, Sack MN. Identification of a novel role for sphingolipid signaling in TNF alpha and ischemic preconditioning mediated cardioprotection. J Mol Cell Cardiol. 2002;34(5):509-18.
46. Hartman MHT, Vreeswijk-Baudoin I, Groot HE, van de Kolk KWA, de Boer RA, Mateo Leach I, et al. Inhibition of Interleukin-6 receptor in a murine model of myocardial ischemia-reperfusion. In: González GE, editor. PLoS One. 11. San Francisco, CA USA2016.
47. Hausenloy DJ, Yellon DM. New directions for protecting the heart against ischaemia-reperfusion injury: targeting the Reperfusion Injury Salvage Kinase (RISK)-pathway. Cardiovascular research. 2004;61(3):448-60.
48. Zhai P, Sadoshima J. Overcoming an energy crisis?: An adaptive role of GSK-3 inhibition in ischemia/reperfusion. Circ Res. 2008;103(9):910-3.
49. Jugdutt BI. Nitric oxide and cardioprotection during ischemia-reperfusion. Heart Fail Rev. 2002;7(4):391-405.
50. Balakirev M, Khramtsov VV, Zimmer G. Modulation of the mitochondrial permeability transition by nitric oxide. Eur J Biochem. 1997;246(3):710-8.
51. Romashkova JA, Makarov SS. NF-kappaB is a target of AKT in anti-apoptotic PDGF signalling. Nature. 1999;401(6748):86-90.
52. Kukreja RC. NFKB activation during ischemia/reperfusion in heart: Friend or foe? Journal of Molecular and Cellular Cardiology. 2002;34(10):1301-4.
53. Lecour S, Suleman N, Deuchar GA, Somers S, Lacerda L, Huisamen B, et al. Pharmacological preconditioning with tumor necrosis factor-alpha activates signal transducer and activator of transcription-3 at reperfusion without involving classic

prosurvival kinases (Akt and extracellular signal-regulated kinase). Circulation. 2005;112(25):3911-8.
54. Lecour S. Activation of the protective Survivor Activating Factor Enhancement (SAFE) pathway against reperfusion injury: Does it go beyond the RISK pathway? J Mol Cell Cardiol. 2009;47(1):32-40.
55. Hattori R, Maulik N, Otani H, Zhu L, Cordis G, Engelman RM, et al. Role of STAT3 in ischemic preconditioning. J Mol Cell Cardiol. 2001;33(11):1929-36.
56. Pfeffer LM, Mullersman JE, Pfeffer SR, Murti A, Shi W, Yang CH. STAT3 as an adapter to couple phosphatidylinositol 3-kinase to the IFNAR1 chain of the type I interferon receptor. Science. 1997;276(5317):1418-20.
57. Nguyen MH, Ho JM, Beattie BK, Barber DL. TEL-JAK2 mediates constitutive activation of the phosphatidylinositol 3'-kinase/protein kinase B signaling pathway. J Biol Chem. 2001;276(35):32704-13.
58. Suranadi IW, Demaison L, Chate V, Peltier S, Richardson M, Leverve X. An increase in the redox state during reperfusion contributes to the cardioprotective effect of GIK solution. J Appl Physiol (1985). 2012;113(5):775-84.
59. Oates A, Nubani R, Smiley J, Kistler L, Hughey S, Theiss P, et al. Myocardial protection of insulin and potassium in a porcine ischemia-reperfusion model. Surgery. 2009;146(1):23-30.
60. Ceremuzynski L, Budaj A, Czepiel A, Burzykowski T, Achremczyk P, Smielak-Korombel W, et al. Low-dose glucose-insulin-potassium is ineffective in acute myocardial infarction: results of a randomized multicenter Pol-GIK trial. Cardiovasc Drugs Ther. 1999;13(3):191-200.
61. Mehta SR, Yusuf S, Diaz R, Zhu J, Pais P, Xavier D, et al. Effect of glucose-insulin-potassium infusion on mortality in patients with acute ST-segment elevation myocardial infarction: the CREATE-ECLA randomized controlled trial. Jama. 2005;293(4):437-46.
62. Timmers L, Henriques JP, de Kleijn DP, Devries JH, Kemperman H, Steendijk P, et al. Exenatide reduces infarct size and improves cardiac function in a porcine model of ischemia and reperfusion injury. J Am Coll Cardiol. 2009;53(6):501-10.
63. Lonborg J, Kelbaek H, Vejlstrup N, Botker HE, Kim WY, Holmvang L, et al. Exenatide reduces final infarct size in patients with ST-segment-elevation myocardial infarction and short-duration of ischemia. Circ Cardiovasc Interv. 2012;5(2):288-95.
64. Fryer RM, Pratt PF, Hsu AK, Gross GJ. Differential activation of extracellular signal regulated kinase isoforms in preconditioning and opioid-induced cardioprotection. J Pharmacol Exp Ther. 2001;296(2):642-9.
65. Manintveld OC, Te Lintel Hekkert M, van den Bos EJ, Suurenbroek GM, Dekkers DH, Verdouw PD, et al. Cardiac effects of postconditioning depend critically on the duration of index ischemia. Am J Physiol Heart Circ Physiol. 2007;292(3):H1551-60.
66. Fujita M, Asanuma H, Hirata A, Wakeno M, Takahama H, Sasaki H, et al. Prolonged transient acidosis during early reperfusion contributes to the cardioprotective effects of postconditioning. Am J Physiol Heart Circ Physiol. 2007;292(4):H2004-8.
67. Federation ID. IDF Diabetes Atlas. 7th Edn ed. Brussels, Belgium: International Diabetes Federation; 2015.
68. CDA. Canadian Diabetes Association 2013 clinical practice guidelines for the prevention and management of diabetes in Canada. Can J Diabetes. 2013;37 Suppl 1:S1-S216.

69. Nokoff N, Rewers M. Pathogenesis of type 1 diabetes: lessons from natural history studies of high-risk individuals. Ann N Y Acad Sci. 2013;1281:1-15.
70. Phillips JE, Couper JJ, Penno MAS, Harrison LC. Type 1 diabetes: a disease of developmental origins. Pediatr Diabetes. 2017;18(6):417-21.
71. Wu Y, Ding Y, Tanaka Y, Zhang W. Risk factors contributing to type 2 diabetes and recent advances in the treatment and prevention. Int J Med Sci. 2014;11(11):1185-200.
72. Boucher J, Kleinridders A, Kahn CR. Insulin receptor signaling in normal and insulin-resistant states. Cold Spring Harb Perspect Biol. 2014;6(1).
73. Zaccardi F, Webb DR, Yates T, Davies MJ. Pathophysiology of type 1 and type 2 diabetes mellitus: a 90-year perspective. Postgrad Med J. 2016;92(1084):63-9.
74. Buchanan TA, Xiang AH. Gestational diabetes mellitus. J Clin Invest. 2005;115(3):485-91.
75. Sorenson RL, Brelje TC. Adaptation of islets of Langerhans to pregnancy: beta-cell growth, enhanced insulin secretion and the role of lactogenic hormones. Horm Metab Res. 1997;29(6):301-7.
76. Radin MS. Pitfalls in hemoglobin A1c measurement: when results may be misleading. J Gen Intern Med. 2014;29(2):388-94.
77. Kannel WB, McGee DL. Diabetes and cardiovascular risk factors: the Framingham study. Circulation. 1979;59(1):8-13.
78. American Heart Association. Cardiovascular Disease & Diabetes. 2015. Available from: http://www.heart.org/HEARTORG/Conditions/More/Diabetes/WhyDiabetesMatters/Cardiovascular-Disease-Diabetes_UCM_313865_Article.jsp/_-_.WZ3W14WAawp. Accessed on: August 2, 2017.
79. Kovacic JC, Castellano JM, Farkouh ME, Fuster V. The relationships between cardiovascular disease and diabetes: focus on pathogenesis. Endocrinol Metab Clin North Am. 2014;43(1):41-57.
80. Haffner SM, Lehto S, Ronnemaa T, Pyorala K, Laakso M. Mortality from coronary heart disease in subjects with type 2 diabetes and in nondiabetic subjects with and without prior myocardial infarction. N Engl J Med. 1998;339(4):229-34.
81. Anand SS, Islam S, Rosengren A, Franzosi MG, Steyn K, Yusufali AH, et al. Risk factors for myocardial infarction in women and men: insights from the INTERHEART study. Eur Heart J. 2008;29(7):932-40.
82. Chavali V, Tyagi SC, Mishra PK. Predictors and prevention of diabetic cardiomyopathy. Diabetes Metab Syndr Obes. 2013;6:151-60.
83. Maisch B, Alter P, Pankuweit S. Diabetic cardiomyopathy--fact or fiction? Herz. 2011;36(2):102-15.
84. Marso SP, Miller T, Rutherford BD, Gibbons RJ, Qureshi M, Kalynych A, et al. Comparison of myocardial reperfusion in patients undergoing percutaneous coronary intervention in ST-segment elevation acute myocardial infarction with versus without diabetes mellitus (from the EMERALD Trial). Am J Cardiol. 2007;100(2):206-10.
85. Alegria JR, Miller TD, Gibbons RJ, Yi QL, Yusuf S. Infarct size, ejection fraction, and mortality in diabetic patients with acute myocardial infarction treated with thrombolytic therapy. Am Heart J. 2007;154(4):743-50.
86. Galiñanes M, Fowler AG. Role of clinical pathologies in myocardial injury following ischaemia and reperfusion. Cardiovascular Research. 2004 61(3):512-21.

87. Lejay A, Fang F, John R, Van JA, Barr M, Thaveau F, et al. Ischemia reperfusion injury, ischemic conditioning and diabetes mellitus. J Mol Cell Cardiol. 2016;91:11-22.
88. Ansley DM, Wang B. Oxidative stress and myocardial injury in the diabetic heart. J Pathol. 2013;229(2):232-41.
89. Giacco F, Brownlee M. Oxidative stress and diabetic complications. Circ Res. 2010;107(9):1058-70.
90. Labieniec-Watala M, Siewiera K, Gierszewski S, Watala C. Chapter 5: Mitochondria function in diabetes - From health to pathology - New perspectives for treatment of diabetes-driven disorders. In: Ghista PDN, editor. Biomedical Science, Engineering and Technology: InTech; 2012.
91. Matsushima S, Kinugawa S, Yokota T, Inoue N, Ohta Y, Hamaguchi S, et al. Increased myocardial NAD(P)H oxidase-derived superoxide causes the exacerbation of postinfarct heart failure in type 2 diabetes. Am J Physiol Heart Circ Physiol. 2009;297(1):H409-16.
92. Yokota T, Kinugawa S, Hirabayashi K, Matsushima S, Inoue N, Ohta Y, et al. Oxidative stress in skeletal muscle impairs mitochondrial respiration and limits exercise capacity in type 2 diabetic mice. Am J Physiol Heart Circ Physiol. 2009;297(3):H1069-77.
93. Sumimoto H. Structure, regulation and evolution of Nox-family NADPH oxidases that produce reactive oxygen species. Febs j. 2008;275(13):3249-77.
94. Ilkun O, Boudina S. Cardiac dysfunction and oxidative stress in the metabolic syndrome: an update on antioxidant therapies. Curr Pharm Des. 2013;19(27):4806-17.
95. Ramakrishna V, Jailkhani R. Oxidative stress in non-insulin-dependent diabetes mellitus (NIDDM) patients. Acta Diabetol. 2008;45(1):41-6.
96. Chu S, Bohlen HG. High concentration of glucose inhibits glomerular endothelial eNOS through a PKC mechanism. Am J Physiol Renal Physiol. 2004;287(3):F384-92.
97. Yakubu MA, Sofola OA, Igbo I, Oyekan AO. Link between free radicals and protein kinase C in glucose-induced alteration of vascular dilation. Life Sci. 2004;75(24):2921-32.
98. Maeno Y, Li Q, Park K, Rask-Madsen C, Gao B, Matsumoto M, et al. Inhibition of insulin signaling in endothelial cells by protein kinase C-induced phosphorylation of p85 subunit of phosphatidylinositol 3-kinase (PI3K). J Biol Chem. 2012;287(7):4518-30.
99. Liu Y, Jin J, Qiao S, Lei S, Liao S, Ge ZD, et al. Inhibition of PKCbeta2 overexpression ameliorates myocardial ischaemia/reperfusion injury in diabetic rats via restoring caveolin-3/Akt signaling. Clin Sci (Lond). 2015;129(4):331-44.
100. Singh VP, Bali A, Singh N, Jaggi AS. Advanced glycation end products and diabetic complications. Korean J Physiol Pharmacol. 2014;18(1):1-14.
101. Bucciarelli LG, Ananthakrishnan R, Hwang YC, Kaneko M, Song F, Sell DR, et al. RAGE and modulation of ischemic injury in the diabetic myocardium. Diabetes. 2008;57(7):1941-51.
102. Esposito K, Nappo F, Marfella R, Giugliano G, Giugliano F, Ciotola M, et al. Inflammatory cytokine concentrations are acutely increased by hyperglycemia in humans: role of oxidative stress. Circulation. 2002;106(16):2067-72.
103. GS H, DL M, LN C, BM S. - Tumor necrosis factor alpha inhibits signaling from the insulin receptor. Proc Natl Acad Sci U S A. 1994;91(11):4854-8.
104. Andersen B, Goldsmith GH, Spagnuolo PJ. Neutrophil adhesive dysfunction in diabetes mellitus; the role of cellular and plasma factors. J Lab Clin Med. 1988;111(3):275-85.

105. Rains JL, Jain SK. Oxidative stress, insulin signaling, and diabetes. Free Radic Biol Med. 2011;50(5):567-75.
106. Panes J, Kurose I, Rodriguez-Vaca D, Anderson DC, Miyasaka M, Tso P, et al. Diabetes exacerbates inflammatory responses to ischemia-reperfusion. Circulation. 1996;93(1):161-7.
107. Hokama JY, Ritter LS, Davis-Gorman G, Cimetta AD, Copeland JG, McDonagh PF. Diabetes enhances leukocyte accumulation in the coronary microcirculation early in reperfusion following ischemia. J Diabetes Complications. 2000;14(2):96-107.
108. Wider J, Przyklenk K. Ischemic conditioning: the challenge of protecting the diabetic heart. Cardiovasc Diagn Ther. 42014. p. 383-96.
109. Kristiansen SB, Lofgren B, Stottrup NB, Khatir D, Nielsen-Kudsk JE, Nielsen TT, et al. Ischaemic preconditioning does not protect the heart in obese and lean animal models of type 2 diabetes. Diabetologia. 2004;47(10):1716-21.
110. Przyklenk K, Maynard M, Greiner DL, Whittaker P. Cardioprotection with postconditioning: loss of efficacy in murine models of type-2 and type-1 diabetes. Antioxid Redox Signal. 2011;14(5):781-90.
111. Tsang A, Hausenloy DJ, Mocanu MM, Carr RD, Yellon DM. Preconditioning the diabetic heart: the importance of Akt phosphorylation. Diabetes. 2005;54(8):2360-4.
112. Miki T, Itoh T, Sunaga D, Miura T. Effects of diabetes on myocardial infarct size and cardioprotection by preconditioning and postconditioning. Cardiovasc Diabetol. 2012;11:67.
113. Li H, Liu Z, Wang J, Wong GT, Cheung CW, Zhang L, et al. Susceptibility to myocardial ischemia reperfusion injury at early stage of type 1 diabetes in rats. Cardiovasc Diabetol. 2013;12:133.
114. Ji L, Zhang X, Liu W, Huang Q, Yang W, Fu F, et al. AMPK-regulated and Akt-dependent enhancement of glucose uptake is essential in ischemic preconditioning-alleviated reperfusion injury. PLoS One. 2013;8(7):e69910.
115. Bouhidel O, Pons S, Souktani R, Zini R, Berdeaux A, Ghaleb B. Myocardial ischemic postconditioning against ischemia-reperfusion is impaired in ob/ob mice. Am J Physiol Heart Circ Physiol. 2008;295(4):H1580-6.
116. Jonassen AK, Aasum E, Riemersma RA, Mjos OD, Larsen TS. Glucose-insulin-potassium reduces infarct size when administered during reperfusion. Cardiovasc Drugs Ther. 2000;14(6):615-23.
117. Jonassen AK, Sack MN, Mjos OD, Yellon DM. Myocardial protection by insulin at reperfusion requires early administration and is mediated via Akt and p70s6 kinase cell-survival signaling. Circ Res. 2001;89(12):1191-8.
118. Gao Y, Moten A, Lin HK. Akt: a new activation mechanism. Cell Res. 2014;24(7):785-6.
119. Carracedo A, Pandolfi PP. The PTEN-PI3K pathway: of feedbacks and cross-talks. Oncogene. 2008;27(41):5527-41.
120. Mocanu MM, Field DC, Yellon DM. A potential role for PTEN in the diabetic heart. Cardiovasc Drugs Ther. 2006;20(4):319-21.
121. Xue R, Lei S, Xia ZY, Wu Y, Meng Q, Zhan L, et al. Selective inhibition of PTEN preserves ischaemic post-conditioning cardioprotection in STZ-induced Type 1 diabetic rats: role of the PI3K/Akt and JAK2/STAT3 pathways. Clin Sci (Lond). 2016;130(5):377-92.

122. Hotta H, Miura T, Miki T, Togashi N, Maeda T, Kim SJ, et al. Angiotensin II type 1 receptor-mediated upregulation of calcineurin activity underlies impairment of cardioprotective signaling in diabetic hearts. Circ Res. 2010;106(1):129-32.
123. Das A, Salloum FN, Filippone SM, Durrant DE, Rokosh G, Bolli R, et al. Inhibition of mammalian target of rapamycin protects against reperfusion injury in diabetic heart through STAT3 signaling. Basic Res Cardiol. 2015;110(3):31.
124. Li H, Yao W, Liu Z, Xu A, Huang Y, Ma XL, et al. Hyperglycemia abrogates ischemic postconditioning cardioprotection by impairing AdipoR1/Caveolin-3/STAT3 signaling in diabetic rats. Diabetes. 2016;65(4):942-55.
125. Riento K, Ridley AJ. Rocks: multifunctional kinases in cell behaviour. Nat Rev Mol Cell Biol. 2003;4(6):446-56.
126. Surma M, Wei L, Shi J. Rho kinase as a therapeutic target in cardiovascular disease. Future Cardiol. 2011;7(5):657-71.
127. Nakagawa O, Fujisawa K, Ishizaki T, Saito Y, Nakao K, Narumiya S. ROCK-I and ROCK-II, two isoforms of Rho-associated coiled-coil forming protein serine/threonine kinase in mice. FEBS letters. 1996;392(2):189-93.
128. Shi J, Wei L. Rho kinase in the regulation of cell death and survival. Arch Immunol Ther Exp (Warsz). 2007;55(2):61-75.
129. Ward Y, Yap SF, Ravichandran V, Matsumura F, Ito M, Spinelli B, et al. The GTP binding proteins Gem and Rad are negative regulators of the Rho-Rho kinase pathway. J Cell Biol. 2002;157(2):291-302.
130. Lowery DM, Clauser KR, Hjerrild M, Lim D, Alexander J, Kishi K, et al. Proteomic screen defines the Polo-box domain interactome and identifies Rock2 as a Plk1 substrate. Embo j. 2007;26(9):2262-73.
131. Lee HH, Tien SC, Jou TS, Chang YC, Jhong JG, Chang ZF. Src-dependent phosphorylation of ROCK participates in regulation of focal adhesion dynamics. J Cell Sci. 2010;123(Pt 19):3368-77.
132. Chuang HH, Yang CH, Tsay YG, Hsu CY, Tseng LM, Chang ZF, et al. ROCKII Ser1366 phosphorylation reflects the activation status. Biochem J. 2012;443(1):145-51.
133. Amano M, Nakayama M, Kaibuchi K. Rho-kinase/ROCK: A key regulator of the cytoskeleton and cell polarity. Cytoskeleton (Hoboken). 2010;67(9):545-54.
134. Wang Y, Zheng XR, Riddick N, Bryden M, Baur W, Zhang X, et al. ROCK isoform regulation of myosin phosphatase and contractility in vascular smooth muscle cells. Circ Res. 2009;104(4):531-40.
135. Maekawa M, Ishizaki T, Boku S, Watanabe N, Fujita A, Iwamatsu A, et al. Signaling from Rho to the actin cytoskeleton through protein kinases ROCK and LIM-kinase. Science. 1999;285(5429):895-8.
136. Fukata Y, Oshiro N, Kinoshita N, Kawano Y, Matsuoka Y, Bennett V, et al. Phosphorylation of adducin by Rho-kinase plays a crucial role in cell motility. J Cell Biol. 1999;145(2):347-61.
137. Fukata Y, Kimura K, Oshiro N, Saya H, Matsuura Y, Kaibuchi K. Association of the myosin-binding subunit of myosin phosphatase and moesin: dual regulation of moesin phosphorylation by Rho-associated kinase and myosin phosphatase. J Cell Biol. 1998;141(2):409-18.

138. Ye Y, Hu SJ, Li L. Inhibition of farnesylpyrophosphate synthase prevents angiotensin II-induced hypertrophic responses in rat neonatal cardiomyocytes: involvement of the RhoA/Rho kinase pathway. FEBS Lett. 2009;583(18):2997-3003.
139. Kuwahara K, Saito Y, Nakagawa O, Kishimoto I, Harada M, Ogawa E, et al. The effects of the selective ROCK inhibitor, Y27632, on ET-1-induced hypertrophic response in neonatal rat cardiac myocytes--possible involvement of Rho/ROCK pathway in cardiac muscle cell hypertrophy. FEBS Lett. 1999;452(3):314-8.
140. Hunter JC, Zeidan A, Javadov S, Kilic A, Rajapurohitam V, Karmazyn M. Nitric oxide inhibits endothelin-1-induced neonatal cardiomyocyte hypertrophy via a RhoA-ROCK-dependent pathway. J Mol Cell Cardiol. 2009;47(6):810-8.
141. Rikitake Y, Oyama N, Wang CY, Noma K, Satoh M, Kim HH, et al. Decreased perivascular fibrosis but not cardiac hypertrophy in ROCK1+/- haploinsufficient mice. Circulation. 2005;112(19):2959-65.
142. Okamoto R, Li Y, Noma K, Hiroi Y, Liu PY, Taniguchi M, et al. FHL2 prevents cardiac hypertrophy in mice with cardiac-specific deletion of ROCK2. Faseb j. 2013;27(4):1439-49.
143. Li Q, Xu Y, Li X, Guo Y, Liu G. Inhibition of Rho-kinase ameliorates myocardial remodeling and fibrosis in pressure overload and myocardial infarction: role of TGF-beta1-TAK1. Toxicol Lett. 2012;211(2):91-7.
144. Zhang YM, Bo J, Taffet GE, Chang J, Shi J, Reddy AK, et al. Targeted deletion of ROCK1 protects the heart against pressure overload by inhibiting reactive fibrosis. FASEB journal : official publication of the Federation of American Societies for Experimental Biology. 2006;20(7):916-25.
145. Yang X, Li Q, Lin X, Ma Y, Yue X, Tao Z, et al. Mechanism of fibrotic cardiomyopathy in mice expressing truncated Rho-associated coiled-coil protein kinase 1. Faseb j. 2012;26(5):2105-16.
146. Mallat Z, Gojova A, Sauzeau V, Brun V, Silvestre JS, Esposito B, et al. Rho-associated protein kinase contributes to early atherosclerotic lesion formation in mice. Circ Res. 2003;93(9):884-8.
147. Wang HW, Liu PY, Oyama N, Rikitake Y, Kitamoto S, Gitlin J, et al. Deficiency of ROCK1 in bone marrow-derived cells protects against atherosclerosis in LDLR(−/−) mice. Faseb j. 222008. p. 3561-70.
148. Zhou Q, Mei Y, Shoji T, Han X, Kaminski K, Oh GT, et al. Rho-associated coiled-coil-containing kinase 2 deficiency in bone marrow-derived cells leads to increased cholesterol efflux and decreased atherosclerosis. Circulation. 2012;126(18):2236-47.
149. Uehata M, Ishizaki T, Satoh H, Ono T, Kawahara T, Morishita T, et al. Calcium sensitization of smooth muscle mediated by a Rho-associated protein kinase in hypertension. Nature. 1997;389(6654):990-4.
150. Mukai Y, Shimokawa H, Matoba T, Kandabashi T, Satoh S, Hiroki J, et al. Involvement of Rho-kinase in hypertensive vascular disease: a novel therapeutic target in hypertension. Faseb j. 2001;15(6):1062-4.
151. Masumoto A, Hirooka Y, Shimokawa H, Hironaga K, Setoguchi S, Takeshita A. Possible involvement of Rho-kinase in the pathogenesis of hypertension in humans. Hypertension. 2001;38(6):1307-10.

152. Zhou H, Li YJ, Wang M, Zhang LH, Guo BY, Zhao ZS, et al. Involvement of RhoA/ROCK in myocardial fibrosis in a rat model of type 2 diabetes. Acta Pharmacol Sin. 2011;32(8):999-1008.
153. Pearson JT, Jenkins MJ, Edgley AJ, Sonobe T, Joshi M, Waddingham MT, et al. Acute Rho-kinase inhibition improves coronary dysfunction in vivo, in the early diabetic microcirculation. Cardiovasc Diabetol. 122013. p. 111.
154. Rao MY, Soliman H, Bankar G, Lin G, MacLeod KM. Contribution of Rho kinase to blood pressure elevation and vasoconstrictor responsiveness in type 2 diabetic Goto-Kakizaki rats. J Hypertens. 2013;31(6):1160-9.
155. Lin G, Craig GP, Zhang L, Yuen VG, Allard M, McNeill JH, et al. Acute inhibition of Rho-kinase improves cardiac contractile function in streptozotocin-diabetic rats. Cardiovasc Res. 2007;75(1):51-8.
156. Soliman H, Gador A, Lu YH, Lin G, Bankar G, MacLeod KM. Diabetes-induced increased oxidative stress in cardiomyocytes is sustained by a positive feedback loop involving Rho kinase and PKCbeta2. Am J Physiol Heart Circ Physiol. 2012;303(8):H989-h1000.
157. Lin G, Brownsey RW, Macleod KM. Complex regulation of PKCbeta2 and PDK-1/AKT by ROCK2 in diabetic heart. PLoS One. 2014;9(1):e86520.
158. Bao W, Hu E, Tao L, Boyce R, Mirabile R, Thudium DT, et al. Inhibition of Rho-kinase protects the heart against ischemia/reperfusion injury. Cardiovasc Res. 2004;61(3):548-58.
159. Wolfrum S, Dendorfer A, Rikitake Y, Stalker TJ, Gong Y, Scalia R, et al. Inhibition of Rho-kinase leads to rapid activation of phosphatidylinositol 3-kinase/protein kinase Akt and cardiovascular protection. Arterioscler Thromb Vasc Biol. 2004;24(10):1842-7.
160. Hamid SA, Bower HS, Baxter GF. Rho kinase activation plays a major role as a mediator of irreversible injury in reperfused myocardium. Am J Physiol Heart Circ Physiol. 2007;292(6):H2598-606.
161. Li Y, Zhu W, Tao J, Xin P, Liu M, Li J, et al. Fasudil protects the heart against ischemia-reperfusion injury by attenuating endoplasmic reticulum stress and modulating SERCA activity: the differential role for PI3K/Akt and JAK2/STAT3 signaling pathways. PloS one. 2012;7(10):e48115.
162. Kitano K, Usui S, Ootsuji H, Takashima S, Kobayashi D, Murai H, et al. Rho-kinase activation in leukocytes plays a pivotal role in myocardial ischemia/reperfusion injury. PloS one. 2014;9(3):e92242.
163. Lee WH, Kang S, Vlachos PP, Lee YW. A novel in vitro ischemia/reperfusion injury model. Arch Pharm Res. 2009;32(3):421-9.
164. Abarbanell AM, Herrmann JL, Weil BR, Wang Y, Tan J, Moberly SP, et al. Animal models of myocardial and vascular injury. J Surg Res. 2010;162(2):239-49.
165. King AJ. The use of animal models in diabetes research. Br J Pharmacol. 2012;166(3):877-94.
166. King A, Austin A. Chapter 10 - Animal models of type 1 and type 2 Diabetes Mellitus. Animal models for the study of human disease. 2nd Edn ed: Elsevier Inc.; 2017. p. 245-65.
167. Cardinal JW, Margison GP, Mynett KJ, Yates AP, Cameron DP, Elder RH. Increased susceptibility to streptozotocin-induced beta-cell apoptosis and delayed autoimmune

diabetes in alkylpurine-DNA-N-glycosylase-deficient mice. Mol Cell Biol. 2001;21(16):5605-13.
168. Charles River Laboratories. Outbred mice. 2015. Available from: http://www.criver.com/files/pdfs/rms/outbred-mice.aspx. Accessed on: August 8, 2017.
169. The Jackson Laboratory. C57BL/6J Mouse strain datasheet 000664. 2017. Available from: https://www.jax.org/strain/000664. Accessed on: August 8, 2017.
170. Guo Y, Flaherty MP, Wu WJ, Tan W, Zhu X, Li Q, et al. Genetic background, gender, age, body temperature, and arterial blood pH have a major impact on myocardial infarct size in the mouse and need to be carefully measured and/or taken into account: Results of a comprehensive analysis of determinants of infarct size in 1074 mice. Basic Res Cardiol. 2012;107(5):288.
171. Zhou Z, Meng Y, Asrar S, Todorovski Z, Jia Z. A critical role of Rho-kinase ROCK2 in the regulation of spine and synaptic function. Neuropharmacology. 2009;56(1):81-9.
172. Thumkeo D, Keel J, Ishizaki T, Hirose M, Nonomura K, Oshima H, et al. Targeted disruption of the mouse rho-associated kinase 2 gene results in intrauterine growth retardation and fetal death. Mol Cell Biol. 2003;23(14):5043-55.
173. Bugger H, Abel ED. Rodent models of diabetic cardiomyopathy. Dis Model Mech. 2009;2(9-10):454-66.
174. Rodrigues B, Cam MC, Kong J, Goyal RK, McNeill JH. Strain differences in susceptibility to streptozotocin-induced diabetes: effects on hypertriglyceridemia and cardiomyopathy. Cardiovasc Res. 1997;34(1):199-205.
175. Nielsen LB, Bartels ED, Bollano E. Overexpression of apolipoprotein B in the heart impedes cardiac triglyceride accumulation and development of cardiac dysfunction in diabetic mice. J Biol Chem. 2002;277(30):27014-20.
176. Zhang Y, Wang JH, Zhang YY, Wang YZ, Wang J, Zhao Y, et al. Deletion of interleukin-6 alleviated interstitial fibrosis in streptozotocin-induced diabetic cardiomyopathy of mice through affecting TGFbeta1 and miR-29 pathways. Sci Rep. 2016;6:23010.
177. Yu X, Tesiram YA, Towner RA, Abbott A, Patterson E, Huang S, et al. Early myocardial dysfunction in streptozotocin-induced diabetic mice: a study using in vivo magnetic resonance imaging (MRI). Cardiovasc Diabetol. 2007;6:6.
178. Moore A, Shindikar A, Fomison-Nurse I, Riu F, Munasinghe PE, Ram TP, et al. Rapid onset of cardiomyopathy in STZ-induced female diabetic mice involves the downregulation of pro-survival Pim-1. Cardiovasc Diabetol. 2014;13:68.
179. Klocke R, Tian W, Kuhlmann MT, Nikol S. Surgical animal models of heart failure related to coronary heart disease. Cardiovasc Res. 2007;74(1):29-38.
180. Thomas JL, Dumouchel J, Li J, Magat J, Balitzer D, Bigby TD. Endotracheal intubation in mice via direct laryngoscopy using an otoscope. J Vis Exp. 2014(86).
181. Mottram PM, Marwick TH. Assessment of diastolic function: what the general cardiologist needs to know. Heart. 2005 91:681-95.
182. Thune JJ, Solomon SD. Left ventricular diastolic function following myocardial infarction. Curr Heart Fail Rep. 2006;3(4):170-4.
183. Arnlov J, Ingelsson E, Riserus U, Andren B, Lind L. Myocardial performance index, a Doppler-derived index of global left ventricular function, predicts congestive heart failure in elderly men. Eur Heart J. 2004;25(24):2220-5.

184. van Zuylen VL, den Haan MC, Roelofs H, Fibbe WE, Schalij MJ, Atsma DE. Myocardial infarction models in NOD/Scid mice for cell therapy research: permanent ischemia vs ischemia-reperfusion. Springerplus. 2015;4:336.
185. Whittington HJ, Babu GG, Mocanu MM, Yellon DM, Hausenloy DJ. The diabetic heart: Too sweet for its own good? Cardiology Research and Practice. 2012;2012(Article ID 845698):15.
186. Rui T, Zhang J, Xu X, Yao Y, Kao R, Martin CM. Reduction in IL-33 expression exaggerates ischaemia/reperfusion-induced myocardial injury in mice with diabetes mellitus. Cardiovasc Res. 2012;94(2):370-8.
187. Liu Y, Qu Y, Wang R, Ma Y, Xia C, Gao C, et al. The alternative crosstalk between RAGE and nitrative thioredoxin inactivation during diabetic myocardial ischemia-reperfusion injury. Am J Physiol Endocrinol Metab. 2012;303(7):E841-52.
188. Lloyd-Jones D, Adams RJ, Brown TM, Carnethon M, Dai S, De Simone G, et al. Heart disease and stroke statistics--2010 update: a report from the American Heart Association. Circulation. 2010;121(7):e46-e215.
189. Sohal DS, Nghiem M, Crackower MA, Witt SA, Kimball TR, Tymitz KM, et al. Temporally regulated and tissue-specific gene manipulations in the adult and embryonic heart using a tamoxifen-inducible Cre protein. Circulation research. 2001;89(1):20.
190. Eguchi M, Kim YH, Kang KW, Shim CY, Jang Y, Dorval T, et al. Ischemia-reperfusion injury leads to distinct temporal cardiac remodeling in normal versus diabetic mice. PloS one. 2012;7(2):e30450.
191. Tsutsumi YM, Patel HH, Lai NC, Takahashi T, Head BP, Roth DM. Isoflurane produces sustained cardiac protection after ischemia-reperfusion injury in mice. Anesthesiology. 2006;104(3):495-502.
192. Gao E, Koch WJ. A novel and efficient model of coronary artery ligation in the mouse. Methods in molecular biology (Clifton, NJ). 2013;1037:299-311.
193. Bohl S, Medway DJ, Schulz-Menger J, Schneider JE, Neubauer S, Lygate CA. Refined approach for quantification of in vivo ischemia-reperfusion injury in the mouse heart. Am J Physiol Heart Circ Physiol. 2009;297(6):H2054-8.
194. Coste A, Dubuquoy L, Barnouin R, Annicotte JS, Magnier B, Notti M, et al. LRH-1-mediated glucocorticoid synthesis in enterocytes protects against inflammatory bowel disease. Proceedings of the National Academy of Sciences of the United States of America. 2007;104(32):13098-103.
195. Lee SH, Huang H, Choi K, Lee DH, Shi J, Liu T, et al. ROCK1 isoform-specific deletion reveals a role for diet-induced insulin resistance. American journal of physiology Endocrinology and metabolism. 2014;306(3):E332-43.
196. Soliman H, Nyamandi V, Garcia-Patino M, Varela JN, Bankar G, Lin G, et al. Partial deletion of ROCK2 protects mice from high-fat diet-induced cardiac insulin resistance and contractile dysfunction. American journal of physiology Heart and circulatory physiology. 2015;309(1):H70-81.
197. Calvert JW. Ischemic heart disease and its consequences. In: Willis M, Homeister J, Stone J, editors. Cellular and Molecular Pathobiology of Cardiovascular Disease: Academic Press; 2014. p. 79–100.
198. Li Z, Dong X, Wang Z, Liu W, Deng N, Ding Y, et al. Regulation of PTEN by Rho small GTPases. Nat Cell Biol. 2005;7(4):399-404.

199. Riento K, Totty N, Villalonga P, Garg R, Guasch R, Ridley AJ. RhoE function is regulated by ROCK I-mediated phosphorylation. The EMBO journal. 2005;24(6):1170-80.
200. Lee DH, Shi J, Jeoung NH, Kim MS, Zabolotny JM, Lee SW, et al. Targeted disruption of ROCK1 causes insulin resistance in vivo. The Journal of biological chemistry. 2009;284(18):11776-80.
201. Noma K, Oyama N, Liao JK. Physiological role of ROCKs in the cardiovascular system. American journal of physiology Cell physiology. 2006;290(3):C661-8.
202. Zhang J, Bian HJ, Li XX, Liu XB, Sun JP, Li N, et al. ERK-MAPK signaling opposes rho-kinase to reduce cardiomyocyte apoptosis in heart ischemic preconditioning. Molecular medicine (Cambridge, Mass). 2010;16(7-8):307-15.
203. Haudek SB, Gupta D, Dewald O, Schwartz RJ, Wei L, Trial J, et al. Rho kinase-1 mediates cardiac fibrosis by regulating fibroblast precursor cell differentiation. Cardiovascular research. 2009;83(3):511-8.
204. Tsang A, Hausenloy DJ, Mocanu MM, Yellon DM. Postconditioning: a form of "modified reperfusion" protects the myocardium by activating the phosphatidylinositol 3-kinase-Akt pathway. Circulation research. 2004;95(3):230-2.
205. Ruan H, Li J, Ren S, Gao J, Li G, Kim R, et al. Inducible and cardiac specific PTEN inactivation protects ischemia/reperfusion injury. Journal of molecular and cellular cardiology.46(2):193-200.
206. Rohrbach S, Troidl C, Hamm C, Schulz R. Ischemia and reperfusion related myocardial inflammation: A network of cells and mediators targeting the cardiomyocyte. IUBMB life. 2015;67(2):110-9.
207. Shimada H, Rajagopalan LE. Rho kinase-2 activation in human endothelial cells drives lysophosphatidic acid-mediated expression of cell adhesion molecules via NF-kappaB p65. The Journal of biological chemistry. 2010;285(17):12536-42.
208. Muller WA. Getting leukocytes to the site of inflammation. Veterinary pathology. 2013;50(1):7-22.
209. Noma K, Rikitake Y, Oyama N, Yan G, Alcaide P, Liu PY, et al. ROCK1 mediates leukocyte recruitment and neointima formation following vascular injury. The Journal of clinical investigation. 2008;118(5):1632-44.
210. Kadmon Corporation. Kadmon initiates placebo-controlled phase 2 clinical trial evaluating KD025 in psoriasis. 2016. Available from: http://kadmon.com/press/kadmon-initiates-placebo-controlled-phase-2-clinical-trial-evaluating-kd025-in-psoriasis/. Accessed on: August 22, 2017.
211. Rawson NSB, Chu R, Ismaila AS, Terres JAR. The aging Canadian population and hospitalizations for acute myocardial infarction: projection to 2020. BMC Cardiovasc Disord. 122012. p. 25.
212. Warfel NA, Niederst M, Newton AC. Disruption of the interface between the pleckstrin homology (PH) and kinase domains of Akt protein is sufficient for hydrophobic motif site phosphorylation in the absence of mTORC2. J Biol Chem. 2011;286(45):39122-9.
213. Sakurai H, Chiba H, Miyoshi H, Sugita T, Toriumi W. IkappaB kinases phosphorylate NF-kappaB p65 subunit on serine 536 in the transactivation domain. J Biol Chem. 1999;274(43):30353-6.
214. Ghaboura N, Tamareille S, Ducluzeau PH, Grimaud L, Loufrani L, Croue A, et al. Diabetes mellitus abrogates erythropoietin-induced cardioprotection against ischemic-

reperfusion injury by alteration of the RISK/GSK-3beta signaling. Basic Res Cardiol. 2011;106(1):147-62.
215. Whittington HJ, Harding I, Stephenson CI, Bell R, Hausenloy DJ, Mocanu MM, et al. Cardioprotection in the aging, diabetic heart: the loss of protective Akt signalling. Cardiovasc Res. 2013;99(4):694-704.
216. Yu Q, Zhou N, Nan Y, Zhang L, Li Y, Hao X, et al. Effective glycaemic control critically determines insulin cardioprotection against ischaemia/reperfusion injury in anaesthetized dogs. Cardiovasc Res. 2014;103(2):238-47.
217. Saini HK, Xu YJ, Zhang M, Liu PP, Kirshenbaum LA, Dhalla NS. Role of tumour necrosis factor-alpha and other cytokines in ischemia-reperfusion-induced injury in the heart. Exp Clin Cardiol. 2005;10(4):213-22.
218. Zanin-Zhorov A, Weiss JM, Trzeciak A, Chen W, Zhang J, Nyuydzefe MS, et al. Cutting Edge: Selective Oral ROCK2 Inhibitor reduces clinical scores in patients with psoriasis vulgaris and normalizes skin pathology via concurrent regulation of IL-17 and IL-10. J Immunol. 2017;198(10):3809-14.
219. Vandervelde S, van Amerongen MJ, Tio RA, Petersen AH, van Luyn MJ, Harmsen MC. Increased inflammatory response and neovascularization in reperfused vs. non-reperfused murine myocardial infarction. Cardiovasc Pathol. 2006;15(2):83-90.
220. Bayzigitov DR, Medvedev SP, Dementyeva EV, Bayramova SA, Pokushalov EA, Karaskov AM, et al. Human induced pluripotent stem cell-derived cardiomyocytes afford new opportunities in inherited cardiovascular disease modeling. Cardiol Res Pract. 2016;2016:3582380.